High Resolution Measurements of the Mean Three-dimensional Flow Field in a Natural River

John Eric Petrie

Dissertation submitted to the faculty of the Virginia Polytechnic Institute and State University in partial fulfillment of the requirements for the degree of

Doctor of Philosophy
In
Civil Engineering

Panayiotis Diplas, Co-Chair
Marte S. Gutierrez, Co-Chair
William E. Cox
W. Cully Hession

April 29, 2013
Blacksburg, VA

Keywords: acoustic Doppler current profiler, field measurements, secondary flows, turbulent flow, hydrokinetic energy generation

High Resolution Measurements of the Mean Three-dimensional Flow Field in a Natural River

John Eric Petrie

ABSTRACT

The flow velocity in a river is three-dimensional (3D), turbulent, and varies in time and space. Capturing this variability in field measurements to support studies of river processes has proven particularly challenging. While originally developed to measure discharge, boat-mounted acoustic Doppler current profilers (ADCP) are increasingly used in field studies to quantify flow features including mean velocity, boundary shear stress, and sediment motion. Two survey procedures are typically employed with an ADCP. Moving-vessel (MV) measurements provide spatially-rich velocity data while temporally-rich data are obtained with fixed-vessel (FV) procedures. Given the relative ease of MV measurements, recent work has focused on developing MV procedures that produce comparable results to FV measurements. At the present, results of this work are inconclusive. Additionally, there is a lack of reported data and procedures for FV measurements.

This work seeks to develop techniques to present 3D velocity data obtained in natural rivers in a unified framework. This framework is based on a stream-fitted coordinate system defined by the flow direction at a cross section and allows for 3D velocity to be decomposed into streamwise, spanwise, and vertical components. Procedures are developed to assure that the velocity profiles measured at fixed locations are (1) not negatively impacted by the inevitable motion of the ADCP, (2) statistically stationary,

and (3) of sufficient record length to determine the mean velocity. The coordinate system allows time-averaged velocity from FV procedures to be compared with spatially-averaged velocity from MV vessels. Significant differences are found between the two survey procedures, particularly for secondary velocity components. Ultimately, integrating results of the two survey procedures leads to an improved representation of the mean flow field. The techniques are applied to data obtained on a study reach on the lower Roanoke River, located in eastern North Carolina.

Dedicated to Margaret Anne Petrie and Hyounae Min (아기곰)

ACKNOWLEDGEMENTS

I am grateful for the support and guidance of my advisors Dr. Panayiotis Diplas and Dr. Marte S. Gutierrez. They provided both the training and flexibility to develop my own ideas and direction. The opportunity to interact closely with scientists of the highest standard has made lasting impact on my life. I would especially like to thank Dr. Diplas for providing the opportunity to return to graduate school. Additionally, I am grateful to my committee members Dr. William E. Cox and Dr. W. Cully Hession for providing ideas and direction for this work.

The financial support provided by Dominion and the U.S. Army Corps of Engineers is gratefully acknowledged. Bob Graham of Dominion deserves special mention for his dedication to our work on the lower Roanoke River. Bob facilitated much of our field data collection, even allowing us to use his personal boat when engine trouble threatened our work. I am grateful to the Hydro Research Foundation. The Hydro Fellowship program has been an amazing experience. I would also like to thank the Civil and Environmental Department at Virginia Tech for financial support. The receipt of the G. V. Loganathan Fellowship was one of the most meaningful events of my graduate studies. Additional financial support from the Virginia Water Resources Research Center, the Edna Bailey Sussman Fund, and the Virginia Water Environment Association is also acknowledged.

Throughout my studies, I have gotten to know a great group of fellow students. Included in this group are Nikolaos Apsilidis, Celso Castro Bolinaga, Polydefkis Bouratsis, Hannah Cardwell, A. Ozan Celik, R. Miles Ellenberg, David Liu, Soonkie Nam, Matthew Rice, Katie Weidner, and Edgardo Zavaleta. A special mention is necessary for Soonkie and David, who survived several lengthy site visits for field work, including 21 straight days at one point. They truly are “Chinese geniuses”, at least in Scotland Neck, NC.

My time in Blacksburg has been more enjoyable playing music with many people. Nathan Alexander, Justin Craig, Paul Deck, Jared Gibbs, and Lou Madsen deserve particular mention. Thank you for tolerating a generally grouchy bass player with a loose interpretation of pitch, harmony, and time.

I would like to express my deepest gratitude to my family in the U.S. and Korea for their patience and understanding. I am especially thankful to my dad, Paul Petrie, for sound advice over the years. Finally, this work would not have been possible without my wife, Hyounae Min, whose warm smile and (mostly) patient support has guided me to this point. Now it’s my turn.

Table of Contents

List of Figures

Chapter 2.

Chapter 3.

Chapter 4.

List of Tables

Chapter 2.

Chapter 3.

Chapter 4.

CHAPTER 1. INTRODUCTION

1.1 Problem Description

The flow of water in a natural river is characterized by three-dimensional (3D) turbulent velocity over a rough boundary, often with complex topography. The boundary may change shape due to erosion and deposition processes. As a result of these characteristics, as well as watershed hydrology, the velocity distribution in a river contains a range of spatial and temporal scales. The importance of the velocity field is well established for studies of sediment transport, erosion, design of in-stream structures and pollutant transport. More recently, velocity has been demonstrated to be an important factor in stream ecology and habitat [*Crowder and Diplas*, 2000] as well as biogeochemical processes [*O'Connor and Hondzo*, 2008]. Understanding of the relation between flow and stream processes is improved by direct measurement of flow velocity in the field. Additionally, field measurements of velocity are needed to support hydrodynamic and computational fluid dynamics models. These high resolution numerical models are increasingly used in fluvial studies and rely on field data for boundary conditions and validation data [*Lane et al.*, 1999; *Shen and Diplas*, 2008].

Capturing the spatial and temporal variability of velocity in natural rivers has proven challenging. High temporal resolution velocity measurements at a single point in a stream have been obtained with electromagnetic current meters [*Roy et al.*, 2004] and acoustic Doppler velocimeters [*Lane et al.*, 1998]. While these technologies have sampling frequencies sufficient to determine turbulent characteristics, quantifying the velocity distribution may require significant time and effort, particularly for larger rivers. More recently, the acoustic Doppler current profiler (ADCP) has emerged as an important tool for field measurements of velocity. A

boat-mounted ADCP measures velocity along a vertical profile and can be operated while traversing the channel (moving-vessel (MV) measurements) or from a fixed location (fixed-vessel (FV) measurement). While the most common application of the ADCP is to measure discharge [e.g., *Yorke and Oberg*, 2002], studies have also investigated the ability of the ADCP to determine mean velocity profiles [*Muste et al.*, 2004], boundary shear stress [*Sime et al.*, 2007], sediment transport rates [*Rennie and Millar*, 2004], turbulence characteristics [*Stacey et al.*, 1999], and habitat quality [*Shields and Rigby*, 2005].

The two survey procedures provide different spatial and temporal resolutions. MV measurements have received more attention due to their ability to efficiently collect data over the width of a river. The velocity field collected during a MV measurement is neither a mean nor instantaneous flow field; rather, the measurement documents the changing turbulent flow field along the path of the ADCP. Mean velocity profiles are obtained with a FV survey procedure but require significantly more time in the field to approach the spatial resolution of MV measurements. Studies comparing the results of both survey procedures have focused on the velocity magnitude and streamwise velocity. Further work is needed to determine if MV surveys can accurately determine mean spanwise and vertical velocity components and to establish appropriate field and data analysis procedures for FV surveys.

1.2 Research Objectives

The primary focus of this research is to quantify the mean 3D flow field in a natural river using a boat-mounted ADCP and to develop appropriate field survey and data analysis procedures. During an extensive field campaign, velocity data were collected using both FV and MV survey procedures at two different study sites and two discharges. A quality assurance plan was developed to ensure that proper field procedures were used for FV measurements, including assessments of ADCP motion, flow stationarity, and sample record length. The mean streamwise velocity profiles were also compared with the theoretical law of the wall for flow over a rough boundary. A framework is presented to align spatially varying data along a cross section defined by the flow characteristics. Using this framework, data obtained from both survey procedures can be directly compared or integrated to present a more complete representation of the mean 3D flow field. In summary, the specific research objectives of this dissertation include:

1. Formulate appropriate field and data analysis procedures, including quality assurance, for mean 3D velocity profiles obtained with FV surveys.
2. Assess the ability of multiple MV measurements to determine 3D velocity profiles comparable to those obtained with a FV procedure.
3. Develop field and data analysis procedures that combine results of the two survey procedures to present a more complete picture of the mean 3D flow field in natural rivers.
4. Demonstrate the application of ADCP field surveys to site assessment for the emerging technology of in-stream hydrokinetic energy generation.

1.3 Organization of Dissertation

This dissertation consists of three self-contained chapters that have been or will be submitted for publication in scholarly journals. Chapter 2 has been published in Water Resources Research, while Chapter 3 is under review in Water Resources Research and Chapter 4 will be submitted to Renewable Energy. The chapters have been formatted for consistency with tables and figures corresponding to each chapter following the text. This formatting may produce minor differences between the chapters of this dissertation and the published articles. While each chapter was designed as a standalone article, when taken together, these articles provide a more complete understanding of the field survey and data analysis procedures required for high resolution velocity measurements in natural rivers.

Chapter 2 – Petrie, J., P. Diplas, M. Gutierrez, and S. Nam (2013), Data evaluation for acoustic Doppler current profiler measurements obtained at fixed locations in a natural river, *Water Resources Research*, *49*(2), 1003-1016.

Chapter 3 – Petrie, J., P. Diplas, M. Gutierrez, and S. Nam (*under review*), Combining fixed- and moving-vessel acoustic Doppler current profiler measurements for improved characterization of the mean flow in a natural river, *Water Resources Research*.

Chapter 4 – Petrie, J., P. Diplas, M. Gutierrez, and S. Nam (*to be submitted*), Characterizing the mean flow field in a river for assessing and monitoring hydrokinetic energy generation sites, *Renewable Energy*.

References

Crowder, D. W., and P. Diplas (2000), Using two-dimensional hydrodynamic models at scales of ecological importance, *Journal of Hydrology*, *230*(3-4), 172-191.

Lane, S. N., P. M. Biron, K. F. Bradbrook, J. B. Butler, J. H. Chandler, M. D. Crowell, S. J. McLelland, K. S. Richards, and A. G. Roy (1998), Three-dimensional measurement of river channel flow processes using acoustic Doppler velocimetry, *Earth Surface Processes and Landforms*, *23*(13), 1247-1267.

Lane, S. N., K. F. Bradbrook, K. S. Richards, P. A. Biron, and A. G. Roy (1999), The application of computational fluid dynamics to natural river channels: three-dimensional versus two-dimensional approaches, *Geomorphology*, *29*(1-2), 1-20.

Muste, M., K. Yu, T. Pratt, and D. Abraham (2004), Practical aspects of ADCP data use for quantification of mean river flow characteristics; Part II: fixed-vessel measurements, *Flow Meas. Instrum.*, *15*(1).

O'Connor, B. L., and M. Hondzo (2008), Enhancement and inhibition of denitrification by fluid-flow and dissolved oxygen flux to stream sediments, *Environ. Sci. Technol.*, *42*(1), 119-125.

Rennie, C. D., and R. G. Millar (2004), Measurement of the spatial distribution of fluvial bedload transport velocity in both sand and gravel, *Earth Surf. Processes Landforms*, *29*(10), 1173-1193.

Roy, A. G., T. Buffin- Bélanger, H. Lamarre, and A. D. Kirkbride (2004), Size, shape and dynamics of large-scale turbulent flow structures in a gravel-bed river, *J. Fluid Mech.*, *500*, 1-27.

Shen, Y., and P. Diplas (2008), Application of two- and three-dimensional computational fluid dynamics models to complex ecological stream flows, *J. Hydrol.*, *348*(1-2), 195-214.

Shields, F. D., and J. R. Rigby (2005), River habitat quality from river velocities measured using acoustic Doppler current profiler, *Environ. Manage.*, *36*(4), 565-575.

Sime, L. C., R. I. Ferguson, and M. Church (2007), Estimating shear stress from moving boat acoustic Doppler velocity measurements in a large gravel bed river, *Water Resour. Res.*, *43*(3), W03418.

Stacey, M. T., S. G. Monismith, and J. R. Burau (1999), Measurements of Reynolds stress profiles in unstratified tidal flow, *J. Geophys. Res.*, *104*(C5), 10933-10949.

Yorke, T. H., and K. A. Oberg (2002), Measuring river velocity and discharge with acoustic Doppler profilers, *Flow Meas. Instrum.*, *13*(5-6), 191-195.

CHAPTER 2. DATA EVALUATION FOR ACOUSTIC DOPPLER CURRENT PROFILER MEASUREMENTS OBTAINED AT FIXED LOCATIONS IN A NATURAL RIVER[1]

Abstract

Methodologies are presented to (1) evaluate the effect of ADCP motion on velocity measurements, (2) assess the stationarity of velocity time series, and (3) ensure that a sample record is of sufficient length for measurements taken with an acoustic Doppler current profiler (ADCP) at a fixed location in a natural river. ADCP motion occurring on the time scale of an ensemble is investigated by comparing single- and multi-ping measurements obtained at the same location under the same flow conditions. Large scale motion occurring over the course of the entire measurement is studied by first examining a set of indicators to determine if motion may have resulted in the ADCP measuring in regions of different flow characteristics and then dividing the record into segments representing the potentially different regions for comparison. If boat motion is significant, the ADCP record is edited accordingly. Stationarity is assessed using statistical trends tests with guidance provided for selecting parameters based on instrument physics and flow conditions. Mean streamwise and spanwise velocity profiles can be calculated after confirming the reliability of a measurement. A set of criteria is presented to evaluate the appropriateness of an assumption of the law of the wall for streamwise velocity profiles. The methodology is demonstrated using 67 fixed-vessel measurements obtained at two sites on the lower Roanoke River for two discharges. The results indicate that an appropriate procedure was

[1] This chapter is a modified version of the published article: Petrie, J., P. Diplas, M. Gutierrez, and S. Nam (2013), Data evaluation for acoustic Doppler current profiler measurements obtained at fixed locations in a natural river, *Water Resources Research*, *49*(2), 1003-1016.

used for securing the ADCP in the channel and that the sample records were sufficient to provide both accurate measurements of mean quantities and assess the stationarity of velocity.

2.1 Introduction

The velocity distribution in a natural river is an important control on morphological processes, contaminant transport, and stream ecology. Prior to the early 1990's obtaining high spatial resolution velocity data was difficult in large rivers due to the available measuring technology. Electromagnetic current meters and acoustic Doppler velocimeters measure two- or three-dimensional velocity components at a single point. Recently the acoustic Doppler current profiler (ADCP) has emerged as a tool that measures three-dimensional velocity components along a vertical profile through the water column. A boat-mounted ADCP fixed in location within a channel provides velocity data along a vertical with a significant decrease in time and overall effort compared to other currently available technologies. Application of the ADCP to studies in geomorphology and river engineering are widespread, investigating discharge [*Yorke and Oberg*, 2002], boundary shear stress [*Sime et al.*, 2007], sediment transport [*Rennie et al.*, 2002; *Rennie and Millar*, 2004], turbulence [*Stacey et al.*, 1999], and habitat quality [*Shields and Rigby*, 2005]. Additionally, recent studies have recognized the ability of the ADCP to support building numerical models [*Shen and Diplas*, 2008, 2010; *Rüther et al.*, 2010; *Rennie and Church*, 2010; *Guerrero and Lamberti*, 2011].

The ADCP has been used to identify flow structures in natural rivers ranging from the River Blackwater, UK (discharge, Q=2.5 m^3 s^{-1}) [*Gunawan et al.*, 2010] to the Río Paraná, Argentina (Q=17,646 m^3 s^{-1}) [*Szupiany et al.*, 2007] with varying planform geometry including meander bends [*Dinehart and Burau*, 2005] and confluences [*Szupiany et al.*, 2009]. Most of these studies

have employed a moving-vessel (MV) survey methodology where the ADCP records velocity and flow depth data while moving across the channel. These measurements span a large portion of the channel width but do not resolve the mean flow field in a time-averaged sense. Time-averaged velocity profiles may be obtained using a fixed-vessel (FV) methodology where the ADCP records continuously at a fixed location within the channel. Due to the increased time associated with FV measurements and the difficulty in maintaining a fixed boat position in a moving current, studies have focused on using MV measurements to provide equivalent results to FV measurements [*Muste et al.*, 2004a, 2004b; *Szupiany et al.*, 2007]. Typically these procedures involve averaging the results of multiple MV measurements.

This study presents a methodology to evaluate the quality of velocity data obtained from a FV boat-mounted ADCP survey. Procedures are developed to demonstrate that motion of the ADCP did not adversely affect FV measurements, establish the stationarity of velocity records, and determine if the sample record length is sufficient. The role of motion is investigated for time scales of an individual ensemble and the entire record. Once the reliability of the velocity data has been verified, basic processing of mean velocity profiles is demonstrated including rotating velocity components to a stream-based coordinate system and estimating boundary shear stress and characteristic roughness using the law of the wall. A set of criteria is presented to provide confidence that the law of the wall is valid for a profile. The methodology is applied to measurements from an extensive field campaign on the lower Roanoke River, North Carolina, USA. ADCP surveys were undertaken for two discharges, one close to the mean annual flow (228 $m^3 s^{-1}$) and another which resulted in bankfull conditions (565 $m^3 s^{-1}$).

2.2 Methodology

2.2.1 Study Site

The lower Roanoke River, shown in Figure 1, is a regulated river flowing through the coastal plain of eastern North Carolina. The lower reach runs from the Roanoke Rapids Dam approximately 210 km to the Albemarle Sound. The Roanoke Rapids Dam, completed in 1951, has significantly reduced the magnitude of peak flows resulting in documented bank retreat along much of the river [*Hupp et al.*, 2009]. Due to a lack of major tributaries and relatively narrow watershed (see Fig. 1), the discharge throughout much of the lower Roanoke River, including the study sites, is largely controlled by reservoir releases.

ADCP measurements were obtained at two sites shown in Figure 2: Site 1, a 180° meander bend and Site 5, a relatively mild bend. Site 1 has a channel width of about 100 m, a ratio of radius of curvature to channel width of 1.6, and a sinuosity of 1.9. These values indicate a meander bend of fairly high curvature for a natural channel. The channel width at Site 5 is approximately 100 m as well, though the bank edges are not well-defined. Measurements were performed in two campaigns occurring in May and June, 2009. The reservoir releases were fairly constant for each survey period as well as for several days prior as demonstrated by the hydrographs in Figure 3. The discharge seen in Figure 3 is measured at the Roanoke Rapids gaging station (USGS 2080500) located 7 km downstream from the dam. The study sites are located about 27 km downstream from the Scotland Neck gaging station (USGS 2081000) and 26 km upstream from the Oak City gaging station (USGS 2081022). The measured gage heights at these stations are included in Figure 3. The steady flow releases in May were the result of spawning operations and produced a discharge, Q, of about 228 m^3 s^{-1}, which is close to the mean annual flow. Flood

control operations produced the high discharge (Q=565 m^3 s^{-1}) in June. This discharge results in bankfull conditions at the study sites. The mean flow depths at Site 1 and Site 5 are 5.6 m (8.6 m) and 3.8 m (7.1 m), respectively, for the mean annual flow (bankfull flow). A maximum measured depth of 17.5 m was measured near the bend apex at Site 1 during the bankfull flow.

2.2.2 Equipment and Measurement Procedures

2.2.2.1 The Acoustic Doppler Current Profiler

The ADCP measures three-dimensional velocity components based on the frequency shift of acoustic pulses, called pings. The water column is divided into equally-spaced depth cells, called bins, and the mean velocity from all pings reflected within each cell is placed at the bin center. A bin size of 0.25 m was used for all measurements in this study. Due to physical limitations of the instrument, velocity measurements are not available near the water surface or near the bed [*Simpson*, 2001]. For the present set up, the first bin was centered at 0.72 m below the water surface and the last bin was located at least 6% of the flow depth above the river bottom. A single recorded measurement of the velocity profile is called an ensemble and may be comprised of a single or multiple pings. In this study, 20 sub-pings sent 50 milliseconds apart were used to create each ensemble. Multi-ping measurements require that the ADCP remain stable to ensure that excess motion does not corrupt the velocity measurements. The mean velocities calculated from the multi-ping measurements are demonstrated to be equivalent to those obtained with a single-ping setting in a subsequent section. Data was collected using Water Mode 12 and Bottom Mode 5 [see *Mueller and Wagner*, 2009].

The raw velocity measured by the ADCP includes contributions from the flowing water and motion of the boat. A measure of the boat velocity, or velocity reference, is required to isolate the flow velocity. The boat velocity may be determined using either bottom tracking or a global positioning system (GPS). While bottom tracking is typically more accurate than GPS, flow velocity will be biased if the bed is moving. Given that bed movement was observed at most locations for the bankfull flow, GPS was used as the velocity reference for all measurements reported here with one exception. During the mean annual flow, a problem with the GPS signal occurred during one profile (S1xs6p2, nomenclature explained in the following section) which required the use of bottom tracking as the velocity reference. Further details on ADCP operational principles can be found in the work of *Gordon* [1989], *Simpson* [2001], and *Mueller and Wagner* [2009].

A 1200 kHz Workhorse Rio Grande ADCP manufactured by Teledyne RD Instruments (Poway, CA) and a Trimble DSM 232 GPS (Sunnyvale, CA) were mounted to a Riverboat tethered boat (Oceanscience, Oceanside, CA). The tethered boat was attached using rope to the starboard (right) side of a motor boat (length=6 m). The ADCP and GPS data were recorded with WinRiver II software (Teledyne RD Instruments). The horizontal accuracy of the GPS is approximately 1.0 m. The measurement locations were selected prior to deployment and found at the field site with HYPACK LITE (HYPACK, Inc., Middletown, CT) surveying software.

2.2.2.2 Survey Procedure

As previously described, two survey procedures are commonly used with a boat-mounted ADCP—moving-vessel (MV) and fixed-vessel (FV) procedures. FV measurements are the focus

here and are obtained by fixing the ADCP within the river channel and recording continuously for a specified time interval. Procedures for fixing the boat include mooring [*Muste et al.*, 2004a], anchoring [*Stacey et al.*, 1999], and, for small rivers, taglines [*Stone and Hotchkiss*, 2007]. Mean velocity profiles are determined by averaging the results of multiple ensembles. *Nystrom et al.* [2007] found good agreement between mean velocity profiles obtained with an ADCP and an acoustic Doppler velocimeter in a laboratory flume. Questions remain as to the appropriate sample record length and influence of boat motion on velocity profiles from FV measurements.

On the lower Roanoke River, anchors were used to fix the boat and ADCP as detailed in *Petrie et al.* [2010]. The procedure to secure the boat involved driving upstream some distance of the desired measurement point and releasing an anchor over the bow (front). The boat was then slowly steered to the desired location where a second anchor was released from the port-side stern (left-side rear). The total set up time ranged from ten minutes to almost one hour depending on flow conditions and the desired location within the channel. During the measurement period, the boat motor was turned off and movement by the operators was minimized. A minimum sample record length of 1200 s was used for all measurements.

Measurements were aligned along cross sections oriented approximately perpendicular to the riverbanks. The cross sections are numbered consecutively from upstream to downstream with six cross sections at Site 1 and two at Site 5 (see Fig. 2). For each discharge between three and five FV measurements were performed along each cross section. The measurement locations for the bankfull flow are shown in Figure 2. While every effort was made to repeat measurements at

the same location in June, some differences were observed due to the difficulty positioning the boat in a fixed location. The average distance between the mean locations measured in May and June is 5.1 m. FV measurement locations at each cross section are labeled consecutively beginning with profile 1 nearest to the left bank when facing downstream. The nomenclature for FV profiles consists of the study site and cross section number followed by the profile number, e.g., S1xs1p1. A total of 25 (26) profiles were measured during the mean annual flow (bankfull flow) at Site 1, while 8 profiles were obtained at Site 5 for each discharge. The surveys were each performed in approximately six days with a three person crew.

The data output from WinRiver II were analyzed using a suite of codes developed in MATLAB® (MathWorks, Natick, MA) at the Baker Environmental Hydraulics Laboratory of Virginia Tech. All velocity, location, and depth measurements marked as "bad" by WinRiver II were removed. Bins that contained "bad" velocity measurements for more than half of the recorded ensembles were removed from the record. This action was necessary for bins nearest the channel bed in a few measurements. No additional smoothing or filtering of the data was performed.

2.3 Effects of ADCP Motion

The inevitable motion that an ADCP undergoes during the course of a FV measurements may adversely affect the measured velocity in two ways. First, motion of the ADCP over the measurement duration, termed large-scale motion, may result in the ADCP moving into a region with distinctly different flow characteristics from the starting position. The statistical properties calculated from this record will then contain a mixture of samples from different populations.

Given that some motion of the ADCP occurs for all FV measurements and the range of acceptable movement is site specific, a quantitative procedure is needed to determine if velocity records contain ensembles from regions of differing flow characteristics. The second way ADCP motion can affect the measured velocity is through movement during the course of a single ensemble, termed small-scale motion. Small-scale motion is important if a multi-ping setting is used, as on the lower Roanoke River. When the ADCP records a single ensemble, in addition to the measured velocity, data are collected for bottom track velocity, flow depth, heading, pitch and roll, and location. A single-ping ensemble records velocity from one ping along with the ancillary data while a multi-ping ensemble records the average velocity of several pings and a single measure of the ancillary data. Multi-ping measurements require stable deployment to ensure that sudden motion does not occur. While no such movement was observed on the lower Roanoke River, comparing the results of multi-ping and single-ping measurements provides further confidence that small-scale motion did not adversely affect the multi-ping measurements.

Analysis of the two types of ADCP motion involves comparing two time series for each bin; thus, the same general procedure is applied to both. For large-scale motion, the two time series are continuous segments taken from the same sample record. For small-scale motion, the two time series come from separate measurements performed at the same location—one using a single-ping setting and the other using a multi-ping setting. To render each velocity time series independent, the autocorrelation coefficient is determined for the velocity record. An edited sample record is then created by selecting every m ensemble, where m is larger than the number of ensemble lags required for the autocorrelation coefficient to go to zero. Hypothesis tests are used to compare the two edited velocity records in each bin. Results of the hypothesis tests

provide quantitative support for assessing the role of ADCP motion on the measured velocity. Examples of this procedure are provided in the following sections.

2.3.1 Large-scale Motion

The effect of large-scale movement of the ADCP on velocity data from FV measurements is difficult to assess given the lack of knowledge regarding the flow field in regions adjacent to the measurement location. Several indirect indicators are available to aid in the identification of measurements that may be adversely impacted by large scale motion. A scatter plot of the ensemble locations from the GPS provides a visual representation of the ADCP footprint (see Fig. 4). The size of the footprint relative to the channel width provides a rough indicator of the significance of ADCP motion. The footprint area, A_f, is a measure of the area covered by the ADCP during the course of a measurement and is defined as the area of the smallest rectangle containing all ensemble locations. The footprint area is used to calculate the mean ensemble separation distance, $D=(A_f/n_e)^{1/2}$, where n_e is the number of ensembles in the sample record. This value represents the mean distance between consecutive ensembles and is analogous to the mean element separation distance in rough-wall boundary layers [see *Raupach et al.*, 1991]. Another indication of the overall boat motion is the boat velocity. For a truly fixed location, the time series and resulting mean of the boat velocity are zero. While the mean boat velocity will not be exactly zero, the value should be small relative to the flow velocity. Plotting the boat velocity time series against the mean boat velocity helps identify trends in ADCP motion. Times within the sample record where boat motion may be significant can be identified by inspecting the area under the boat velocity time series. A time series plot of the measured flow depths also provides evidence as to whether or not the ADCP remained in a region where the flow can be considered

homogeneous. While the measured depth in each beam will not be constant over the entire sample record due to bed forms and other topographical features, each beam depth should remain within a reasonable range considering the site characteristics.

While none of the above indicators alone provides conclusive evidence of homogeneity, measurements that may be affected by excessive boat motion can be identified. Once identified, these measurements can be further investigated to determine if motion of the ADCP has adversely impacted the measured velocity. The procedure is to first identify the time at which the potentially excessive motion takes place, then divide the velocity magnitude sample record into two records containing the ensembles believed to be in regions of differing flow characteristics. Hypothesis tests are then applied to the two records as described above. These tests can be applied to the means using the two sample *t*-test assuming equal variance or to the entire distributions using the Kolmogorov-Smirnov test. The Kolmogorov-Smirnov test is a non-parametric test that evaluates the null hypothesis that two samples have the same cumulative distribution function [*Gibbons and Chakraborti*, 2011]. The preliminary assessment of the lower Roanoke River data identified five measurements that required further investigation.

The procedure to determine if the ADCP moved into a region of different flow characteristics is demonstrated using S1xs6p3 from the mean annual flow. Figures 4 and 5 show the measured GPS locations and time series of boat velocity and flow depth, respectively. The range of boat motion for S1t6p3 was by far the largest seen in the dataset, with A_f=84.6 m^2 and D=0.29 m. The excessive movement was noted by the technicians on the boat; however, the measurement was not canceled because the motion took place relatively late in the sample record. The wide range

of ensemble locations seen in the east direction is the first indication that the boat motion may be significant. The boat velocity deviates substantially from the mean near 860 s which corresponds to a change in flow depth (see Fig. 5). Around 950 s the flow depth becomes relatively constant and the boat velocity decreases. Thus, it appears that the ADCP measured at one location up to 860 s; the boat then drifted about 10 m and settled at a second location at 950 s. To determine if the two regions have different flow characteristics, the velocity magnitude record in each bin was divided into two—one from 0 to 860 s, the other from 950 to 1254 s. Applying the Kolmogorov-Smirnov test, the hypothesis of equivalent distributions was rejected in five out of nine bins. While the original measurement contained 11 bins, the two bins closest to the bed did not contain data for the second location due to the decrease in flow depth. The hypothesis of equivalent means was rejected in six out of nine bins using the two sample *t*-test. Both tests were performed at the 0.05 level of significance. The results of the hypothesis tests indicate that the flow characteristics between the two regions are different for more than half the bins and, accordingly, ensembles after 860 s are removed from the record. After editing, the footprint area and mean ensemble separation distance decrease to 4.25 m^2 and 0.08 m, respectively. Applying this procedure to the five measurements identified using the preliminary indicators resulted in one other measurement being edited. Ensembles past 1160 s were removed from S1xs6p3 for the bankfull flow. The records for S1xs6p3 for both discharges were the only measurements with record lengths less than 1200 s. The velocity time series for the two edited records are demonstrated to be stationary in a subsequent section—indicating that the difference in velocity is due to changes in boat position and not nonstationarity of the flow velocity.

The values for the footprint area, A_f, and mean ensemble separation distance, D, given in Table 1 use the results of the edited records. The mean and maximum A_f for the mean annual flow (bankfull flow) are 2.8 m^2 (5.5 m^2) and 6.7 m^2 (23.0 m^2), respectively. The mean ensemble separation distance shows a similar trend with a mean value for the mean annual flow (bankfull flow) of 0.05 m (0.08 m). The eight largest values of A_f and the seven largest values for D occurred during the bankfull flow. For over 75% of the measurement locations, larger values of A_f and D were observed during the bankfull flow. The increase in boat motion is likely due to the rise in current velocity which made it more difficult to maintain the boat in a fixed location with anchors. The average of all depth-averaged velocities increased from 0.59 m s^{-1} for the mean annual to 0.85 m s^{-1} for the bankfull flow. The small number of measurements exhibiting the influence of boat motion (2 out of 67), however, suggests that the procedure employed to fix the boat in the channel was successful for the conditions encountered at the field site.

2.3.2 Small-scale Motion

Three measurements were obtained using both single- and multi-ping settings: S5xs1p2 for the bankfull flow and S5xs2p1 for both discharges. The single-ping measurements immediately followed the completion of the multi-ping measurement with all other instrument settings kept the same. The single-ping (multi-ping) setting resulted in an average time between ensembles of about 0.5 s (1.7 s). The measured flow depth, flow direction, and footprint area are similar between settings at each location. While the mean velocity magnitude for the two settings differs by less than 5% in each bin, the variance will not agree due to the averaging of subpings in the multi-ping ensembles. The appropriate hypothesis test to compare the two means is the two sample *t*-test with unequal variances. The hypothesis of equal means was rejected in only 2 out

of 8 bins for S5xs2p1 during the mean annual flow (0.05 level of significance). Given that the test failed to reject the hypothesis for the majority of bins (>95%), the mean velocities calculated from single- and multi-ping measurements are considered equivalent. These results indicate that individual multi-ping ensembles were not adversely impacted by motion of the ADCP.

2.4 Stationarity of Velocity Records

If a sample record of a random process such as a velocity time series in turbulent flow is stationary, its statistical properties are time invariant. Data can be further classified as weakly stationary, where the mean and autocorrelation do not vary with time, or strongly stationary, where all moments and joint moments do not vary. In practice, data are assumed to be strongly stationary once weak stationarity has been established [*Bendat and Piersol*, 1986]. It is important to establish the stationarity of a velocity time series in turbulent flow as the common data analysis techniques assume stationarity [*Tennekes and Lumley*, 1972].

The general procedure for assessing the stationarity of a time series given by *Bendat and Piersol* [1986] can be summarized in three steps: (1) the sample record is divided into consecutive N subsamples using equal time intervals, (2) the mean square value is calculated for each subsample, and (3) a statistical test is performed on the sequence of mean square values to determine if a trend is present. By testing a sequence of mean square values, stationarity of the first two moments is assessed, implying weak stationarity. Non-parametric tests are preferred because the sampling distribution is typically unknown. The run test and reverse arrangements test are two such tests appropriate for evaluating the stationarity of velocity data [*Bendat and*

Piersol, 1986]. Both test the null hypothesis that the sequence of data contains no underlying trends against the alternative hypothesis that a trend is present.

The run test compares the number of runs present in a sequence against the expected number of runs in a uniform random distribution, where a run is defined as a group of identical observations preceded and followed by a different observation or no observation. When applied to a sequence of mean square values the observation is whether each value is above or below the median of the sequence. A sequence containing too few runs indicates a tendency for like values to cluster while too many runs indicate a tendency for values to alternate. The run test has been used to evaluate stationarity in velocity records from a river measured with an ADCP [*Muste et al.*, 2004a] and tidal flow measured with an electromagnetic current meter [*Soulsby*, 1980]. The reverse arrangements test compares the number of reverse arrangements present in a sequence against the expected number for a uniform random distribution, where a reverse arrangement is defined as a count of the number of times an observation is larger than a subsequent observation. The total number of reverse arrangements in a sequence is the sum of the reverse arrangements for all observations. Too few reverse arrangements indicate an increasing trend in the data while too many indicate a decreasing trend. Comparing the two trend tests, the reverse arrangements test is better suited for capturing monotonic trends while the run test better identifies periodic trends. Further details on these tests can be found in *Bendat and Piersol* [1986], *Himelblau et al.* [1993], *Brandt* [2011], and *Gibbons and Chakraborti* [2011].

A factor that requires consideration before evaluating stationarity is the appropriate length for the time interval used to divide the sample record. Both *Soulsby* [1980] and *Muste et al.* [2004a] use

30 s for this interval. Given the wide range of flow conditions found in environmental flows, it is unlikely that a single interval length will be appropriate for all datasets. Guidance for selecting the appropriate value is found by examining the factors that influence the upper and lower bounds on the interval.

The upper bound results from the requirement that a sufficient sample size is needed to reach a statistically meaningful conclusion. *Brandt* [2011] states that a minimum sample size of 20 should be used for the run test as the test becomes weak for small sample sizes. *Himelblau et al.* [1993] provide guidance for selecting both the sample size and the level of significance for the reverse arrangements test. A minimum sample size of 20 is recommended; however, sample sizes as low as 10 can be used along with a level of significance of 0.10. For sample sizes between 20 and 40, a level of significance of 0.05 is recommended. The reverse arrangements test becomes very powerful with increasing sample size—sample sizes above 40 are not recommended as small time variations of questionable physical significance may be captured. To allow a comparison between the two trend tests, a minimum sample size of 20 is used here for both tests resulting in a maximum interval length of 60 s for the 1200 s sample records.

The lower bound on the interval length is derived from the requirement that the individual velocity measurements be independent. The interval length should be larger than the integral timescale—the length of time over which the velocity is dependent on itself [*Tennekes and Lumley*, 1972]. The integral timescale, τ, is defined as

$$\tau = \int_0^\infty R_{xx}(s)ds \qquad (1)$$

where $R_{xx}(s)$ is the autocorrelation coefficient for lag time, s. In turbulent flows, the autocorrelation coefficient theoretically decreases to zero resulting in a finite integral timescale. In practice, however, the autocorrelation coefficient typically decreases from its maximum value of one and oscillates about zero. To estimate the integral timescale from ADCP velocity data, the autocorrelation coefficient is calculated by numerical integration of the time series of velocity magnitude. The first zero crossing of the autocorrelation coefficient is considered the point where oscillation about zero begins and becomes the upper limit of integration. When interpreting the calculated integral timescale, it is important to note that the resolution of the integral timescale is limited by the size of the sample volume. The characteristic length of the sample volume is an effective diameter approximated as the horizontal distance between the centerlines of beams contained in the same vertical plane for each bin. Taylor's frozen turbulence hypothesis is used to convert this characteristic length scale to the minimum measureable integral timescale where the mean velocity magnitude for each bin serves as the characteristic velocity [*Soulsby*, 1980]. Calculated values of the integral timescale below the corresponding minimum value were not used in the analysis. The maximum calculated integral timescale that was above the minimum measurable value was found to be 26 s.

The integral timescale can also be estimated by dividing the flow depth, H, by the depth-averaged velocity, U. This approach uses Taylor's frozen turbulence hypothesis to convert from a length scale to a time scale. When this procedure is applied to measurements on the lower Roanoke River, the maximum estimated integral timescale is 23 s. The value for S1xs4p5 at the mean annual flow is excluded from this analysis—the low velocity at this location results in an

integral timescale more than twice the next largest estimate. While the maximum estimated value is close to that found by integrating the autocorrelation coefficient, it is noted that the two maximum values occurred at different locations. Nonetheless, estimating the integral timescale provides reasonable results with less effort for the analysis here.

A conservative minimum interval length to evaluate stationarity must be larger than the maximum integral timescale. An appropriate interval for the lower Roanoke River data is then between 26 and 60 s. To ensure the independence of all intervals, an averaging interval of 60 s is used here—more than twice the maximum integral timescale. Combining the interval length of 60 s with the minimum sample size of 20, results in a minimum sample record length of 1200 s to assess stationarity.

Stationarity for all bins in each profile is evaluated using the general procedure described above with both the run test and reverse arrangements test at the 0.05 level of significance. The ratio of nonstationary bins determined by each trend test to the total number of bins for each profile is reported in Table 1. Both trend tests determined that more than half of the total measurements contained no bins which were nonstationary. The majority of measurements, 59 out of 67 for both trend tests, had less than 10% of the bins in the profile found to be nonstationary. These findings are consistent with the flow conditions observed at the study sites (see Fig. 3).

The reverse arrangements test rejected the hypothesis of stationarity for 5.0% of the total bins (70 out of 1409) while the run test rejected the hypothesis for 3.9% of the total bins (55 out of 1409). Less than 1% of bins (9 out of 1409) were found to be nonstationary by both tests. Neither

test exhibited a significant change in the total number of nonstationary bins with discharge. While the highest percentage of bins in a single measurement determined to be nonstationary was found by the run test for S1xs3p5 during the mean annual flow (3 out of 6 bins), only the reverse arrangements test found five or more bins to be nonstationary in single measurements. The largest total number of nonstationary bins in a single measurement was found for S1xs3p2 during the bankfull flow (15 out of 35 bins). These results agree with the statement of *Bendat and Piersol* [1986] that the reverse arrangements test is the more sensitive test. Given that the tests are relatively simple to perform and require little processing time, it is recommended to evaluate stationarity using both tests. This procedure provides confidence in the stationarity of the flow when both determine a large majority of the bins to be stationary. Additionally, if measurements are obtained during unsteady flow, such as a flood wave, the time over which the velocity may be considered stationary can be determined by applying this procedure to progressively larger record lengths.

Large numbers of nonstationary bins in a measurement may provide information on the local hydrodynamics. For example, during the mean annual flow S1xs4p5 is located within a recirculation zone—regions well known for complex hydrodynamics [*e.g., Ferguson et al.*, 2003]. At this location, 9 out of 22 bins were found to be nonstationary. Of the nonstationary bins, 6 adjacent bins were located between relative flow depths of y/H=0.44 to 0.6. *Ferguson et al.* [2003] found that flow near the surface in a recirculation zone moved upstream while flow near the bed moved downstream. The mean velocity profile at S1xs4p5 exhibits similar behavior with the mean crossover point from upstream to downstream flow located near y/H=0.5. The majority of nonstationary bins are located in a region where the velocity is expected to fluctuate

in both magnitude and direction. The other two measurements with large numbers of nonstationary bins are S1xs3p2 (15 out of 35) and S5xs1p3 (9 out of 23), both for the bankfull flow. While neither measurement is located in an obvious region of flow complexity, both measurements contained large numbers of adjacent bins which were found to be nonstationary. For S5xs1p3, the top nine bins were nonstationary while for S1xs3p2, the top seven and bottom five were nonstationary. For all bins in both measurements, the hypothesis of stationarity was rejected based on too many reverse arrangements. This indicates a decelerating trend in the velocity at these locations. Further measurements in the vicinity are needed to better quantify the local flow field. In general, for almost all measurements with two or more nonstationary bins, nonstationarity was observed in adjacent bins.

2.5 Sample Record Length

Selecting the appropriate sample record length is an important step for field measurements of velocity. Typically the sample record length must be specified before detailed information on flow conditions at the site is available. While longer records will yield more accurate results, excessive time in the field may be required to achieve the desired spatial resolution. Additionally, long record lengths may prevent the collection of adequate measurements if the flow is unsteady. The minimum sample record length is one that is long enough to be representative of the current flow conditions and no longer. Studies have demonstrated that the minimum record length is also dependent on the statistical quantity of interest [*Soulsby*, 1980]. Detailed investigations of sample record length have been carried out for electromagnetic current meters and acoustic Doppler velocimeters [*Soulsby*, 1980; *Buffin-Bélanger and Roy*, 2005]; however, results from these studies are not directly applicable to the ADCP. The low sampling

frequency of the ADCP requires prohibitive record lengths to compute standard errors—even when using a bootstrap approach similar to *Buffin-Bélanger and Roy* [2005]. A common approach to assess the sample record length is to plot statistics such as the mean for progressively increasing record length, resulting in a running mean. If the statistic converges to a single value, the record length is judged to be sufficient [*Sukhodolov and Rhoads*, 2001]. This approach has been applied to ADCP measurements of flow velocity by *Muste et al.* [2004a] and *Stone and Hotchkiss* [2007] as well as measurements of bed velocity by *Rennie et al.* [2002]. For the Mississippi River (Q=1550 m^3 s^{-1}), *Muste et al.* [2004a] report that the mean and standard deviation become approximately stable after 11 minutes, while *Stone and Hotchkiss* [2007] found that a five minute record produced almost identical results to a 20 minute record in shallow streams (H=0.75–1.1 m). The advantages of the running procedure are that it can be applied to a variety of statistics and it maintains the autocorrelation characteristics of the velocity record. For the results to be meaningful, the original record must be long enough to characterize the flow.

The running mean and standard deviation were computed for all bins in each measurement. The running statistics are compared to the values for the entire sample record, termed the long-term record with length T_∞, mean velocity U_∞, and standard deviation σ_∞. A statistic is considered converged once it remains within 10% of the long-term record value. When applied to a single measurement, this procedure results in profiles of minimum record lengths for the mean and standard deviation. The minimum sample record length for the mean, T_μ, and the standard deviation, T_σ, for each measurement is the maximum value for the appropriate statistic in the profile. Figure 6 demonstrates this procedure for S1xs5p5 during the mean annual flow—the

location of the maximum T_μ. The minimum record lengths for all measurements are provided in Table 1. The average, minimum, and maximum values of T_μ at the mean annual flow (bankfull flow) are 70.2 s (54.4 s), 2.5 s (5.0 s), and 352 s (217 s), respectively. The average, minimum, and maximum values of T_σ at the mean annual flow (bankfull flow) are 382 s (523 s), 111 s (243 s), and 744 s (871 s), respectively. Both the running mean and standard deviation remained within 10% of the long time values for more than 5 minutes at each measurement. These statistics do not include the results from S1xs4p5 for the mean annual flow. As discussed previously, this measurement is located in a recirculation region which results in complex flow not found at other locations. Comparing T_μ and T_σ reveals that the standard deviation requires a longer record to converge at all but two measurements. While no clear trends in the vertical or horizontal distribution of minimum sample record length are seen, some general comments can be made. No consistent location of T_μ and T_σ was seen in the profiles, although the largest record lengths for the mean were mostly found in the bottom half of the profile. The largest values of T_μ and T_σ at each cross-section were often found at measurement locations nearest one of the banks, likely due to increased flow complexity. Comparing the two study sites, the average value of T_μ for both discharges is smaller at Site 5 than Site 1 while the average values of T_σ are larger at Site 5. When considering both sites together, no consistent trend was found when comparing the minimum record lengths for the two discharges, suggesting that discharge is not a good indicator for sample record length. The variability in the minimum sample record length suggests that a single long record may not be sufficient to determine an appropriate record length for other locations at a site. While it may not be possible to specify the minimum record length a priori, examining the behavior of the running mean and standard deviation provides confidence that the selected record length is sufficient.

2.6 Mean Velocity Profiles

Once a measurement has been confirmed as homogeneous, stationary, and of sufficient record length, mean velocity components can be obtained by averaging all ensembles within each bin. To aid in the interpretation of mean velocity data, the horizontal components are often rotated from a Cartesian coordinate system defined by east, E, and north, N, axes, to a "channel-fitted" curvilinear coordinate system defined by streamwise, s, and normal, n, axes, referred to as the stream coordinate system. Rotation of velocity components is a pure rotation in the horizontal plane where the E and N axes are rotated clockwise by an angle equal to the direction of primary flow, α, measured from the N axis. While a number of approaches have been proposed to define the primary flow, or streamwise, direction [see *Hey and Rainbird*, 1996; *Lane et al.*, 2000], FV measurements are limited to the approach of *Rozovskii* [1957; see also *Bathurst et al.*, 1977]. In this approach the direction of primary flow along a vertical profile is defined as the direction which results in zero net secondary discharge across the vertical, or equivalently, the direction of the depth-averaged velocity vector. The Rozovskii definition has been widely applied to ADCP data [e.g., *Barua and Rahman*, 1998; *Rennie et al.*, 2002; *Rennie and Church*, 2010; *Parsons et al.*, 2007; *Szupiany et al.*, 2007, 2009]. This definition produces a flow direction that is local to the individual vertical. Thus, flow direction will not necessarily remain constant along a cross-section. This is an important consideration when interpreting secondary circulation [see *Dietrich and Smith*, 1983; *Lane et al.*, 2000].

The streamwise flow direction, α, the streamwise depth-averaged velocity, U, and flow depth, H, for all measurements are provided in Table 1. The flow direction generally follows the channel

boundary as expected for within bank flows with one exception. At S1xs4p5 during the mean annual flow the primary flow direction is moving upstream with a small magnitude (U=0.066 m s^{-1}). This result suggests that this location is within a region of flow separation and recirculation. Separation zones at the inner bank of a meander bend have been observed in both the laboratory [*Leopold et al.*, 1960] and natural rivers [*Ferguson et al.*, 2003]. The separation zone was not captured during the bankfull flow although a significant decrease in velocity is seen at S1xs4p5. Separation may have occurred but would likely have moved further inward where ADCP measurements could not be obtained. For the mean annual flow (bankfull flow), U ranges from 0.066 (0.47) to 0.75 m s^{-1} (1.06 m s^{-1}). The mean ratios of U and H for the bankfull flow to the mean annual flow at each location are 1.7 and 1.6, respectively. At most cross-sections, the maximum measured U-value occurs within the outer half of the channel. For both discharges, U decreases in the vicinity of the bend apex at Site 1 to accommodate the increase in flow depth.

The logarithmic law of the wall, or log law, can be used to estimate the boundary shear stress, τ_o, and characteristic roughness, k_s from mean streamwise velocity profiles. For flows over fully rough boundaries, the log law can be written

$$\frac{u_s}{u_\tau} = \frac{1}{\kappa}\ln\left(\frac{z}{k_s}\right) + 8.5 \qquad (2)$$

where u_s = streamwise velocity, u_τ = shear velocity = $(\tau_o/\rho)^{0.5}$, ρ = fluid density, κ = von Kármán constant = 0.41, and z = elevation above the bed. This relation is strictly valid for two-dimensional flows over flat boundaries; however, it is commonly applied to velocity profiles in natural rivers. For flow over a flat boundary, k_s is the Nikuradse equivalent sand grain roughness while for a river flow, k_s is a composite of grain and form roughness. Given that the log law is derived for two-dimensional flows, the Rozovskii definition is the proper approach to determine

the streamwise velocity as the spanwise component is minimized. The log law is valid for approximately the lower 20% of the depth, though it is common to assume it valid for the entire flow depth. The location of the bin nearest the riverbed depends on both the flow depth and the bin size. For the lower Roanoke River, 13 out of 33 (28 out of 34) measurements contained at least one bin within the lower 20% of the flow depth during the mean annual flow (bankfull flow).

To demonstrate the use of the log law with streamwise velocity profiles from FV measurements, a least squares regression is used to fit measured data to equation (2). This general procedure for determining the log law parameters, u_τ and k_s, is commonly used with ADCP data [*Rennie et al.*, 2002; *Rennie and Church*, 2010; *Sime et al.*, 2007; *Stone and Hotchkiss*, 2007]. To determine the bins that will be used in the regression procedure, the measured streamwise velocity is plotted against the logarithm of elevation for all bins. Consecutive bins nearest the bed which appear to follow a linear trend are selected. A minimum of three bins is used for all measurements. While the selection of the appropriate bins is somewhat subjective, this approach acknowledges the limitations of the log law. A similar procedure has been applied to laboratory flume data by *Coleman* [1981]. Additionally, a visual inspection found that the majority of velocity profiles are not linear for the entire flow depth.

The primary results of the regression procedure—the log law parameters and the coefficient of determination, R^2—are given in Table 1. To determine if the assumption of the log law is valid for a velocity profile, the following set of criteria is applied. First, all measurements with a value of R^2 below 0.90 are regarded as not following the log law. While a high R^2-value does not

necessarily mean that the log law is valid, a low R^2-value indicates that the relationship is not linear and, accordingly, the data do not follow the log law. A total of nine measurements have R^2 below 0.90. These measurements were taken at locations closest to the banks near the bend apex at Site 1 (S1xs3, S1xs4, and S1xs5). Next, measurements producing a negative shear velocity are eliminated from consideration. This nonphysical result occurs in profiles where the velocity increases as the bed is approached and is seen in five measurements, all located at S1xs4 and S1xs5. Finally, following *Rennie and Church* [2010], measurements producing k_s less than 1 mm or greater than 5 m are not considered. Twelve measurements, ten of which were taken during the mean annual flow, produce values lower than the lower limit while four measurements, three of which were taken during the mean annual flow, produce values above the upper limit. After removing measurements from consideration, 17 out of the original 33 (26 out of 34) measurements were found to be adequately described by the log law for the mean annual flow (bankfull flow) based on the criteria introduced above. In general, the log law was found to be not valid at locations of lower flow depth and/or locations with highly three-dimensional flow. This is highlighted by the large number of measurements found to not follow the log law during the mean annual flow and the fact that for the bankfull flow, all measurements found to not follow the log law were at S1xs4 and S1xs5. For both discharges, the largest spanwise velocities occurred at S1xs4 and S1xs5.

Examples of mean streamwise and spanwise velocity profiles from S1xs1 during the bankfull flow are shown in Figure 7. The logarithmic equation determined by regression is shown along with the streamwise measured velocities. Each fit used the bottom four bins in the profile. This cross section is near the entrance to the meander bend, and the streamwise profiles appear

logarithmic for much of the flow depth. At S1xs1p1 the larger magnitude of the spanwise velocity near the water surface induces a velocity dip, causing the profile to deviate significantly from logarithmic. Most of the mean spanwise velocities are less than 5% of the depth-averaged streamwise velocity, supporting the assumption of two-dimensional flow required by the log law. The largest values of both u_τ and k_s are found near the middle of the channel at S1xs1p2. The k_s-value at S1xs1p2 is two orders of magnitude larger than the value at S1xs1p3 with similar ranges seen at other cross-sections. Without information regarding the grain size distribution of the bed or the presence of bed forms during the measurement, it is difficult to evaluate the reliability of these values. Given that the lower Roanoke River has a sand bed, larger k_s-values suggest the presence of bed forms. The spanwise velocity profile at S1xs1p2 suggests a circulation pattern with flow near the surface towards the outer bank, a well-recognized feature of flow through meander bends. While at S1xs1p1, a cell rotating counter to this cell is implied near the water surface. A similar feature has been documented near the apex of meander bends in natural rivers [*Sukhodolov*, 2012]. At this location, further measurements are required to resolve the spatial distribution of spanwise velocity. It is important to note that the spanwise velocities shown in Figure 7 do not occur in the same vertically-oriented plane as a result of the Rozovskii definition. At this cross-section, though, the maximum difference between flow directions is 2.3°. This difference is close to the reported ADCP compass accuracy of 2 degrees [*RD Instruments*, 2007].

2.7 Discussion

The standard approach for evaluating the stationarity of a time series is adapted here to ADCP velocity measurements. Given the importance of this assumption for many data analysis procedures, verification of stationarity should be performed for each location and flow

condition—especially for field sites lacking gaging stations or where an assumption of stationarity is suspect. Based on the lower Roanoke River data, identifying the most appropriate location to evaluate stationarity is difficult without prior knowledge of site characteristics as local geometry and flow features appear to influence stationarity. A conservative approach is to select a sample record length that allows an evaluation of stationarity for all FV measurements.

The sample record length required to assess stationarity is controlled by the integral timescale of the measured flow and the minimum sample size requirement for the statistical trend test. Knowledge of the integral timescale is necessary to determine the minimum length for the averaging interval over which mean square values are calculated. Few studies have reported values for the integral timescale in natural rivers. *McQuivey* [1973] reports integral timescales ranging from 2.45 s to 11.50 s for the Missouri and Mississippi Rivers from hot-film measurements while *Roy et al.* [2004] use electromagnetic current meters and report integral timescales on the order of 1 s in a shallow stream (H=0.46-0.59 m). When using ADCP data, resolution of the integral timescale is limited by the sample volume. The minimum resolvable integral timescale is estimated using Taylor's frozen turbulence hypothesis. Using only values above this minimum, the integral timescales calculated from the lower Roanoke River data range from 3.0 s to 26.2 s with over 90% of the results below 15 s. Reasonable agreement was generally seen between the calculated integral timescale and that estimated using Taylor's frozen turbulence hypothesis. The estimated integral timescales ranged from 4.5 s to 23.2 s, disregarding the result at S1xs4p5during the mean annual flow. Considering the available data, a maximum integral timescale of 30 s appears conservative. Accordingly, a minimum averaging interval of 30 s should be used to divide the sample record for evaluating stationarity.

Calculating the integral timescale using the autocorrelation coefficient or Taylor's frozen turbulence hypothesis is recommended to identify an appropriate site-specific interval. An averaging interval of 30 s results in a minimum sample record length of 600 s. This minimum sample record length is larger than T_μ for 66 out of 67 measurements and larger than T_σ for 46 out of 67 measurements. Thus, the record length required to assess stationarity may be longer than that required for flow statistics to stabilize.

The results of both tests for stationarity support the observations presented in Figure 3 by finding the majority of velocity time series to be stationary. For the bins found to be nonstationary, two explanations exist: (1) the result of the trend test rejects the hypothesis of stationarity when in fact the record is stationary (*Type I Error*) and (2) the record length is insufficient to characterize flow at this location. The probability of a *Type I Error* is equal to the level of significance used for the hypothesis test. For both trend tests, the hypothesis of stationarity was rejected for a percentage of bins less than or equal to the level of significance. In other words, the expected number or less of *Type I Errors* was observed for the dataset. Despite this result, the possibility of an insufficient record length exists, particularly as the value of T_μ or T_σ approaches T_∞ (see S1xs4p5 during the mean annual flow). Thus, locations where highly three-dimensional velocity may occur, such as a recirculation zone, are not recommended for evaluating the stationarity of a study reach.

The relatively low sampling frequency of the ADCP has prevented a detailed study of the effect of record length on standard errors similar to those carried out for other instruments [*e.g.*, *Soulsby*, 1980; *Buffin-Bélanger and Roy*, 2005]. To address this deficiency, running statistics

have been applied to different quantities to evaluate the adequacy of a record length. Table 2 summarizes the record lengths used for FV ADCP measurements. Considering the range of rivers and discharges seen in Table 2 it is unlikely that a single minimum record length applies to all rivers and parameters of interest. Rather, the record length is controlled by the flow characteristics, parameter of interest, and accuracy requirements. The level of accuracy for running statistics is typically based on a comparison with the statistic for the entire sample record (see Fig. 6). This highlights the primary weakness of the running approach—by definition the running statistic must converge to the long-term value. Accordingly, running statistics that converge close to the end of a record suggest that the sample record is not long enough to characterize the statistic of interest. Further work is needed to quantify an acceptable length of time for a running statistic to remain converged. It is likely that the minimum time of 5 min observed here is conservative. In all but the study of *Holmes and Garcia* [2008], a similar evaluation of running statistics leads to the recommended record lengths beyond which the statistics are considered stable given in Table 2.

The strong influence of the parameter of interest is highlighted by comparing the studies of *Rennie et al.* [2002] and *Guerrero and Lamberti* [2011]. The well-documented variability in bed load transport rates results in a minimum record length of 25 min. Conversely, the depth-averaged velocity can be accurately represented with only a few ensembles. This point is further demonstrated by examining the running mean for the depth-averaged velocity in Figure 6. The location shown corresponds to the highest T_μ; however, the depth-averaged velocity remains close to the long-term value from the first ensemble. For studies investigating mean velocity profiles, the recommended record lengths range from 5 to 15 min for a wide range of flow

conditions. The more stringent requirement of *Barua and Rahman* [1998] arises from the use of a running turbulence intensity to determine the record length. Both *Stone and Hotchkiss* [2007] and *Szupiany et al.* [2007] rely on a running mean while *Muste et al.* [2004a] use a running mean and standard deviation. Similar results were observed on the lower Roanoke River with the running standard deviation requiring longer record lengths (<15 min) than the running mean (<6 min). Considering the present results and those in Table 2, a record length of 20 min seems to be appropriate for mean velocity profiles covering a wide range of flow conditions—allowing for the first two statistical moments to stabilize and evaluation of stationarity for the measured velocity.

Once the reliability of the measured velocity is established, mean profiles can be used to investigate the site hydrodynamics. For studies of sediment transport, quantifying the boundary shear stress and characteristic roughness is often performed by fitting measured velocity profiles to the log law. While the ADCP does provide velocity profiles throughout much of the water column, its inability to measure near-bed velocity is a significant disadvantage when applying the log law. The approach presented here is consistent with the derivation of the log law by using measured velocities nearest the bed. Additionally, the appropriateness of the fit is evaluated using a set of criteria. In general, two reasons explain why measured velocity profiles do not follow the log law: (1) insufficient or no measurements were captured in the logarithmic region and (2) the log law is not valid for the local flow conditions. Examples of both are seen in the lower Roanoke River data. The lack of near-bed measurements becomes more problematic for lower flow depths as seen in the larger number of measurements found to not follow the log law during the mean annual flow. The majority of the velocity profiles at the two cross-sections near

the apex of the bend, S1xs4 and S1xs5, were found to not follow the log law. The fact that several profiles at these locations produced high R^2-values demonstrates that a good regression fit does not guarantee the validity of the log law. The present data suggest that application of the log law to velocity profiles in natural rivers for regions of highly three-dimensional flow results in inaccurate and, often, nonphysical estimates of the log law parameters, u_τ and k_s. A more complete assessment of the ability of the log law to quantify boundary shear stress awaits the development of techniques to directly measure boundary shear stress over complex, rough boundaries. In spite of these limitations, ADCP data can help to build and validate CFD models which may be able to provide a more accurate representation of the boundary shear stress distribution [see *Shen and Diplas*, 2008, 2010].

2.8 Conclusions

Procedures have been presented to evaluate FV ADCP measurements for the influence of boat motion, stationarity, and adequate sample record length. An extensive dataset comprised of 67 FV measurements taken during two discharges is used to demonstrate each procedure. The analysis of ADCP motion indicates that the anchoring procedure employed on the lower Roanoke River prevents excessive motion. Assessing stationarity was aided by steady flows due to flow regulation and unique watershed characteristics. The results agree with measured hydrographs and predict overwhelmingly that velocity time series are stationary. Additionally, a region of highly three-dimensional flow was identified, and later confirmed analyzing velocity profiles, using locations of nonstationary bins. Running statistics cannot predict an appropriate record length a priori; however, they do provide a means to determine if records of sufficient length were obtained. The sample record length of 20 min used on the lower Roanoke River is

satisfactory for the site conditions encountered. It is important to recognize that record length requirements to assess stationarity may be longer than those required for flow statistics to stabilize.

Upon confirmation of negligible ADCP motion, stationarity, and adequate record length, mean velocity profiles can be used to investigate the site hydrodynamics. On the lower Roanoke River, secondary circulation and flow separation at the inner bank were both observed in mean velocity profiles rotated to a stream-based coordinate system. A consistent procedure is used to apply the log law to mean velocity profiles. The procedure is limited to profiles which contain data within the logarithmic region and to regions where the assumptions of the log law are valid.

Mean velocity profiles from FV ADCP surveys provide boundary conditions, as well as calibration and validation data, to build numerical models [*e.g.*, *Rüther et al.*, 2010; *Shen and Diplas*, 2010]. The analysis procedures presented here help support the growing role of CFD in fluvial studies. Recent work has also focused on describing the spatial distribution of flow and related parameters with MV ADCP surveys [*e.g.*, *Dinehart and Burau*, 2005; *Rennie and Church*, 2010; *Jamieson et al.*, 2011]. FV measurements complement these studies by providing time-averaged velocity profiles that can be used to determine the accuracy of the MV measurements as well as investigate the temporal development of flow features. Thus, viewing FV and MV survey procedures as complementary may lead to the development of improved methods to quantify the hydrodynamics in natural rivers.

Notation

A_f footprint area (m^2)

D mean ensemble separation distance (m)

H flow depth (m)

k_s characteristic bed roughness (m)

Q discharge ($m^3\ s^{-1}$)

R^2 coefficient of determination

T_μ minimum sample record length for the mean (s)

T_σ minimum sample record length for the standard deviation (s)

T_∞ long-term record length (s)

u_n spanwise velocity ($m\ s^{-1}$)

u_s streamwise velocity ($m\ s^{-1}$)

u_τ shear velocity ($m\ s^{-1}$)

U depth-averaged streamwise velocity ($m\ s^{-1}$)

U_∞ mean velocity of the long-term record ($m\ s^{-1}$)

y depth below water surface (m)

z elevation above channel bed (m)

α streamwise flow direction (°)

κ von Kármán constant

ρ fluid density ($kg\ m^{-3}$)

R_{xx} autocorrelation coefficient

σ_∞ standard deviation of the long-term record ($m\ s^{-1}$)

τ integral timescale (s)

τ_o boundary shear stress (N m^{-2})

Acknowledgements

The authors acknowledge the financial support of Dominion, the U.S. Army Corps of Engineers, the Hydro Research Foundation, and the Edna Bailey Sussman Foundation. Ozan Celik and Nikos Apsilidis assisted with the field measurements. Bob Graham graciously provided a boat when engine trouble threatened to cut our field campaign short. The authors thank three anonymous reviewers and the associate editor for criticism that improved the presentation of this work.

References

Barua, D. K., and K. H. Rahman (1998), Some aspects of turbulent flow structure in large alluvial rivers, *J. Hydraul. Res.*, *36*(2), 235-252.

Bathurst, J. C., C. R. Thorne, and R. D. Hey (1977), Direct measurements of secondary currents in river bends, *Nature*, *269*(5628), 504-506.

Bendat, J. S., and A. G. Piersol (1986), *Random data: analysis and measurement procedures*, 2nd ed., 566 pp., John Wiley, New York.

Brandt, A. (2011), *Noise and vibration analysis: signal analysis and experimental procedures*, 438 pp., John Wiley, Chichester.

Buffin-Bélanger, T., and A. G. Roy (2005), 1 min in the life of a river: selecting the optimal record length for the measurement of turbulence in fluvial boundary layers, *Geomorphology*, *68*, 77-94. doi:10.1016/j.geomorph.2004.09.032.

Coleman, N. L. (1981), Velocity profiles with suspended sediment, *J. Hydraul. Res.*, *19*(3), 211-

229.

Dietrich, W. E., and J. D. Smith (1983), Influence of the point-bar on flow through curved channels, *Water Resour. Res.*, *19*(5), 1173-1192.

Dinehart, R. L., and J. R. Burau (2005), Averaged indicators of secondary flow in repeated acoustic Doppler current profiler crossings of bends, *Water Resour. Res.*, *41*(9), W09405, doi:10.1029/2005WR004050.

Ferguson, R. I., D. R. Parsons, S. N. Lane, and R. J. Hardy (2003), Flow in meander bends with recirculation at the inner bank, *Water Resour. Res.*, *39*(11), 1322, doi:10.1029/2003WR001965.

Gibbons, J. D., and S. Chakraborti, (2011), *Nonparametric statistical inference*, 5th ed., 630 pp., CRC Press, Boca Raton.

Gordon, R. L. (1989), Acoustic Measurement of River Discharge, *J. Hydraul. Eng.*, *115*(7), 925-936.

Guerrero, M., and A. Lamberti (2011), Flow Field and Morphology Mapping Using ADCP and Multibeam Techniques: Survey in the Po River, *J. Hydraul. Eng.*, *137*(12), 1576-1587. doi:10.1061/ (ASCE)HY.1943-7 900.000046 4

Gunawan, B., M. Sterling, and D. W. Knight (2010), Using an acoustic Doppler current profiler in a small river, *Water Environ. J.*, *24*(2), 147-158. doi:10.1111/j.1747-6593.2009.00170.x.

Hey, R. D., and P. C. B. Rainbird (1996), Three-dimensional flow in straight and curved reaches, in *Advances in Fluvial Dynamics and Stratigraphy*, edited by P. A. Carling and M. R. Dawson, pp. 33-66, John Wiley, Chichester, UK.

Himelblau, H., A. G. Piersol, J. H. Wise, and M. R. Grundvig, (1993), *Handbook for dynamic*

data acquisition and analysis, 307 pp., Institute of Environmental Sciences, Mount Prospect, Illinois.

Holmes, R. R., and M. H. Garcia (2008), Flow over bedforms in a large sand-bed river: A field investigation, *J. Hydraul. Res.*, *46*(3), 322-333, doi:10.3826/jhr.2008.3040.

Hupp, C. R., E. R. Schenk, J. M. Richter, R. K. Peet, and P. A. Townsend (2009), Bank erosion along the dam-regulated lower Roanoke River, North Carolina, in *Management and Restoration of Fluvial Systems with Broad Historical Changes and Human Impacts*, edited by L. A. James, et al., pp. 97-108. doi:10.1130/2009.2451(06).

Jamieson, E. C., C. D. Rennie, R. B. Jacobson, and R. D. Townsend (2011), 3-D flow and scour near a submerged wing dike: ADCP measurements on the Missouri River, *Water Resour. Res.*, *47*(7), W07544, doi:10.1029/2010WR010043.

Lane, S. N., K. F. Bradbrook, K. S. Richards, P. M. Biron, and A. G. Roy (2000), Secondary circulation cells in river channel confluences: measurement artefacts or coherent flow structures?, *Hydrol. Processes*, *14*(11-12), 2047-2071.

Leopold, L. B., R. A. Bagnold, M. G. Wolman, and J. L. M. Brush (1960), Flow resistance in sinuous or irregular channels, *Geological Survey Professional Paper 282-D*, U. S. Geol. Surv., Washington, D.C.

McQuivey, R. S. (1973), Summary of turbulence data from rivers, conveyance channels, and laboratory flumes; turbulence in water, 66 pp., *U.S. Geol. Surv. Professional Paper 802-B*, Washington, DC.

Mueller, D. S., and C. R. Wagner (2009), Measuring discharge with acoustic Doppler current profilers from a moving boat, *U.S. Geological Survey Techniques and Methods 3A-22*, 72 pp., U.S. Geol. Surv., Reston, VA.

Muste, M., K. Yu, T. Pratt, and D. Abraham (2004a), Practical aspects of ADCP data use for quantification of mean river flow characteristics; Part II: fixed-vessel measurements, *Flow Meas. Instrum.*, *15*(1), 17-28, doi:10.1016/j.flowmeasinst.2003.09.002.

Muste, M., K. Yu, and M. Spasojevic (2004b), Practical aspects of ADCP data use for quantification of mean river flow characteristics; Part 1: moving-vessel measurements, *Flow Meas. Instrum.*, *15*(1), 1-16, doi:10.1016/j.flowmeasinst.2003.09.001.

Nystrom, E. A., C. R. Rehmann, and K. A. Oberg (2007), Evaluation of mean velocity and turbulence measurements with ADCPs, *J. Hydraul. Eng.*, *133*(12), 1310-1318, doi:10.1061/(ASCE)0733-9429(2007)133:12(1310).

Parsons, D. R., J. L. Best, S. N. Lane, O. Orfeo, R. J. Hardy, and R. Kostaschuk (2007), Form roughness and the absence of secondary flow in a large confluence-diffluence, Rio Parana, Argentina, *Earth Surf. Processes Landforms*, *32*(1), 155-162.

Petrie, J., P. Diplas, S. Nam, and M. S. Gutierrez (2010), Local boundary shear stress estimates from velocity profiles measured with an ADCP, paper presented at River Flow 2010, Int. Assoc. Hydraul. Eng. and Res., Braunschweig, Germany.

Raupach, M. R., R. A. Antonia, and S. Rajagopalan (1991), Rough-wall turbulent boundary layers, *Appl. Mech. Rev.*, *44*(1), 1-25.

RD Instruments (2007), *Work Horse Rio Grande Acoustic Doppler Current Profiler Technical Manual*, San Diego, Calif.

Rennie, C. D., and M. Church (2010), Mapping spatial distributions and uncertainty of water and sediment flux in a large gravel bed river reach using an acoustic Doppler current profiler, *J. Geophys. Res.*, *115*(F3), F03035, doi:10.1029/2009JF001556.

Rennie, C. D., and R. G. Millar (2004), Measurement of the spatial distribution of fluvial bedload transport velocity in both sand and gravel, *Earth Surf. Processes Landforms*, *29*(10), 1173-1193, doi:10.1002/esp.1074.

Rennie, C. D., R. G. Millar, and M. A. Church (2002), Measurement of bed load velocity using an acoustic Doppler current profiler, *J. Hydraul. Eng.*, *128*(5), 473-483.

Roy, A. G., T. Buffin- Bélanger, H. Lamarre, and A. D. Kirkbride (2004), Size, shape and dynamics of large-scale turbulent flow structures in a gravel-bed river, *J. Fluid Mech.*, *500*, 1-27.

Rozovskii, I. L., *Flow of Water in Bends of Open Channels* (in Russian), Acad. of Sci. of the Ukrainian SSR, Kiev, 1957. (English translation, Isr. Program for Sci. Transl., Jerusalem, 1961.)

Rüther, N., J. Jacobsen, N. R. B. Olsen, and G. Vatne (2010), Prediction of the three-dimensional flow field and bed shear stresses in a regulated river in mid-Norway, *Hydrol. Res.*, *41*(2), 145-152, doi:10.2166/nh.2010.064.

Shen, Y., and P. Diplas (2008), Application of two- and three-dimensional computational fluid dynamics models to complex ecological stream flows, *J. Hydrol.*, *348*(1-2), 195-214, doi:10.1016/j.jhydrol.2007.09.060.

Shen, Y., and P. Diplas (2010), Modeling unsteady flow characteristics of hydropeaking operations and their implications on fish habitat, *J. Hydraul. Eng.*, *136*(12), 1053-1066, doi:10.1061/(ASCE)HY.1943-7900.0000112.

Shields, F. D., and J. R. Rigby (2005), River habitat quality from river velocities measured using acoustic Doppler current profiler, *Environ. Manage.*, *36*(4), 565-575, doi: 10.1007/s00267-004-0292-6.

Sime, L. C., R. I. Ferguson, and M. Church (2007), Estimating shear stress from moving boat acoustic Doppler velocity measurements in a large gravel bed river, *Water Resour. Res.*, *43*(3), W03418, doi:10.1029/2006WR005069.

Simpson, M. R. (2001), Discharge measurements using a broad-band acoustic Doppler current profiler, *Open File Report 01-1*,123 pp., U. S. Geol. Surv., Sacramento, CA.

Soulsby, R. L. (1980), Selecting record length and digitization rate for near-bed turbulence measurements, *J. Phys. Oceanogr.*, *10*(2), 208-219.

Stacey, M. T., S. G. Monismith, and J. R. Burau (1999), Measurements of Reynolds stress profiles in unstratified tidal flow, *J. Geophys. Res.*, *104*(C5), 10933-10949.

Stone, M. C., and R. H. Hotchkiss (2007), Evaluating velocity measurement techniques in shallow streams, *J. Hydraul .Res.*, *45*(6), 752-762.

Sukhodolov, A. N. (2012), Structure of turbulent flow in a meander bend of a lowland river, *Water Resour. Res.*, *48*(1), W01516, doi:10.1029/2011WR010765.

Sukhodolov, A. N., and B. L. Rhoads (2001), Field investigation of three-dimensional flow structure at stream confluences 2. Turbulence, *Water Resour. Res.*, *37*(9), 2411-2424.

Szupiany, R. N., M. L. Amsler, J. L. Best, and D. R. Parsons (2007), Comparison of fixed- and moving-vessel flow measurements with an aDp in a large river, *J. Hydraul. Eng.*, *133*(12), 1299-1309, doi:10.1061/(ASCE)0733-9429(2007)133:12(1299)

Szupiany, R. N., M. L. Amsler, D. R. Parsons, and J. L. Best (2009), Morphology, flow structure, and suspended bed sediment transport at two large braid-bar confluences, *Water Resour. Res.*, *45*, W05415, doi:10.1029/2008WR007428.

Tennekes, H., and J. L. Lumley (1972), *A first course in turbulence*, 300pp., MIT Press, Cambridge, Mass.

Yorke, T. H., and K. A. Oberg (2002), Measuring river velocity and discharge with acoustic Doppler profilers, *Flow Meas. Instrum.*, *13*(5-6), 191-195.

Table 1. Summary of fixed-vessel velocity profiles

		mean annual flow												bankfull flow										
Site 1		U	H	α	A_f	D	RT[a]	RA[b]	T_μ	T_σ	u_τ	k_s	R^2	U	H	α	A_f	D	RT[a]	RA[b]	T_μ	T_σ	u_τ	k_s	R^2
xs1	p1	0.52	5.1	92.5	3.1	0.07	0 /15	1 /15	187	613	0.132	11.43	0.99	0.86	7.7	92.9	1.4	0.04	0 /25	1 /25	20	553	0.050	0.06	1.00
	p2	0.65	4.7	95.7	1.4	0.04	0 /13	0 /13	11	265	0.086	3.03	1.00	0.99	7.3	94.0	2.4	0.05	2 /23	1 /23	74	530	0.080	0.66	1.00
	p3	0.63	4.6	91.8	1.1	0.04	0 /12	0 /12	44	444	0.037	0.08	0.99	0.92	7.3	95.2	4.0	0.07	0 /23	0 /23	127	309	0.067	0.39	1.00
xs2	p1	0.71	6.4	131.2	0.8	0.03	1 /17	0 /17	15	283	0.034	0.02	0.99	0.90	9.5	132.5	18.9	0.15	4 /30	2 /30	12	302	0.050	0.08	0.98
	p2	0.67	5.7	134.1	2.3	0.05	0 /17	0 /17	19	260	0.017	<1E-3	0.99	1.01	9.0	130.5	6.7	0.09	1 /29	0 /29	38	278	0.061	0.10	1.00
	p3	0.68	4.9	132.3	1.2	0.04	3 /14	0 /14	20	281	0.020	<1E-3	1.00	0.96	8.3	133.0	2.4	0.05	2 /27	0 /27	28	623	0.058	0.12	1.00
	p4	0.70	3.5	125.7	0.7	0.03	0 /9	0 /9	3	143	0.032	0.01	0.99	0.99	6.7	129.7	8.2	0.10	2 /20	0 /20	28	351	0.075	0.39	1.00
xs3	p1	0.47	5.7	173.8	3.2	0.06	0 /13	0 /13	75	269	0.008	<1E-3	0.74	0.73	9.9	167.5	4.0	0.08	1 /25	0 /25	99	312	0.091	4.29	0.94
	p2	0.64	8.3	166.7	1.4	0.04	0 /24	0 /24	31	293	0.063	1.94	0.99	0.99	11.4	170.6	6.4	0.10	0 /35	15 /35	25	871	0.109	2.37	1.00
	p3	0.68	5.8	166.0	1.1	0.04	2 /16	4 /16	3	388	0.029	0.005	0.98	1.00	9.2	168.3	23.0	0.18	1 /29	2 /29	19	286	0.049	0.02	1.00
	p4	0.56	4.6	167.1	0.6	0.03	0 /13	1 /13	21	240	0.026	0.01	0.99	0.88	7.6	167.1	0.9	0.04	0 /23	0 /23	21	351	0.080	1.16	1.00
	p5	0.21	2.2	162.2	6.2	0.08	3 /6	0 /6	278	111	0.002	<1E-3	0.82	0.69	5.2	161.2	0.4	0.02	0 /15	0 /15	21	463	0.035	0.01	0.98
xs4	p1	0.57	6.2	227.8	2.8	0.05	2 /12	0 /12	294	153	0.194	44.11	0.65	0.91	5.8	198.1	2.5	0.06	0 /13	0 /13	11	819	0.143	6.26	0.99
	p2	0.70	11.0	232.4	6.7	0.09	2 /30	3 /30	14	431	<0	>100	1.00	0.98	12.2	206.0	3.9	0.08	0 /28	0 /28	11	607	<0	>100	1.00
	p3	0.58	13.5	190.0	1.1	0.04	0 /45	1 /45	60	460	0.014	<1E-3	0.91	0.90	16.7	196.7	4.1	0.09	0 /56	0 /56	29	449	0.040	0.02	0.99
	p4	0.48	11.8	188.0	6.1	0.10	1 /37	0 /37	176	744	0.030	0.10	0.98	0.82	13.7	185.9	9.0	0.13	1 /43	0 /43	71	669	0.088	4.19	0.85
	p5	0.07	7.8	77.3	3.2	0.07	3 /22	9 /22	1025	1090	0.009	52.07	0.69	0.52	11.0	187.4	11.1	0.14	3 /32	0 /32	217	718	0.054	3.69	0.70
xs5	p1	0.48	4.5	221.7	3.8	0.07	0 /8	1 /8	352	439	0.032	0.16	1.00	0.54	5.4	222.3	4.8	0.07	0 /13	0 /13	67	505	0.058	1.96	0.80
	p2	0.57	8.7	223.3	6.5	0.08	1 /27	1 /27	46	504	0.025	0.01	0.99	0.91	12.0	228.9	4.1	0.08	2 /38	2 /38	15	619	0.028	<1E-3	0.95
	p3	0.56	7.1	227.2	2.0	0.05	1 /21	5 /21	49	328	<0	>100	0.98	0.88	10.3	231.9	3.5	0.07	2 /33	1 /33	47	243	0.020	<1E-3	0.98
	p4	0.57	5.2	227.1	2.2	0.05	4 /15	0 /15	10	260	0.017	<1E-3	0.95	0.80	8.2	236.3	6.9	0.10	1 /26	2 /26	174	576	<0	>100	0.03
	p5	0.41	3.8	228.9	2.0	0.05	0 /10	0 /10	304	520	<0	>100	0.41	0.47	5.4	233.9	5.3	0.09	4 /14	0 /14	156	649	0.020	0.01	1.00
xs6	p1	0.75	7.0	256.9	2.8	0.05	0 /19	1 /19	11	535	0.051	0.32	0.98	1.06	10.5	268.2	1.9	0.05	0 /34	0 /34	5	506	0.061	0.24	0.99
	p2	0.61	5.5	257.8	0.3	0.02	0 /16	0 /16	17	485	0.078	3.44	1.00	0.98	7.8	266.8	2.6	0.06	0 /25	0 /25	8	462	0.050	0.04	1.00
	p3	0.61	4.0	260.7	4.3	0.08	1 /11	3 /11	47	649	0.046	0.27	0.99	0.87	7.2	267.9	2.4	0.05	1 /23	0 /23	128	332	0.047	0.08	0.99
	p4	---	---	---	---	---	---	---	---	---	---	---	---	0.70	6.2	265.9	2.6	0.06	1 /18	3 /18	28	491	0.054	0.34	1.00

[a] ratio of nonstationary bins to total bins for the run test

[b] ratio of nonstationary bins to total bins for the reverse arrangements test

Table 1. continued

		mean annual flow											bankfull flow										
Site 5		U	H	α	A_f	D	RT[a]	RA[b]	T_μ	T_σ	u_τ	k_s	R^2	U	H	α	A_f	D	RT[a]	RA[b]	T_μ	T_σ	u_τ	k_s	R^2
xs1	p1	0.61	3.2	177.9	5.2	0.07	0 /8	0 /8	4	259	0.042	0.12	1.00	0.70	6.3	180.3	14.4	0.14	1 /20	0 /20	51	481	0.039	0.05	1.00
	p2	0.72	3.3	183.2	1.8	0.04	0 /8	0 /8	3	607	0.014	<1E-3	0.99	0.89	7.0	185.4	5.1	0.08	0 /21	0 /21	105	675	0.094	2.32	1.00
	p3	0.66	4.0	180.5	1.1	0.03	0 /11	0 /11	27	222	0.044	0.13	1.00	0.94	7.4	186.6	3.2	0.07	0 /23	9 /23	7	826	0.061	0.18	1.00
	p4	0.71	4.7	180.1	1.6	0.04	0 /14	0 /14	23	283	0.022	<1E-3	1.00	0.81	8.1	182.8	3.6	0.06	0 /26	0 /26	118	663	0.062	0.46	1.00
xs2	p1	0.57	3.2	174.8	3.8	0.06	0 /8	0 /8	9	307	0.033	0.04	1.00	0.72	6.4	176.3	4.6	0.07	1 /20	0 /20	53	645	0.035	0.02	1.00
	p2	0.65	3.5	174.9	4.5	0.07	0 /9	0 /9	55	432	0.031	0.01	1.00	0.86	6.9	176.2	6.0	0.09	0 /21	0 /21	12	372	0.103	3.00	1.00
	p3	0.72	4.0	173.6	3.6	0.06	1 /11	0 /11	9	298	0.009	<1E-3	0.95	0.98	7.7	175.5	6.2	0.09	0 /25	1 /25	18	411	0.064	0.17	1.00
	p4	0.71	5.0	171.3	5.4	0.07	0 /15	0 /15	31	727	0.018	<1E-3	1.00	0.89	8.3	175.3	1.2	0.04	0 /27	1 /27	7	836	0.051	0.11	1.00

[a] ratio of nonstationary bins to total bins for the run test

[b] ratio of nonstationary bins to total bins for the reverse arrangements test

Table 2. Sample records lengths from the literature

Study	River	Q	Parameter of interest	Sample record length (min)	
				used	recommended
Barua and Rahman [1998]	Brahmaputra River, Bangladesh	19,600	mean velocity and turbulence parameters	33-127	15
Rennie et al. [2002]	Fraser River, Canada	5,600-6,800	bed load velocity	2-112	25
Muste et al. [2004a]	Mississippi River, USA	900-1,500	mean velocity	16	11
Stone and Hotchkiss [2007]	St. Maries river and Potlatch River, USA	7.9-11.4	mean and std. dev. of velocity	20	5
Szupiany et al. [2007]	Paraná River, Argentina	12,127-24,682	mean velocity	10	7
Holmes and Garcia [2008]	Missouri River, USA	1,407-3,160	mean velocity	10-30	NA
Guerrero and Lamberti [2011]	Po River, Italy	974	depth-averaged velocity	3.3	"some tens of seconds"

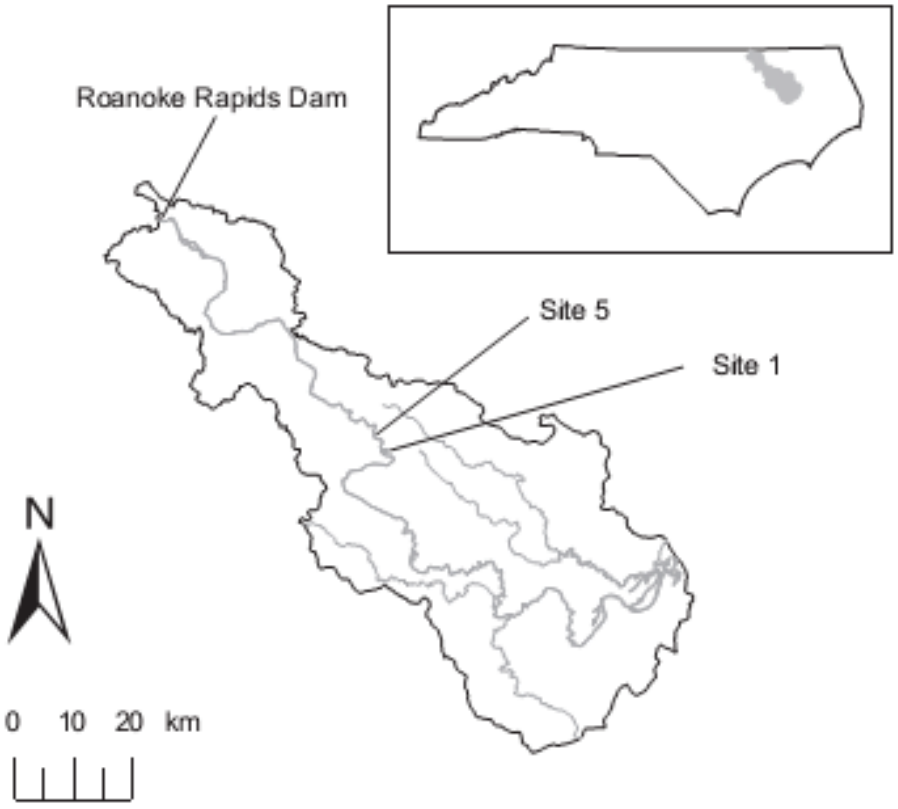

Figure 1. Map of the portion of the lower Roanoke River watershed located within North Carolina. Location of the watershed in North Carolina is shown in gray in the box.

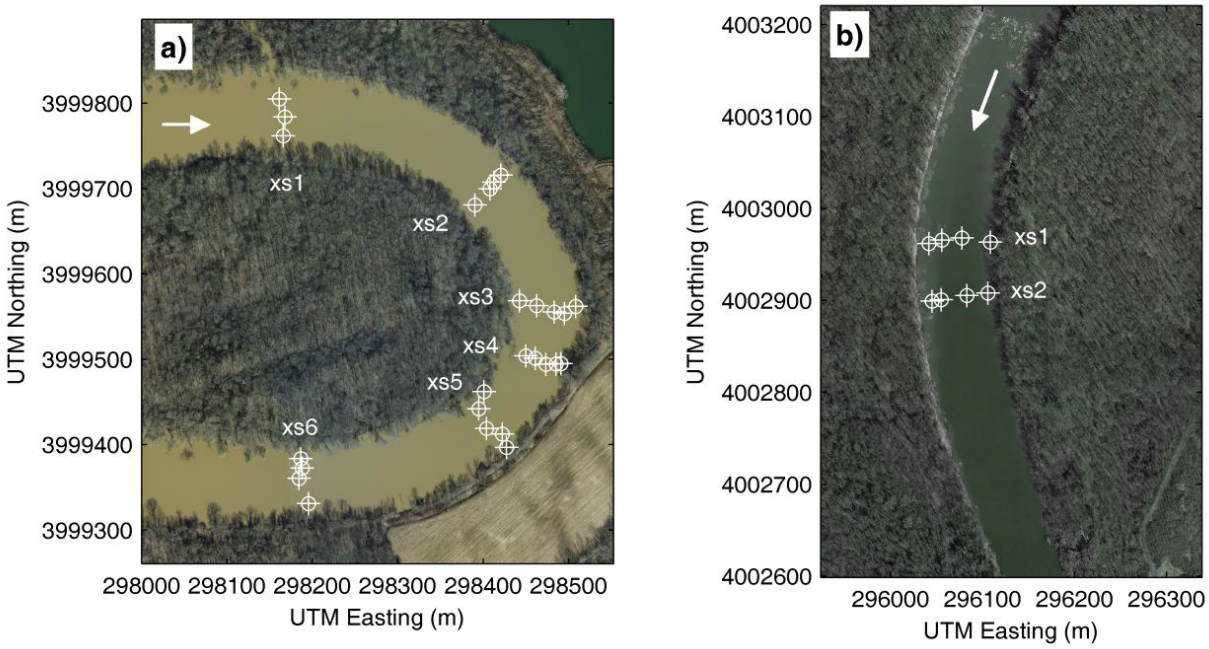

Figure 2. Locations of the FV ADCP measurements for the bankfull flow at (a) Site 1 and (b) Site 5. Arrows indicate the approximate direction of flow.

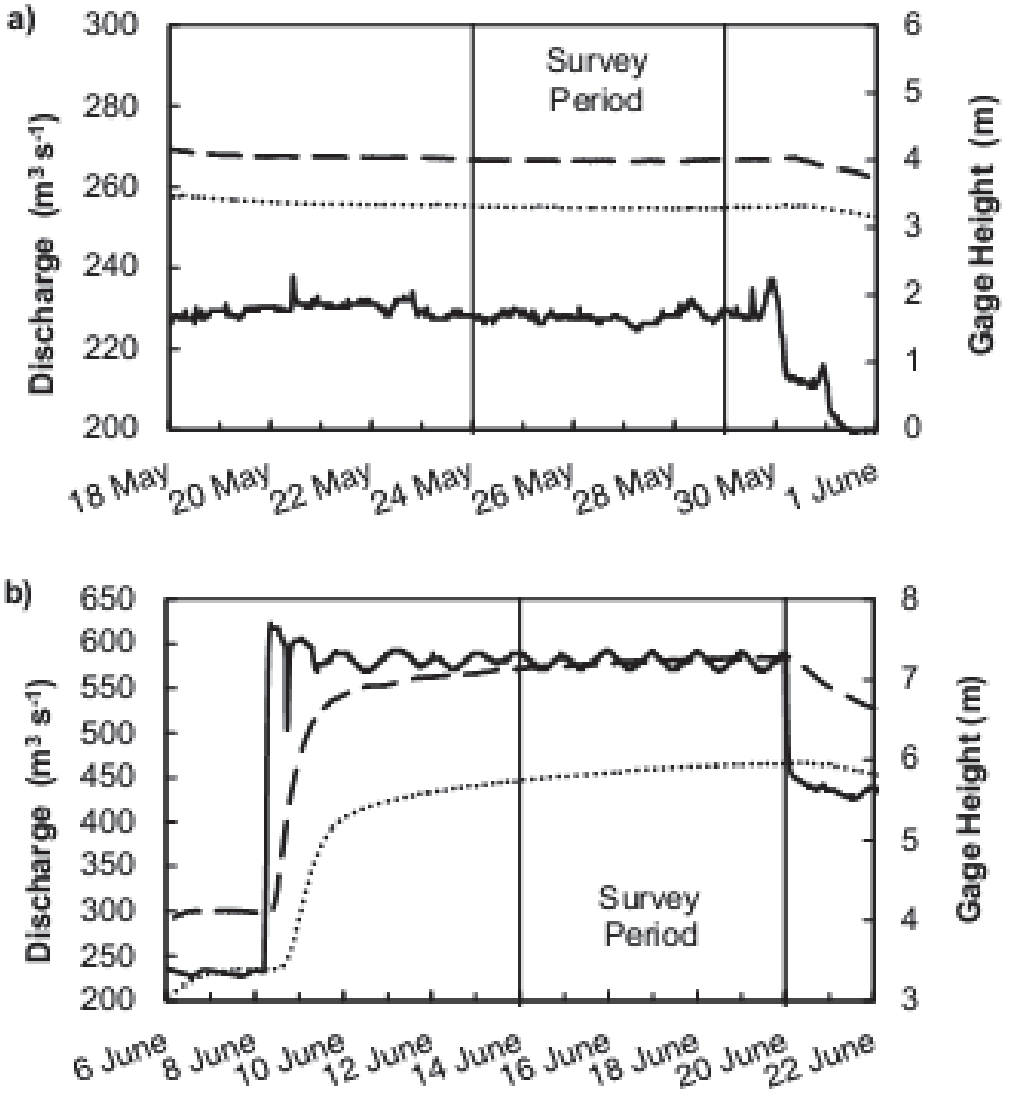

Figure 3. Discharge (Roanoke Rapids, solid line) and stage (Scotland Neck, dashed line, and Oak City, dotted line) during the field surveys in (a) May and (b) June, 2009.

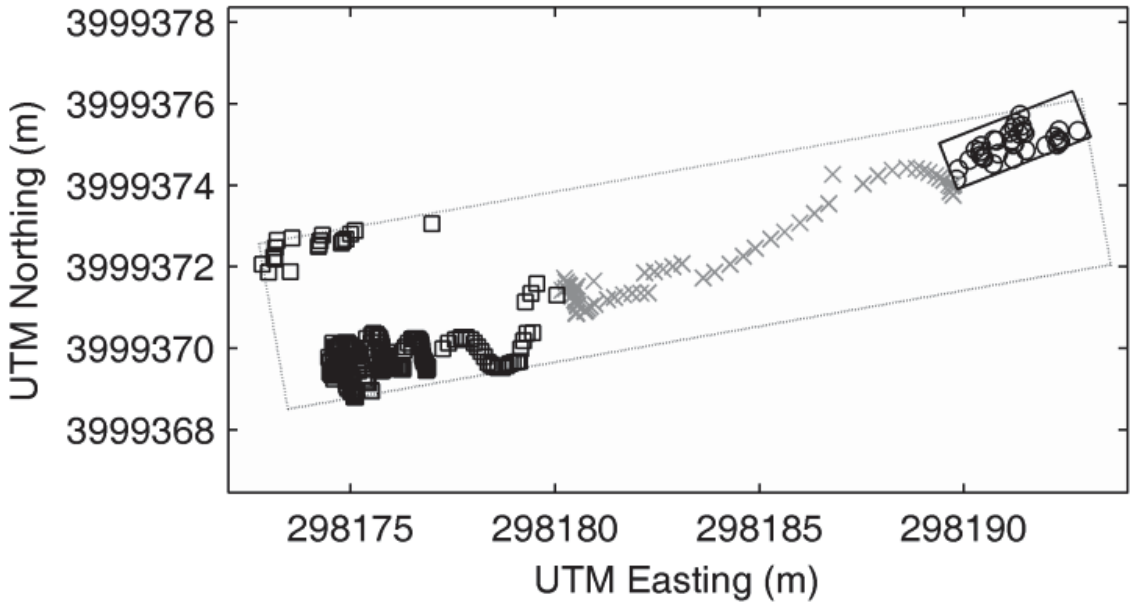

Figure 4. Ensemble locations for S1xs6p3 during the mean annual flow. Every twentieth Ensemble measured before 860 s is shown with a circle, ensembles measured after 950 s are shown with squares, and those measured between 860 and 950 s are shown with an "×". The rectangle corresponding to the footprint area of the edited (unedited) record is shown with a solid (dashed) line.

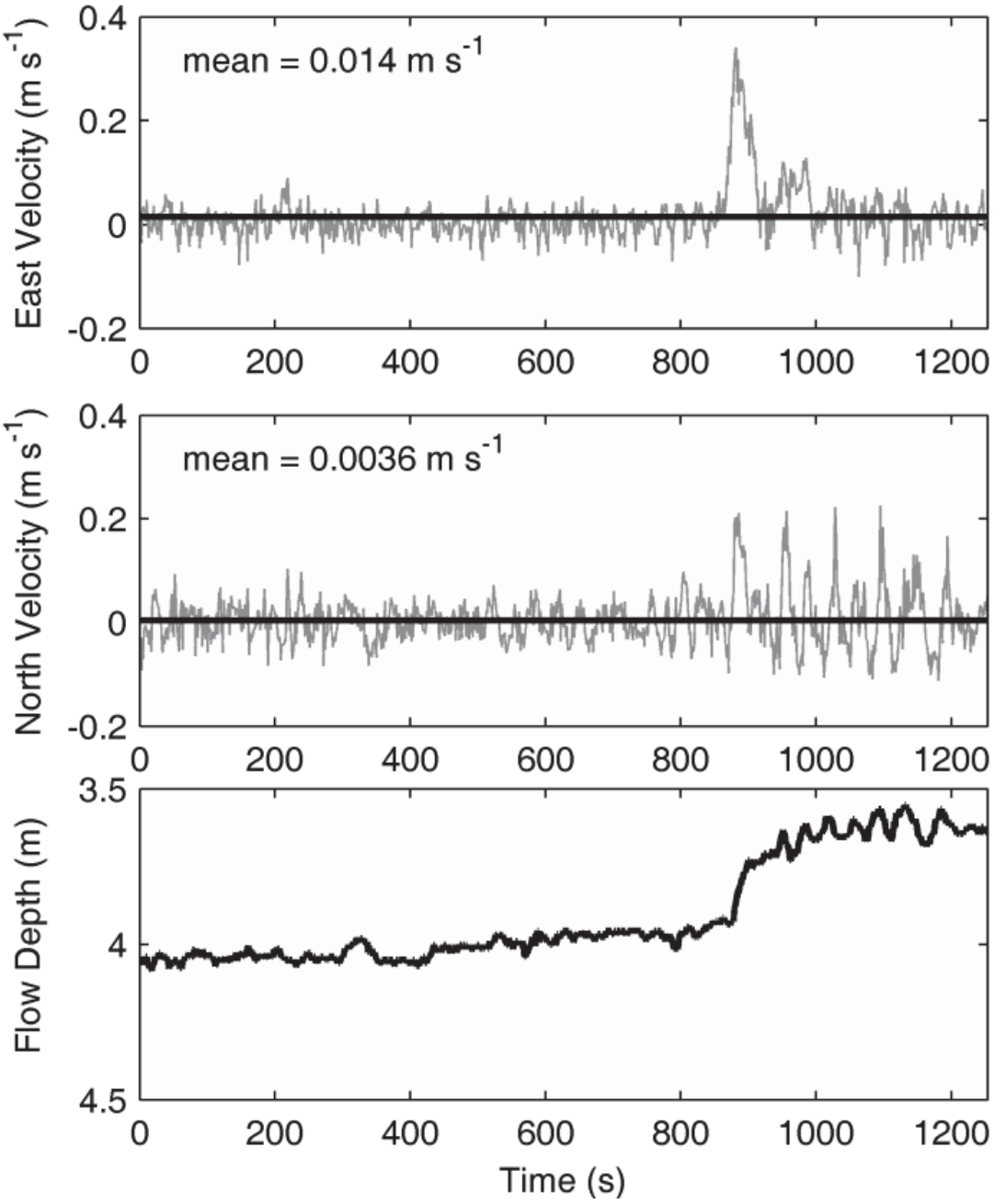

Figure 5. Times series of the horizontal components of boat velocity and flow depth for S1xs6p3 at the mean annual flow. The mean boat velocity is shown with a solid black line.

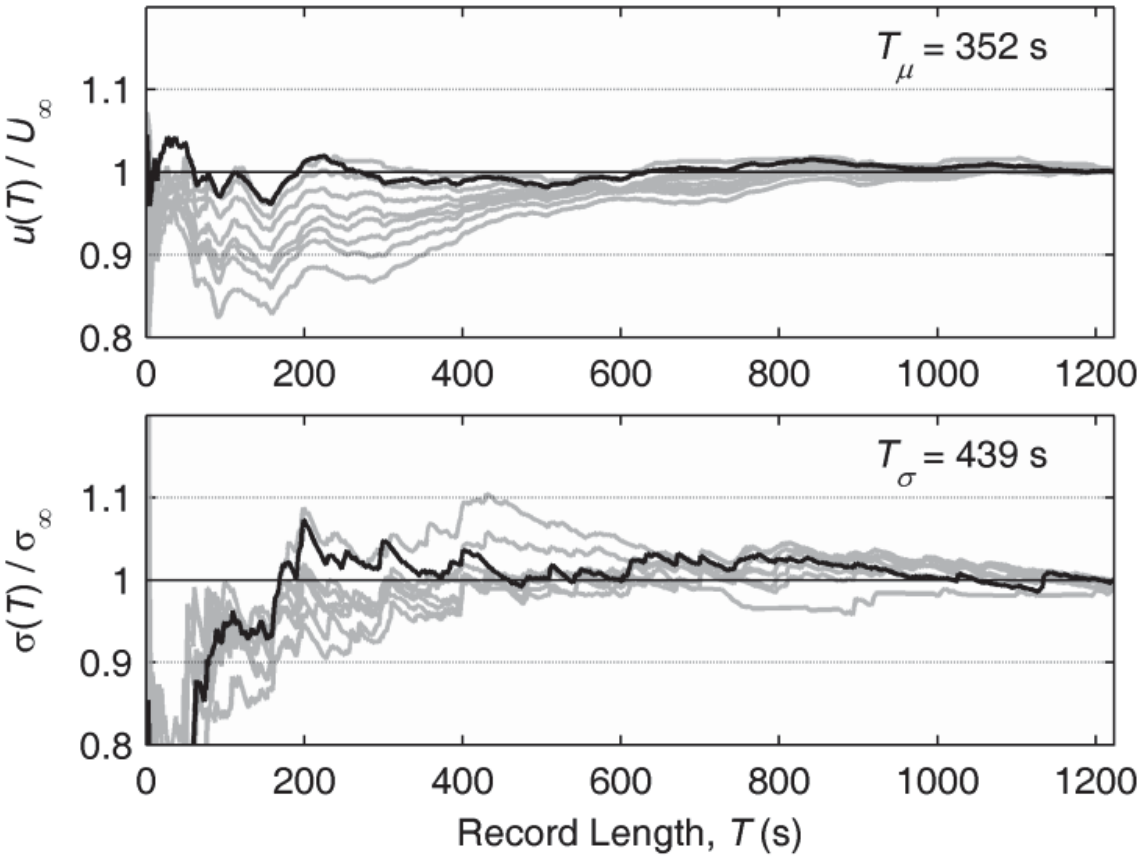

Figure 6. Normalized running mean and standard deviation for S1xs5p5 for the mean annual flow. The running statistics for the depth-averaged velocity are shown with a black line.

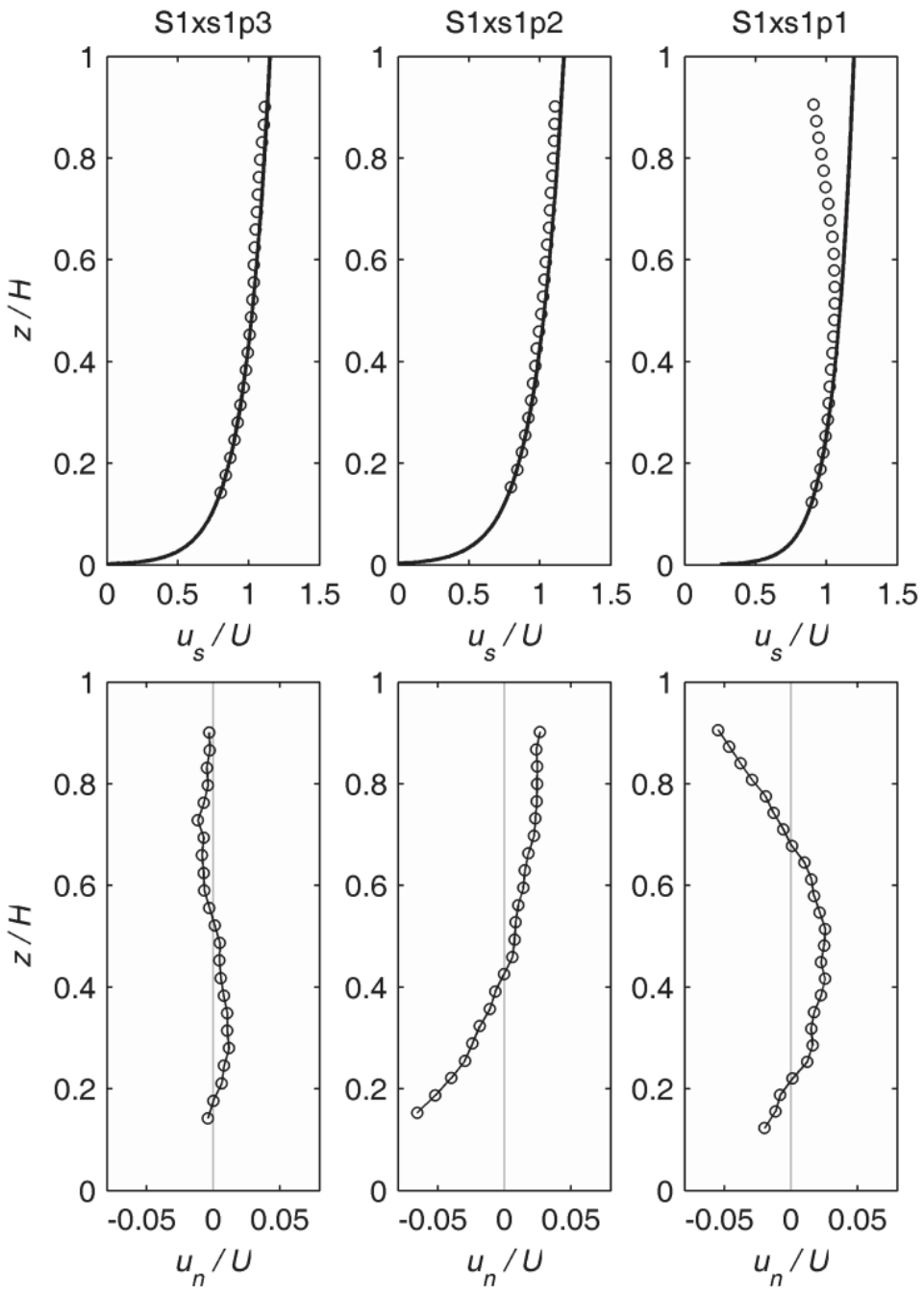

Figure 7. Streamwise and spanwise velocity profiles at S1xs1 during the bankfull flow.

CHAPTER 3. COMBINING FIXED- AND MOVING-VESSEL ACOUSTIC DOPPLER CURRENT PROFILER MEASUREMENTS FOR IMPROVED CHARACTERIZATION OF THE MEAN FLOW IN A NATURAL RIVER[2]

Abstract

A methodology is presented to quantify the mean flow field in a natural river with a boat-mounted acoustic Doppler current profiler (ADCP). Moving-vessel (MV) and fixed-vessel (FV) survey procedures are used in a complementary fashion to provide an improved representation of mean three-dimensional velocity profiles along a cross section. Mean velocity profiles determined with FV measurements are rotated to a stream-fitted orthogonal coordinate system. The orientation of the coordinate system is established using MV measurements. The methodology is demonstrated using measurements obtained at two study sites on the lower Roanoke River for the mean annual flow (228 m^3 s^{-1}) and a flow that produces bankfull conditions at the sites (565 m^3 s^{-1}). Results at a meander bend identify well known flow features including a main circulation cell, outer-bank circulation, and separation at the inner bank. This methodology also provides a framework for comparing time-averaged velocity profiles from FV measurements with spatially-averaged profiles from MV measurements. Results indicate that MV measurements can provide a reasonable estimate of the streamwise velocity at many locations. The MV measurements obtained here, however, were not sufficient to resolve the spanwise velocity component.

---

[2] This chapter is currently under review: Petrie, J., P. Diplas, M. Gutierrez, and S. Nam (*under review*), Combining fixed- and moving-vessel acoustic Doppler current profiler measurements for improved characterization of the mean flow in a natural river, *Water Resources Research*.

3.1 Introduction

The flow field in natural rivers is characterized by turbulent three-dimensional (3D) velocity. The 3D nature of velocity is due to channel planform curvature and pronounced channel topography [e.g., *Rozovskii*, 1957; *Dietrich and Smith*, 1983] as well as anisotropic turbulence [*Tominaga et al.*, 1989]. To interpret field data, velocity measurements are often decomposed into orthogonal components in the streamwise, spanwise, and vertical directions. Orientation of the horizontal components is dependent on the definition of the primary flow direction. Typically, the streamwise flow direction is prescribed using either channel geometry or flow characteristics. Velocity components in the plane perpendicular to the streamwise direction formed by the spanwise and vertical axes are referred to as secondary velocities and are known to influence channel morphology [e.g., *Blanckaert*, 2011] and ecology [e.g., *Shen and Diplas*, 2008, 2010]. Interpretation of secondary velocity patterns is complicated due to the small magnitudes relative to the streamwise component as well as when only the horizontal velocity is measured and vertical velocity must be inferred. *Lane et al.* [2000] advocated the use of 3D computational fluid dynamics (CFD) models to directly represent velocity vectors as an alternative to interpreting orthogonal components. Flows in natural rivers are particularly challenging to model due to the presence of moving boundaries—including both the channel boundary and free-surface, complex topography, turbulence, and boundary roughness. Despite these complexities CFD has been applied to flows in natural rivers with promising results [e.g., *Ferguson et al.*, 2003; *Shen and Diplas*, 2008, 2010; *Rüther et al.*, 2010]. High resolution field data for boundary conditions and validation are needed to support the expanding role of CFD in fluvial hydraulics.

A boat-mounted acoustic Doppler current profiler (ADCP) is a versatile tool for riverine studies that can provide measurements of 3D velocity and channel topography. The spatial and temporal resolution of the velocity measurements is dependent on the type of deployment. During moving-vessel (MV) measurements the ADCP records continuously while the boat traverses the channel. This is the most common boat-mounted survey procedure and provides accurate measurements of discharge [*Oberg and Mueller*, 2007]. Fixed-vessel (FV) measurements are performed while the boat is held at a constant position within the channel. The improved temporal resolution can be used to determine mean, e.g. time-averaged, velocity profiles [*Petrie et al.*, 2013] and bed load velocity [*Rennie et al.*, 2002]. Due to the increased effort required to collect FV measurements, several studies have investigated mean velocity profiles from MV measurements using spatial averaging or interpolation [*Muste et al.*, 2004a, 2004b; *Dinehart and Burau*, 2005; *Szupiany et al.*, 2007]. Recently, kriging has been used to interpolate planform maps of flow quantities including depth-averaged velocity, boundary shear stress, and bed load velocity from MV measurements [*Rennie and Church*, 2010; *Guerrero and Lamberti*, 2011]. *Jamieson et al.* [2011] and *Tsubaki et al.* [2012] have extended this work to interpolate the 3D velocity field. While these maps do not represent mean quantities in a strict time-averaged sense, *Jamieson et al.* [2011] argue that interpolated maps may better represent a complex flow field than averaging repeat transects that are not coincident and introduce spatial averaging. Nonetheless, a detailed comparison of interpolated maps to time-averaged velocities has yet to be reported.

This study presents a methodology to quantify the mean flow field in a natural river with a boat-mounted ADCP using both MV and FV survey procedures. This approach capitalizes on the relative advantage of each procedure with the MV measurements providing the direction of

primary flow and channel topography, while the FV measurements determine the mean velocity profiles. A comparison of mean velocity profiles from FV and MV measurements is performed to determine if the MV measurements can quantify the spatial distribution of the mean secondary velocity. The methodology is then demonstrated by examining mean velocity profiles throughout a meander bend.

3.2 Field Measurements

3.2.1 Study Sites

ADCP measurements were obtained in May and June, 2009 at two study sites shown in Figure 1 on the lower Roanoke River in eastern North Carolina. Flow to the lower reach is primarily controlled by releases from the Roanoke Rapids Dam. The effect of this flow regulation on bank retreat has been the subject of recent investigations [*Hupp et al.*, 2009; *Nam et al.*, 2010, 2011]. Reservoir releases were relatively steady for both survey periods, with the discharge Q in May close to the mean annual flow (Q=228 m^3 s^{-1}) and at bankfull in June (Q=565 m^3 s^{-1}). Further information on the study sites and flow conditions are provided in *Petrie et al.* [2013].

3.2.2 Equipment and Measurement Procedures

The ADCP measures 3D velocity components by applying the Doppler principle to the frequency shift of reflected acoustic pulses, called pings. Measurements are assigned to equally-spaced discrete locations in the water column, called bins. A bin size of 0.25 m was used for all measurements in this study. Limitations of the instrument prevent velocity measurements from being obtained near the water surface or near the bed [see *Simpson*, 2001]. An ensemble is one measurement of the velocity profile and may be comprised of a single ping or the average of

several pings. For the FV measurements, 20 sub-pings sent 50 milliseconds apart were used to create each ensemble. The recommended settings provided by the ADCP software were used for the MV measurements. For the mean annual flow, this resulted in 7 sub-pings sent 40 milliseconds apart to create an ensemble for most transects and 1 sub-ping sent 70 milliseconds apart for most transects during the bankfull flow. Data were collected using Water Mode 12 and Bottom Mode 5 [see *Mueller and Wagner*, 2009]. Global positioning system (GPS) was used as the velocity reference for all measurements with the exception of one FV measurement, S1xs6p2 (nomenclature explained in the following section) during the mean annual flow, due to a problem with the GPS signal. The decision to use GPS was based on observations of bed movement, especially during the bankfull flow. Further details on ADCP operational principles can be found in the work of *Gordon* [1989], *Simpson* [2001], and *Mueller and Wagner* [2009].

A 1200 kHz Workhorse Rio Grande ADCP (Teledyne RD Instruments, Poway, CA) and a Trimble DSM 232 GPS (Sunnyvale, CA) were mounted to a tethered boat (Oceanscience, Oceanside, CA). The GPS antenna is positioned directly above the ADCP at a height of about 50 cm from the water surface. Rope was used to attach the tethered boat (length=1.2 m) to the starboard (right) side of a motor boat (length=6 m). The tethered boat remained on the starboard side near center of the motor boat for both survey procedures. The ADCP and GPS data were recorded with WinRiver II software provided by the ADCP manufacturer. The horizontal accuracy of the GPS was approximately 1.0 m. Measurement locations were found during deployment with HYPACK LITE (HYPACK, Inc., Middletown, CT).

Both MV and FV survey procedures were performed at each study site. FV measurements were performed by anchoring the boat within the channel and measuring continuously for 1200 s. A data assurance procedure was performed on each individual measurement to verify that the measured velocity was (1) statistically stationary, (2) not adversely influenced by motion of the ADCP, and (3) of sufficient sample record length [*Petrie et al.*, 2013]. MV measurements consisted of driving the boat from one bank edge to the other in a path approximately perpendicular to the flow direction with the ADCP measuring continuously. One pass across the river produces a single measurement and is referred to as a transect. Four transects, two starting at each bank, were performed at each cross section of interest. Directional errors were observed near the end of some transects as a result of acceleration due to the ADCP turning near the bank edge. The affected ensembles were removed from the sample record.

Measurements were aligned along cross sections, six at Site 1 and two at Site 5, oriented approximately perpendicular to the riverbanks. The cross-sections are numbered consecutively from upstream to downstream as shown in Figure 2. For each discharge between three and five FV measurements were performed followed by four MV transects at each cross section. Difficulty positioning the ADCP prevented measurements from occurring at the exact same locations during June 2009. The average distance between the FV locations for the two discharges is 5.1 m. Each FV measurement is labeled to identify the site, cross-section, and profile number, e.g. S1xs1p1, where the profile nearest the left bank is designated profile number 1. A total of 25 (26) profiles were measured during the mean annual flow (bankfull flow) at Site 1 and 8 profiles were obtained at Site 5 for each discharge. The surveys required approximately six days with a three person crew. Data processing for both FV and MV measurements was

performed with in-house codes developed in MATLAB® (MathWorks, Natick, MA) at the Baker Environmental Hydraulics Laboratory of Virginia Tech.

3.3 Data Analysis

Interpreting flow data in a natural river can be difficult due to complex channel topography and the turbulent, 3D nature of velocity. A methodology is presented here that allows velocity data obtained with MV and FV survey procedures to be presented in a consistent framework. The velocity data is first rotated to a common coordinate system and then translated to a two-dimensional plane representing a cross-section. This procedure allows a comparison of measured velocity from different survey procedures as well as a hybrid approach to presenting velocity patterns at a cross-section, e.g. using the MV measurements to quantify the channel bathymetry and FV measurements to determine mean velocity profiles.

Velocity components are presented in a stream-based coordinate system. As the orientation of the coordinate system may not be known prior to field measurements, ADCP velocity data are output in a Cartesian coordinate system defined by east, E, north, N, and vertical, Z, axes, more specifically the Universal Transverse Mercator (UTM) geographic coordinate system; referred to here as the geographic coordinate system. The geographic components are rotated in the horizontal plane by an angle, α, to the stream coordinate system—a "channel-fitted" curvilinear coordinate system defined by streamwise, s, spanwise, n, and vertical, z, axes. The angle of rotation, α, is measured clockwise from the N-axis to the s-axis. Representing velocity in stream coordinates allows the velocity vectors to be decomposed into a primary component, oriented along the s-axis, and secondary components, occurring within the secondary plane—the plane

formed by the *n*- and *z*-axes. The angle of rotation, α, is referred to as the direction of primary flow, the streamwise direction, or simply the flow direction.

The direction of primary flow may be defined using channel geometry or flow characteristics [*Hey and Rainbird*, 1996; *Lane et al.*, 2000]. Channel curvature referenced to either the bank edge or channel centerline has been used to define the flow direction in curved laboratory channels [*De Vriend*, 1976; *Blanckaert and Graf*, 2001] as well as field sites [*Dinehart and Burau*, 2005; *Nanson*, 2010; *Sukhodolov*, 2012]. Difficulties may be encountered when applying this approach to natural rivers including problems identifying the bank edge or channel centerline, non-uniformity between the right and left bank edges, changing channel curvature, and other complex features such as bifurcations and confluences. Definitions using flow characteristics to determine flow direction depend on the spatial extent over which the flow direction is defined with one-, two-, and three-dimensional approaches being available. The most commonly applied definition is the one-dimensional approach of *Rozovskii* [1957], where the direction of primary flow along a vertical profile is defined as the direction that results in a zero net secondary discharge across the vertical. Requiring a zero net secondary discharge ensures that both positive and negative spanwise velocity values exist in all profiles. The Rozovskii definition is applied to individual velocity profiles; thus, it provides a local flow direction which may vary for different locations along a cross section. *Paice* [1990] defines the direction of primary flow as the direction that results in the maximum discharge through a vertically-oriented plane, a two-dimensional approach. Equivalently, this definition results in zero net secondary discharge in the cross-section plane. The Paice definition produces a single flow direction for a cross-section allowing for regions of unidirectional spanwise velocity to exist.

The choice of definition for the flow direction will influence the interpretation of secondary velocity and depends on the available data. For example, the local flow direction resulting from the Rozovskii definition may obscure flow features when secondary profiles are viewed along a cross-section [*Dietrich and Smith*, 1983]. The Paice definition was selected due to the fact that it provides a consistent flow direction along a cross section. The algorithm for computing the flow direction using the Paice definition [see *Hey and Rainbird*, 1996] can be adapted to MV transects using the following steps.

1. Perform a MV transect in the same manner as obtaining a discharge measurement.
2. Calculate the streamwise and spanwise velocity components in each bin for all possible angles of rotation from 0° to 360°.
3. For each angle of rotation compute the net spanwise discharge for the transect.
4. The angle of rotation in step 3 which produces a zero net spanwise discharge is the direction of primary flow, α.

Both *Paice* [1990] and *Markham and Thorne* [1992] apply a similar procedure after collecting velocity profiles along a cross section with a current meter and applying the mid-section method to compute discharge. MV transects with a boat-mounted ADCP provide spatial resolution of velocity that produce improved estimates of discharge and, likely, the flow direction as well. Calculating discharge in the streamwise and spanwise directions from MV measurements requires a modification to the standard discharge equation presented in *Christensen and Herrick* [1982] and used in WinRiver II. Modification is necessary due to the fact that the standard

discharge equation computes the total net horizontal discharge independent of coordinate system [*Simpson*, 2001]. Reintroducing the dependence on coordinate system results in the following equation for the spanwise discharge for the i^{th} ensemble:

$$Q_{ni} = \sum_{j=1}^{m} u_{nj} \left(V_s\right)_i \Delta t_i \Delta z \tag{1}$$

where the ensemble contains $j = 1, 2, \ldots, m$ bins, u_{nj} is the spanwise velocity component of the j^{th} bin, $(V_s)_i$ is the streamwise component of the boat velocity for the ensemble, Δt_i is time elapsed between ensembles i and i–1, and Δz is the bin height. Summing over all ensembles provides the total discharge in the spanwise direction:

$$Q_n = \sum_{i=1}^{k} Q_{ni} \tag{2}$$

where the transect contains $i = 1, 2, \ldots, k$ ensembles. A derivation of equations (1) and (2) is provided in the appendix. As with discharge measurements [see *Mueller and Wagner*, 2009], multiple transects should be obtained at each cross-section and the flow direction computed from the average of the individual transect results.

To present the velocity component in a single plane, velocity data are translated onto the secondary plane. *Dinehart and Burau* [2005] refer to this procedure as "section straightening". While care is taken to obtain measurements close to the cross-section, measurements will inevitably vary in location. Multiple MV transects will not be coincident due to difficulty

keeping the boat moving along the same straight path while traversing the river channel. Likewise, difficulty fixing the boat at an exact location in the river may prevent the FV measurement locations from lying along the MV transects. *Dinehart and Burau* [2005] define the horizontal orientation of the plane by fitting a mean line through multiple boat paths then rotating the ADCP data about a distant point onto the mean line with cosine rotation. It is not explicitly stated how the mean line is fit through the boat paths. Two options are to visually estimate the mean line or perform a linear regression on the horizontal locations from the boat path as discussed by *Szupiany et al.* [2007].

Following the general approach of *Dinehart and Burau* [2005] and *Szupiany et al.* [2007], the procedure for section straightening presented here fits a straight line through the boat paths of the MV transects. The slope of this line is prescribed to produce a line coincident to the spanwise axis, n, in local stream coordinates. The motivation for using the orientation of the spanwise axis is to provide a convenient physical interpretation for velocity data visualized in the secondary plane. Specifically, when mean spanwise and vertical velocity components are plotted, the resulting patterns occur within the plane as shown. Once the direction of primary flow is determined, section straightening is performed with the following steps.

1. Rotate the location of all ensembles from MV transects from geographic to stream coordinates.
2. Translate the MV locations to a local stream coordinate system where the location of the spanwise axis (s=0) is set to the location of the average streamwise location. The location

of the primary axis (n=0) is set to the mean of the spanwise locations to approximate the channel centerline.

3. Translate the locations of MV or FV data perpendicularly to lie on the secondary plane. Following *Dinehart and Burau* [2005], the translated velocity data remain unchanged.

Once section straightening is performed, any location may be presented in either geographic or stream coordinates. As the stream coordinate system changes for each cross section, geographic coordinates are preferred when representing data from multiple cross sections. Figure 3 demonstrates section straightening for S1xs2 during the mean annual flow. In Figure 3a, the gray line shows the location of the spanwise axis and the vector arrows indicate the direction of primary flow. Figure 3b shows the FV and MV measurement locations in stream coordinates. The distance required to translate each FV profile to the secondary plane is provided in Table 1. The mean and maximum translation distances for the mean annual flow (bankfull flow) are 7.7 m (8.8 m) and 17.4 m (20.1 m), respectively.

3.4 Results

3.4.1 Mean Velocity Profiles from MV and FV Procedures

While time-averaged velocity profiles cannot be directly determined from MV transects, spatial averaging of multiple transects has been used to produce mean profiles [*Dinehart and Burau*, 2005; *Szupiany et al.*, 2007]. The dataset from the lower Roanoke River is used to evaluate the adequacy of spatially-averaged velocity profiles derived from MV transects to represent mean, i.e. time-averaged, velocity profiles. The velocity profiles from the MV transects at a cross-section are compared with time-averaged velocity profiles from FV measurements obtained

along the cross-section. Mean velocity profiles were obtained from multiple transects by first applying the section straightening procedure to the individual transects. Each geographic velocity component is interpolated at locations corresponding to the bins in the FV measurement of interest, resulting in a velocity profile for each transect. The velocity profiles interpolated from the individual transects are then averaged to create the mean velocity profile. A similar procedure is employed by *Dinehart and Burau* [2005] to represent secondary velocity components. To provide a consistent coordinate system for comparison, the mean geographic velocity components are rotated using the flow direction determined with the Rozovskii definition from the corresponding FV measurement. The results at two locations are excluded from this analysis: (1) S1xs4p5 for the mean annual flow which is located in a recirculation region and (2) S1xs5p5 for the bankfull flow due to the fact that the FV measurement location falls outside of the transects.

The FV and MV results for the streamwise and spanwise velocity components for all bins are compared in Figure 4. Generally, closer agreement is seen in the streamwise component. The majority of bins which show large spanwise velocity from the MV results occur in four profiles: S1xs2p1, S1xs4p1, S1xs4p2, and S1xs4p4 during the mean annual flow. The spanwise velocities at these locations are shown in gray in Figure 4b. Example velocity profiles from FV and MV measurements along S5xs1 during the bankfull flow are provided in Figure 5. Reasonable agreement is seen in the streamwise velocity profiles while the spanwise profiles show differences in both magnitude and direction. As expected, the time-averaged FV results have a smoother velocity distribution for all profiles.

Table 2 presents the mean percent difference and the maximum percent difference between the MV and FV results for each profile of velocity magnitude and streamwise velocity. The median value of the mean percent difference for all profiles is about 10% or less, demonstrating that MV transects can provide reasonable estimates of the time-averaged velocity magnitude and streamwise velocity profiles (see Fig. 5). The maximum percent difference within each profile, however, was found to be as large as 96% with median values over 20%. Thus, values at specific locations within the profile may vary considerably. The largest differences were generally seen in cross-sections near the bend apex at Site 1 (S1xs2 through S1xs5), particularly at locations near the inner bank. The percent difference values for the spanwise velocity component are not reported in Table 2 due to the fact that the values were uniformly large—only two profiles have a mean percent difference less than 100%. The median value of the mean absolute difference for the spanwise velocity profiles during the mean annual flow (bankfull flow) was 0.052 m s^{-1} (0.070 m s^{-1}). These differences are the same order of magnitude as the mean spanwise velocities measured with the FV procedure. The differences in spanwise velocity are observed in both magnitude and direction (see Figure 4 and Figure 5).

Also included in Table 2 is the absolute difference between the local flow directions calculated from the FV and MV mean profiles using the Rozovskii definition. Good agreement was found for most profiles with a median difference less than 4° for both discharges and 68% (44 out of 65) of the profiles having differences less than 5°. Despite the generally good agreement, two profiles—S1xs4p1 and S1xs4p2 during the mean annual—had absolute differences of about 40°.

3.4.2 Direction of Primary Flow

The flow direction at each cross section is found by averaging the individual results of the four MV transects. For each transect, discharge was recomputed using the rotated velocity components and compared to the value produced by the standard equation. The mean difference between the two discharges for all transects was 2.0%. The mean flow direction along with the standard deviation and range for all cross-sections are provided in Table 3. The results show good agreement amongst the individual transect estimates with low standard deviations and reasonable ranges considering the ADCP compass accuracy of 2° [*RD Instruments*, 2007] at all but two cross-sections: S1xs4 and S1xs5 during the mean annual flow. Site and flow conditions prevented the transect boat paths from aligning with the planned path at these sites. For the majority of cross-sections, an increase in discharge leads to a decrease in both the standard deviation and range, indicating a reduction in variability between the individual transect estimates. This improved agreement is likely related to the increased percentage of the flow area measured for a higher discharge. Analogous to discharge measurements, the accuracy of flow direction estimates will increase as the measured region of the channel increases.

The flow direction generally follows the channel curvature around the bend with no significant change resulting from the increase in discharge (see Fig. 2 and Table 3). The flow uniformity at the two discharges can be attributed to the fact that the flow remains within the outer bank. At bankfull discharge, however, an increased area of the inner bank is submerged. While ADCP measurements in the inner bank region were not possible due to the presence of trees and other vegetation, the flow was visually judged to be moving slowly and, thus, would contribute little to

the measured discharge. These results indicate that similar flow directions are likely present for all within bank flows.

The flow direction at each FV location using the Rozovskii definition is provided in Table 1. Comparing these values with the flow direction determined from the Paice definition with MV transects at each cross-section gives a median difference of 2.8° (1.9°) for the mean annual (bankfull) flow. Three locations at each discharge have a difference larger than 10° with all six measurements located at S1xs4. The greatest difference is found at S1xs4p5 during the mean annual flow—a location within a recirculation zone [see *Petrie et al.*, 2013]. Table 3 provides estimates of the flow direction based on channel geometry. This geometric flow direction is found by visually positioning a spanwise axis that is perpendicular to the bank edge. The geometric flow direction remains constant for changes in discharge as a single aerial photo was used. Good agreement is seen between the flow directions determined from channel geometry and the Paice definition at all but two cross-sections, S1xs3 and S1xs4. The high curvature at Site 1 directs the flow towards the outer bank in the vicinity of the apex, resulting in a flow direction from the Paice definition oriented towards the outer bank and not parallel to the banks as produced by the geometric flow direction. The effect of different definitions of flow direction on the velocity profiles is addressed in Section 5.

3.4.3 Velocity Distribution in the Meander Bend at Site 1

3.4.3.1 Depth-averaged Velocity

The mean depth-averaged velocity in the streamwise flow direction using the Paice definition, U, and flow depth, H, for each FV profile is provided in Table 1. The flow depth was determined

using the average of the four beam measurements over the entire sample record. For the mean annual flow (bankfull flow), U ranges from −0.02 (0.47) to 0.75 m s^{-1} (1.06 m s^{-1}). As the flow moves through the bend, U decreases in the vicinity of the bend apex, S1xs4 and S1xs5, to accommodate the increase in flow depth. At each cross-section, the maximum U-value occurs within the outer half of the channel. The depth-averaged velocity at S1xs4p5 for the mean annual flow is a small negative value (U = −0.02 m s^{-1}), indicating that the mean flow is moving upstream at this location. This result suggests that this location is within a region of flow separation and recirculation as observed in both the laboratory [*Leopold et al.*, 1960] and natural rivers [*Ferguson et al.*, 2003]. The separation region was not captured for the bankfull flow although a significant decrease in velocity is seen at S1xs4p5. Separation may still occur but has moved further inward where ADCP measurements could not be obtained.

3.4.3.2 Primary Velocity Profiles

The primary or streamwise velocity profiles for all FV measurements are shown in Figure 6. The profiles are non-dimensionalized with the depth-averaged velocity and flow depth. Many of the non-dimensional profiles show a similar distribution of velocity for both discharges. The largest deviation between discharges appears to occur at S1xs4. Another notable feature is the presence of a velocity dip in several profiles, particularly at locations near the banks. The velocity dip is an indicator of strong secondary velocity (see Fig. 7). The primary velocity profiles at S1xs4p1 and S1xs4p2 at the bankfull flow both exhibit a sudden decrease in velocity as the free surface is approached. This behavior is due to the presence of a large tree protruding almost perpendicularly from the bank just upstream of the measurement location. At bankfull discharge, a portion of the tree is submerged. While it was not possible to determine the submerged depth of

the tree, the distance is estimated to be ~2-3 m, based on visual observation at lower flows. The small, negative depth-averaged velocity at S1xs4p5 for the mean annual flow results in a non-dimensional profile that extends over a large range with both positive and negative values. Positive values of u_s/U indicate upstream flow for the mean annual flow at S1xs4p5.

3.4.3.3 Secondary Velocity Profiles

The mean secondary, i.e. spanwise and vertical, velocity profiles determined using the flow direction determined from the MV measurements are show in Figure 7. The velocity scale is the same for all cross-sections with the exception of S1xs4. The maximum secondary velocity magnitude in each profile is typically on the order of 20% of U or less. The change in discharge produces no clear trend in the secondary velocity magnitude with both increasing and decreasing magnitudes relative to U. The largest magnitudes of relative secondary velocity are found at S1xs4 for the mean annual flow. In particular, S1xs4p1 and S1xs4p2 have secondary velocity magnitudes close to U while the secondary velocity magnitude at S1xs4p5 is several times larger than U.

Several well-established features of flow in natural meander bends are identified in Figure 7. A circulation cell can be seen in several profiles for both discharges at S1xs2, S1xs3, S1xs4, and S1xs6. This main circulation cell is generated by channel curvature and has been observed in both the laboratory [e.g., *Kikkawa et al*., 1976; *Blanckaert and Graf*, 2001] and field [e.g., *Thorne et al*., 1985; *Sukhodolov*, 2012]. The cell appears to move from the central region of the channel at S1xs2 to the inner half of the channel at S1xs6. It is possible that the strong negative spanwise velocities seen near the outer bank at S1xs4 may be responsible, in part, for this shift in

location. Evidence of a circulation cell rotating counter to the main circulation cell is also seen near the outer bank at the apex in the profile S1xs3p1 at bankfull discharge. *Sukhodolov* [2012] observed an outer bank cell that developed near the bend apex and strengthened downstream. This outer bank cell may exist at other locations as well; however, it was not captured due to the difficulty in obtaining measurements with the ADCP near the steep outer bank.

Further effects of channel topography on the velocity field are seen at the inner bank and in the vicinity of a scour hole located just downstream of the bend apex. Topographic steering of the flow over the inner bank in the form of unidirectional positive spanwise velocities occurs in profiles for the mean annual discharge at S1xs2p4, S1xs3p5, and S1xs4p5 and for the bankfull flow at S1xs3p5. Figure 8 shows a region of increased flow depth centered approximately at S1xs4p3. Downward vertical velocities are seen in Figure 7 as the flow approaches this region in S1xs3 and S1xs4 followed by upward vertical velocities as the flow exits the scour hole at S1xs5.

3.5 Discussion

The results from the lower Roanoke River show that spatially-interpolated and averaged velocity profiles from MV transects do not adequately predict time-averaged profiles from FV measurements. While general trends can be reasonably identified in the streamwise direction, agreement was poor for the spanwise velocity component. Two reasons that may explain the differences are (1) the MV transects and FV measurements were obtained at locations with differing velocity characteristics and (2) measurements were insufficient to describe the mean flow. *Petrie et al.* [2013] demonstrate that the FV measurements were adequate to represent the

mean flow at each location and MV transects were performed while monitoring the boat path with GPS ensuring reasonable agreement among individual transect locations. When performing section straightening, however, the locations of some FV profiles were translated up to 20 m. It is possible that, following translation, the FV and MV velocity data correspond to regions with different flow characteristics. Support for the agreement of the two measurement procedures is found by observing the flow depths measured by the MV transects and FV profiles. In Figure 7, the length of the line indicating the profile location corresponds to the measured flow depth from the FV measurement while the channel boundary is the average of the flow depths measured during the MV transects. Good agreement can be seen at all cross sections with the exception of S1xs4 (discussed below).

For a stationary flow, the ability of a FV measurement to describe the mean flow field is controlled by the sample record length, while the number of transects controls the ability of the MV measurements to accurately reproduce the spatial distribution of the mean flow. *Petrie et al.* [2013] found the flow field at the lower Roanoke River study sites to be stationary for both discharges and the sample record length of 1200 s to be sufficient for all FV measurements. The four transects collected at each cross-section, however, are likely not sufficient to determine the mean velocity. As the boat traverses the channel for each transect, the flow field is changing due to turbulent fluctuations. While guidelines are available for discharge [e.g., *Mueller and Wagner*, 2009], the variability in transect timing and location along with flow turbulence makes is difficult to prescribe a minimum number of transects required to accurately represent the spatial distribution of the mean flow. Turbulence is especially problematic when considering the secondary velocity components. Using detached-eddy simulation of a river confluence, *Tsubaki*

et al. [2012] found that the maximum value of the turbulence intensity was similar for all three components. Accordingly, even if the mean values are small, sufficient individual transects are needed to ensure that these large fluctuations do not bias the resulting mean value. Previous studies comparing velocity profiles derived from transects with time-averaged values [e.g., *Muste et al.*, 2004b; *Szupiany et al.*, 2007] have focused on streamwise velocity or velocity magnitude and not explicitly investigated secondary velocity components. Based on the reasonable agreement of both the measured flow depths and streamwise velocity profiles using both FV and MV measurements at many locations, the likely cause of the discrepancy between FV and MV mean velocities is an insufficient number of transects at each cross-section.

While ADCP transects are well-suited to determine flow direction with the Paice algorithm, especially when compared to point velocity measurement techniques, two issues related to the accuracy of the flow direction require further discussion. First, the flow direction is determined only by the measured region of the cross section, excluding areas near the bed, bank, and water surface. This issue applies to flow directions determined from both FV measurements using the Rozovskii definition and MV measurements applying the Paice definition. The unmeasured region near the water surface would likely have the stronger influence on the calculated flow direction as the velocity and, thus, discharge is expected to be larger than in regions close to the channel boundary. Given that the majority of the discharge is contained within the measured portion of the cross-section and the difficulty in estimating vector components of velocity, it is recommended to determine the flow direction using only measured velocity data without extrapolation to unmeasured regions. The final estimate of flow direction is also dependent on the number of transects obtained at each cross section. The four transects per cross section

obtained at the study sites were originally performed to measure discharge. Table 3 shows good agreement among the transects at all cross-sections except S1xs4, indicating that four transects are sufficient for most cross sections at the study sites. Further study on the effect of transect number on flow direction is necessary to establish guidelines similar to those for discharge measurements [see *Mueller and Wagner*, 2009].

While not investigated here, the time required to complete each transect may influence the flow direction from the Paice definition and the ability of transects to represent the mean flow. *Oberg and Mueller* [2007] found that measurement duration was more important to the accuracy of a discharge estimate than the number of transects performed. Estimates of flow direction, a bulk quantity like discharge, make likewise benefit from increased durations. Additionally, the higher spatial resolution resulting from longer duration transects may improve the ability of these transects to predict mean velocity components.

The MV transects at each cross section were designed to be performed perpendicular to the banks as the channel geometry gives a first approximation of the flow direction. Perpendicular boat paths were not always possible due to difficulties maneuvering the boat, the flow conditions encountered, and other factors. Figure 8 shows the boat paths and secondary plane orientation for S1xs3-S1xs5 during the bankfull flow. While reasonable agreement between the boat paths and secondary plane are seen at S1xs3 and S1xs5, significant differences occur at S1xs4. An area of vegetation near the inner bank not visible in the aerial photograph forced the boat paths to diverge from the planned course. This region shows spatial variability in channel topography and likely flow characteristics as well. The variability in topography can be seen in Figure 7 by

examining the flow depths measured with FV and MV procedures at S1xs4p4 and S1xs4p5. The difference in the boat paths and the FV measurement locations along with the changes in bathymetry suggest that the MV transects and FV measurements at S1xs4p4 and S1xs4p5 are measuring regions where the flow may not be considered homogeneous. Whenever possible, the location of a cross section should be selected so that sufficient boat access is available to perform transects.

The different definitions of the primary flow direction all provide a means to visualize three-dimensional velocity data in an orthogonal coordinate system. Figure 9 shows the mean secondary velocity profiles at S1xs3 for the bankfull flow considering three different definitions: (1) Rozovskii, (2) Paice, and (3) channel geometry. As noted previously, the Rozovskii definition produces a flow direction for each profile (see Table 1) making the presentation of velocity in Figure 9 somewhat misleading. At this cross-section, the range of flow directions from the Rozovskii definition is 9.4° with a mean value close to the primary flow direction determined with the Paice definition. Despite this agreement differences in the secondary velocity patterns are seen in two profiles: S1xs3p2 and S1xs3p5. The flow direction based on the channel geometry differs from that of the Paice definition by more than 10°. The strong curvature of the meander bend directs the flow towards the outer bank in the vicinity of the apex as shown in Figures 2 and 8. By not considering the flow conditions, the channel geometry definition results in a significantly different pattern of secondary velocity. The spanwise component using the channel geometry definition is directed almost entirely towards the outer bank obscuring the circulation pattern observed with the Paice definition. The results presented in Figure 9 highlight two advantages of the Paice definition when presenting secondary velocity

profiles at a cross-section: (1) the velocity at each profile occurs in the plane as shown and (2) the orientation of the secondary plane is determined by the flow characteristics at the site, clarifying secondary velocity patterns of small magnitude and removing the need for decisions regarding channel orientation. The fact that both cross-sections at Site 5 show similar secondary velocity profiles with the Paice and channel geometry definitions for both discharges demonstrates that results of the two definitions diverge as channel curvature increases.

3.6 Conclusions

A methodology has been proposed to quantify the mean 3D velocity distribution in natural rivers using a boat-mounted ADCP. The approach benefits from the advantages of the different survey procedures. The high spatial resolution of MV transects define the coordinate system for cross sections and establish the cross-section bathymetry. FV measurements obtained along the cross section provide mean 3D velocity profiles at discrete locations. The methodology can be adapted to present spatially-averaged velocity from MV measurements and time-averaged velocity from FV measurements in the stream-based coordinate system. Comparing 65 mean velocity profiles obtained with both FV and MV procedures demonstrates that MV transects can often provide reasonable estimates of velocity magnitude profiles, streamwise velocity profiles, and local flow direction. The spanwise velocity profiles from the two survey procedures show sizeable differences likely stemming from the inability of the four transects obtained at each cross-section to adequately represent secondary velocity. This comparison demonstrates the need for high temporal resolution FV measurements to quantify mean secondary velocity components. Applying the methodology to a meander bend, several well-known flow features are captured

including a main circulation cell, an outer bank circulation cell, unidirectional flow over the inner bank, and separation at the inner bank.

The orientation of the coordinate system is specified with the Paice definition which has several advantageous characteristics. The flow direction is constant for a cross section allowing secondary velocity to be visualized in a single plane defined by the spanwise and vertical axes. Additionally, flow characteristics determine the flow direction, removing the uncertainty associated with geometric approaches to defining the flow direction in natural channels. The presentation of velocity data along cross section allows the field data to be integrated with numerical models to provide boundary conditions, calibration data, and validation data.

While the procedure performs well for the conditions encountered at the study site, further testing should be undertaken for a variety of flow conditions and channel geometries. For example, the procedure could be expanded to confluences where individual flow directions are computed from each tributary following the recommendation of *Lane et al.* [2000]. Studies at confluences and other complex flows may require further investigation of the effects of repeat transects and transect duration on the average flow direction.

Appendix A: Derivation of Equations to Calculate Discharge

Applying the Paice definition to MV transects requires that the streamwise or spanwise discharge be calculated for a specified angle of rotation. While the equations developed here are necessary to apply the Paice method, they are not meant to replace the traditional discharge calculation method. Derivations of the equation used to calculate the total discharge from a MV transect can

be found in *Christensen and Herrick* [1982] and *Simpson and Oltmann* [1993]. Derivation of the equation for the discharge in the streamwise flow direction is demonstrated and a similar procedure may be followed for the spanwise discharge. Discharge in a river is defined as

$$Q = \int\int_A \mathbf{V} \bullet \mathbf{n} dA \tag{A1}$$

where Q is the discharge across the surface A, $\mathbf{V}$ is the velocity vector of the river flow, $\mathbf{n}$ is the normal vector to A, and dA is the differential area of A. The surface A is specified by the angle of rotation and is the plane defined by the two axes mutually orthogonal to the primary flow direction as shown in Figure A1, i.e., the spanwise, n, and vertical, z, axes. By definition, A is perpendicular to the streamwise axis and, therefore, $\mathbf{n}$ is constant. The integrand in equation (A1) becomes

$$\mathbf{V} \bullet \mathbf{n} = u_s \tag{A2}$$

where u_s is the streamwise component of velocity. The differential area can be rewritten as

$$dA = dn\, dz \tag{A3}$$

where dn is the differential distance along the spanwise axis and dz is the differential distance along the vertical axis. The distance dn is found by projecting the boat path onto the plane A using the boat velocity in stream coordinates (see Fig. A1).

$$dn = V_{bn} dt \tag{A4}$$

where V_{bn} is the spanwise component of the boat velocity and dt is the differential elapsed time. Substituting equations (A2), (A3), and (A4) into equation (A1) yields the general equation for the discharge in the primary flow direction:

$$Q_s = \int_0^T \int_0^H u_s V_{bn} dz\, dt \tag{A5}$$

where T is the total elapsed time for the transect and H is the flow depth. The discrete form of equation (A5) is better suited for ADCP data. Following a similar approach to that presented by *Simpson* [2001, p. 27-29], the discharge in the primary flow direction for the ith ensemble is

$$Q_{si} = \sum_{j}^{m} u_{sj} \left(V_{bn}\right)_i \Delta t_i \Delta z \tag{A6}$$

where the ensemble contains $j = 1, 2, \ldots, m$ bins, u_{sj} is the primary velocity component of the jth bin, $(V_{bn})_i$ is the spanwise component of the boat velocity of the ensemble, Δz is the bin size, Δt_i is the time elapsed between ensembles i and i–1. Summing over all ensembles provides the total discharge in the primary direction:

$$Q_s = \sum_{i}^{k} Q_{si} \tag{A7}$$

where the transect contains $i = 1, 2, \ldots, k$ ensembles. Following a similar procedure, the discharge in the secondary direction for the ith ensemble and the total secondary discharge are calculated with equations (1) and (2).

Notation

H flow depth (m)

n unit normal vector

Q discharge ($m^3\ s^{-1}$)

Q_n discharge in the spanwise direction ($m^3\ s^{-1}$)

Q_s discharge in the streamwise direction ($m^3\ s^{-1}$)

u_n spanwise velocity ($m\ s^{-1}$)

u_s streamwise velocity ($m\ s^{-1}$)

U depth-averaged streamwise velocity ($m\ s^{-1}$)

$\mathbf{V}$ river velocity vector (m s^{-1})

V_n spanwise boat velocity (m s^{-1})

V_s streamwise boat velocity (m s^{-1})

y depth below water surface (m)

α streamwise flow direction (°)

Δt time elapsed between ensembles (s)

Δz bin size (m)

Acknowledgements

The authors acknowledge the financial support of Dominion, the U.S. Army Corps of Engineers, the Hydro Research Foundation, and the Edna Bailey Sussman Foundation. Ozan Celik and Nikos Apsilidis assisted with the field measurements. Bob Graham graciously provided a boat when engine trouble threatened to cut our field campaign short. The comments and criticisms of three anonymous reviewers and the associate editor have improved the presentation of this work.

References

Blanckaert, K. (2011), Hydrodynamic processes in sharp meander bends and their morphological implications, *J. Geophys. Res.*, *116*(F1), F01003. doi:10.1029/2010JF001806.

Blanckaert, K., and W. H. Graf (2001), Mean flow and turbulence in open-channel bend, *J. Hydraul. Eng.*, *127*(10), 835-847.

Christensen, J. L., and L. E. Herrick (1982), Final Report: DCP4400/300 Mississippi River Test Volume 1, report, prepared by AMETEK for U. S. Geol. Surv., El Cajon, CA.

De Vriend, H. J. (1979), Flow measurements in a curved rectangular channel, Internal Report 9-79, Delft University of Technology, Delft, The Netherlands.

Dietrich, W. E., and J. D. Smith (1983), Influence of the point-bar on flow through curved channels, *Water Resour. Res.*, *19*(5), 1173-1192.

Dinehart, R. L., and J. R. Burau (2005), Averaged indicators of secondary flow in repeated acoustic Doppler current profiler crossings of bends, *Water Resour. Res.*, *41*(9), W09405, doi:10.1029/2005WR004050.

Ferguson, R. I., D. R. Parsons, S. N. Lane, and R. J. Hardy (2003), Flow in meander bends with recirculation at the inner bank, *Water Resour. Res.*, *39*(11), 1322, doi:10.1029/2003WR001965.

Gordon, R. L. (1989), Acoustic measurement of river discharge, *J. Hydraul. Eng.*, *115*(7), 925-936.

Guerrero, M., and A. Lamberti (2011), Flow field and morphology mapping using ADCP and multibeam techniques: Survey in the Po River, *J. Hydraul. Eng.*, *137*(12), 1576-1587. doi:10.1061/ (ASCE)HY.1943-7 900.000046 4

Hey, R. D., and P. C. B. Rainbird (1996), Three-dimensional flow in straight and curved reaches, in *Advances in Fluvial Dynamics and Stratigraphy*, edited by P. A. Carling and M. R. Dawson, pp. 33-66, John Wiley, Chichester, UK.

Hupp, C. R., E. R. Schenk, J. M. Richter, R. K. Peet, and P. A. Townsend (2009), Bank erosion along the dam-regulated lower Roanoke River, North Carolina, in *Management and Restoration of Fluvial Systems with Broad Historical Changes and Human Impacts*, edited by L. A. James, et al., pp. 97-108. doi:10.1130/2009.2451(06).

Jamieson, E. C., C. D. Rennie, R. B. Jacobson, and R. D. Townsend (2011), 3-D flow and scour near a submerged wing dike: ADCP measurements on the Missouri River, *Water Resour. Res.*, *47*(7), W07544, doi:10.1029/2010WR010043.

Kikkawa, H., S. Ikeda, and A. Kitagawa (1976), Flow and bed topography in curved open channels, *J. Hydraul. Eng.*, *102*(9), 1327-1342.

Lane, S. N., K. F. Bradbrook, K. S. Richards, P. M. Biron, and A. G. Roy (2000), Secondary circulation cells in river channel confluences: measurement artefacts or coherent flow structures?, *Hydrol. Processes*, *14*(11-12), 2047-2071.

Leopold, L. B., R. A. Bagnold, M. G. Wolman, and J. L. M. Brush (1960), Flow Resistance in Sinuous or Irregular Channels, *Geological Survey Professional Paper 282-D*, U. S. Geol. Surv., Washington, D.C.

Markham, A. J., and C. R. Thorne (1992), Geomorphology of gravel-bed river bends, in *Dynamics of Gravel-bed Rivers*, edited by P. Billi, R. D. Hey, C. R. Thorne and P. Tacconi, pp. 433-450, John Wiley, Chichester.

Mueller, D. S., and C. R. Wagner (2009), Measuring Discharge with Acoustic Doppler Current Profilers from a Moving Boat, *U.S. Geological Survey Techniques and Methods 3A-22*, 72 pp., U.S. Geol. Surv., Reston, VA.

Muste, M., K. Yu, T. Pratt, and D. Abraham (2004a), Practical aspects of ADCP data use for quantification of mean river flow characteristics; Part II: fixed-vessel measurements, *Flow Meas. Instrum.*, *15*(1), 17-28, doi:10.1016/j.flowmeasinst.2003.09.002.

Muste, M., K. Yu, and M. Spasojevic (2004b), Practical aspects of ADCP data use for quantification of mean river flow characteristics; Part 1: moving-vessel measurements, *Flow Meas. Instrum.*, *15*(1), 1-16, doi:10.1016/j.flowmeasinst.2003.09.001.

Nam, S., M. Gutierrez, P. Diplas, and J. Petrie (2011), Determination of the shear strength of unsaturated soils using the multistage direct shear test, *Eng. Geol.*, *122*(3–4), 272-280, doi: 10.1016/j.enggeo.2011.06.003.

Nam, S., M. Gutierrez, P. Diplas, J. Petrie, A. Wayllace, N. Lu, and J. J. Munoz (2010), Comparison of testing techniques and models for establishing the SWCC of riverbank soils, *Eng. Geol.*, *110*(1-2), 1-10 doi: 10.1016/j.enggeo.2009.09.003.

Nanson, R. A. (2010), Flow fields in tightly curving meander bends of low width-depth ratio, *Earth Surf. Processes Landforms*, *35*(2), 119-135, doi: 10.1002/esp.1878.

Oberg, K., and D. S. Mueller (2007), Validation of streamflow measurements made with acoustic Doppler current profilers, *J. Hydraul. Eng.*, *133*(12), 1421-1432, doi:10.1061/(ASCE)0733-9429(2007)133:12(1421).

Paice, C. (1990), Hydraulic Control of River Bank Erosion: An Environmental Approach, PhD. thesis, School of Environmental Sciences, University of East Anglia, Norwich, UK.

Petrie, J., P. Diplas, M. Gutierrez, and S. Nam (2013), Data evaluation for acoustic Doppler current profiler measurements obtained at fixed locations in a natural river, *Water Resour. Res.*, *49*, 1-14, doi:10.1002/wrcr.20112.

RD Instruments (2007), *Work Horse Rio Grande Acoustic Doppler Current Profiler Technical Manual*, San Diego, Calif.

Rennie, C. D., and M. Church (2010), Mapping spatial distributions and uncertainty of water and sediment flux in a large gravel bed river reach using an acoustic Doppler current profiler, *J. Geophys. Res.*, *115*(F3), F03035, doi:10.1029/2009JF001556.

Rennie, C. D., R. G. Millar, and M. A. Church (2002), Measurement of bed load velocity using an acoustic Doppler current profiler, *J. Hydraul. Eng.*, *128*(5), 473-483.

Rozovskii, I. L. (1957), *Flow of Water in Bends of Open Channels* (in Russian), Acad. of Sci. of the Ukrainian SSR, Kiev. (English translation, Isr. Program for Sci. Transl., Jerusalem, 1961.)

Rüther, N., J. Jacobsen, N. R. B. Olsen, and G. Vatne (2010), Prediction of the three-dimensional flow field and bed shear stresses in a regulated river in mid-Norway, *Hydrol. Res.*, *41*(2), 145-152, doi:10.2166/nh.2010.064.

Shen, Y., and P. Diplas (2008), Application of two- and three-dimensional computational fluid dynamics models to complex ecological stream flows, *J. Hydrol.*, *348*(1-2), 195-214, doi:10.1016/j.jhydrol.2007.09.060.

Shen, Y., and P. Diplas (2010), Modeling unsteady flow characteristics of hydropeaking operations and their implications on fish habitat, *J. Hydraul. Eng.*, *136*(12), 1053-1066, doi:10.1061/(ASCE)HY.1943-7900.0000112.

Simpson, M. R. (2001), Discharge Measurements using a Broad-band Acoustic Doppler Current Profiler, *Open File Report 01-1*,123 pp., U. S. Geol. Surv., Sacramento, CA.

Simpson, M. R., and R. N. Oltmann (1993), Discharge-measurement System Using an Acoustic Doppler Current Profiler with Applications to Large Rivers and Estuaries, Water-Supply Paper 2395, 32 pp., U. S. Geol. Surv., Reston, VA.

Sukhodolov, A. N. (2012), Structure of turbulent flow in a meander bend of a lowland river, *Water Resour. Res.*, *48*(1), W01516, doi:10.1029/2011WR010765.

Szupiany, R. N., M. L. Amsler, J. L. Best, and D. R. Parsons (2007), Comparison of fixed- and moving-vessel flow measurements with an aDp in a large river, *J. Hydraul. Eng.*, *133*(12), 1299-1309, doi:10.1061/(ASCE)0733-9429(2007)133:12(1299).

Thorne, C. R., L. W. Zevenbergen, J. C. Pitlick, S. Rais, J. B. Bradley, and P. Y. Julien (1985), Direct measurements of secondary currents in a meandering sand-bed river, *Nature*, *315*(6022), 746-747.

Tominaga, A., I. Nezu, K. Ezaki, and H. Nakagawa (1989), Three-dimensional turbulent structure in straight open channel flows, *J. Hydraul. Res.*, *27*(1), 149-173.

Tsubaki, R., Y. Kawahara, Y. Muto, and I. Fujita (2012), New 3-D flow interpolation method on moving ADCP data, *Water Resour. Res.*, *48*(5), W05539, doi:10.1029/2011WR010867.

Table 1. Summary of FV velocity profiles

		Mean Annual Flow				Bankfull Flow			
		U (m s^{-1})	H (m)	Rozovskii flow direction (°)	translation distance (m)	*U* (m s^{-1})	H (m)	Rozovskii flow direction (°)	translation distance (m)
S1xs1	p1	0.52	5.1	92.5	7.1	0.86	7.7	92.9	6.9
	p2	0.65	4.7	95.7	9.2	0.99	7.3	94.0	0.6
	p3	0.63	4.6	91.8	6.3	0.92	7.3	95.2	0.6
S1xs2	p1	0.71	6.4	131.2	9.8	0.90	9.5	132.5	15.6
	p2	0.66	5.7	134.1	7.2	1.01	9.0	130.5	13.9
	p3	0.68	4.9	132.3	10.6	0.96	8.3	133.0	15.3
	p4	0.70	3.5	125.7	4.6	0.99	6.7	129.7	12.6
S1xs3	p1	0.46	5.7	173.8	8.8	0.73	9.9	167.5	10.5
	p2	0.64	8.3	166.7	8.3	0.99	11.4	170.6	15.2
	p3	0.68	5.8	166.0	6.2	1.00	9.2	168.3	10.9
	p4	0.56	4.6	167.1	1.7	0.88	7.6	167.1	1.0
	p5	0.21	2.2	162.2	9.3	0.69	5.2	161.2	11.1
S1xs4	p1	0.44	6.2	227.8	8.1	0.89	5.8	198.1	17.3
	p2	0.51	11.0	232.4	8.2	0.92	12.2	206.0	18.2
	p3	0.58	13.5	190.0	13.7	0.88	16.7	196.7	20.1
	p4	0.48	11.8	188.0	8.9	0.82	13.7	185.9	14.1
	p5	-0.02	7.8	77.3	5.2	0.52	11.0	187.4	12.4
S1xs5	p1	0.48	4.5	221.7	15.1	0.54	5.4	222.3	9.0
	p2	0.57	8.7	223.3	16.7	0.91	12.0	228.9	3.2
	p3	0.56	7.1	227.2	16.4	0.88	10.3	231.9	13.3
	p4	0.57	5.2	227.1	17.4	0.79	8.2	236.3	5.9
	p5	0.41	3.8	228.9	8.3	0.47	5.4	233.9	11.2
S1xs6	p1	0.75	7.0	256.9	2.5	1.06	10.5	268.2	0.2
	p2	0.61	5.5	257.8	14.6	0.98	7.8	266.8	8.8
	p3	0.61	4.0	260.7	1.5	0.87	7.2	267.9	4.4
	p4	---	---	---	---	0.70	6.2	265.9	5.4
S5xs1	p1	0.61	3.2	177.9	4.3	0.69	6.3	180.3	2.9
	p2	0.72	3.3	183.2	1.0	0.89	7.0	185.4	0.7
	p3	0.65	4.0	180.5	3.9	0.94	7.4	186.6	4.7
	p4	0.71	4.7	180.1	10.2	0.81	8.1	182.8	9.5
S5xs2	p1	0.57	3.2	174.8	0.7	0.72	6.4	176.3	3.6
	p2	0.65	3.5	174.9	0.4	0.86	6.9	176.2	4.9
	p3	0.72	4.0	173.6	3.7	0.98	7.7	175.5	7.7
	p4	0.71	5.0	171.3	3.7	0.89	8.3	175.3	8.4

Table 2. Percent difference in velocity and absolute difference in flow direction between mean velocity profiles obtained from FV and MV procedures.

	Velocity magnitude		Primary velocity		Flow direction
	mean	max	mean	max	
		mean annual flow			
range	3.2-58%	9.4-96%	3.1-36%	9.5-94%	0.04-42°
median	10.8%	20.4%	11.3%	23.3%	3.6°
		bankfull flow			
range	5.3-42%	14.9-76%	5.6-43%	15.1-73%	0.4-12.7°
median	8.6%	25.6%	8.9%	25.3%	3.3°

Table 3. Direction of primary flow from MV transects and channel geometry (°)

	mean annual flow			bankfull flow			channel geometry
	mean	std dev	range	mean	std dev	range	
S1xs1	92.6	1.5	3.5	92.4	2.3	4.8	93.7
S1xs2	130.1	4.8	10.8	127.3	4.4	9.1	132.8
S1xs3	166.8	3.4	7.6	166.7	2.5	6.1	180.3
S1xs4	189.3	10.9	23.8	186.2	1.9	4.3	204.4
S1xs5	224.4	6.0	14.4	231.3	1.7	3.9	229.3
S1xs6	263.9	0.8	1.7	266.1	0.8	1.8	264.8
S5xs1	185.1	2.0	4.5	184.5	1.9	3.9	185.7
S5xs2	174.0	4.3	9.2	176.3	1.2	2.7	173.8

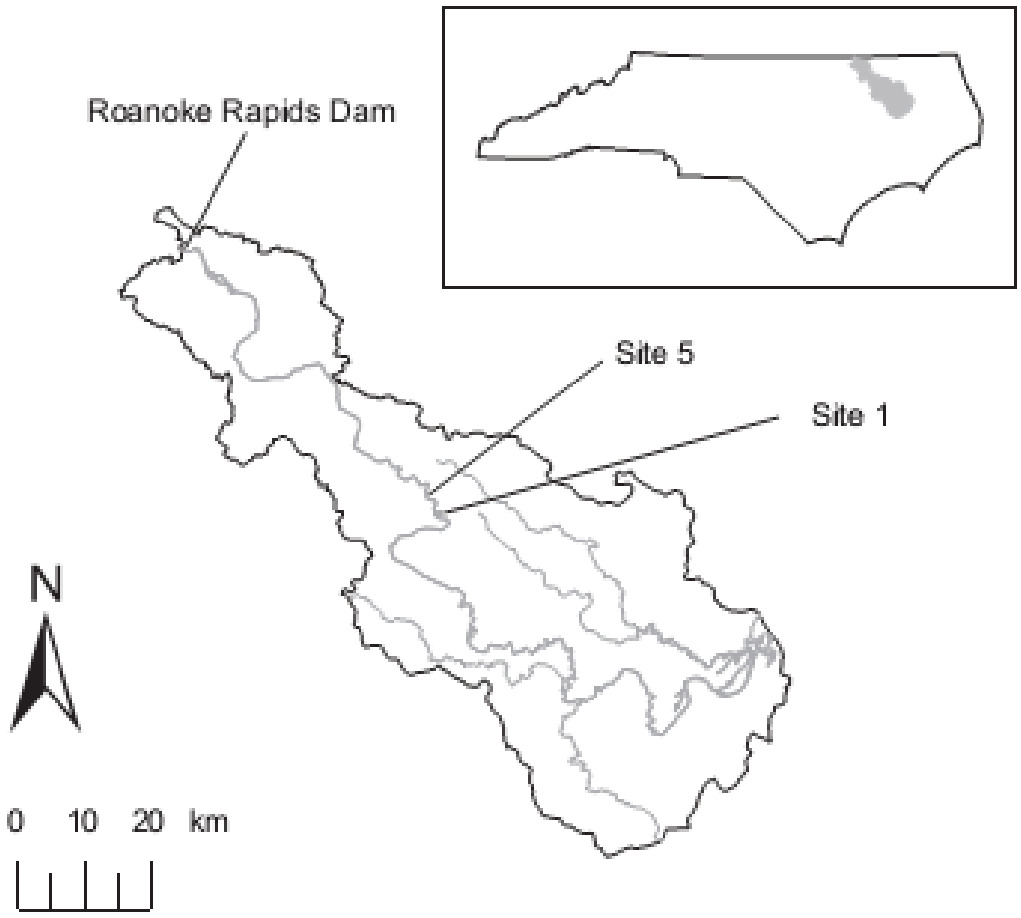

Figure 1. Map of the portion of the lower Roanoke River watershed located within North Carolina. The location of the watershed in North Carolina is shown in gray in the box [from *Petrie et al.*, 2013].

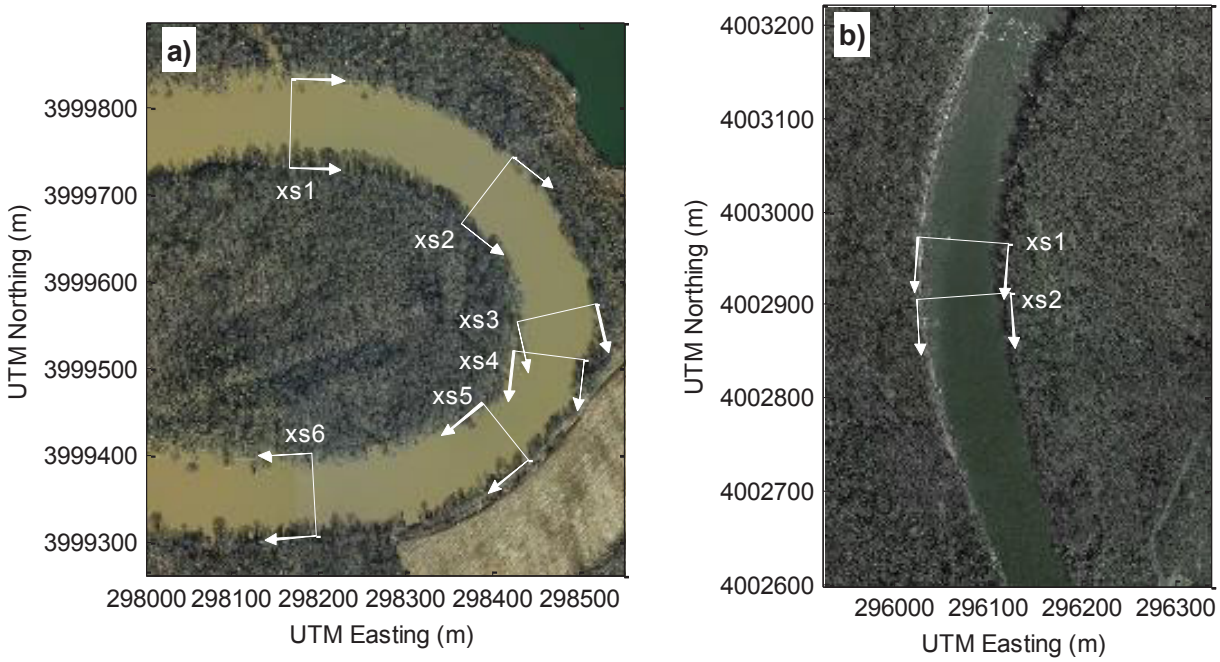

Figure 2. Orientation of the streamwise and spanwise axes at each cross-section during the bankfull flow for (a) Site 1 and (b) Site 5.

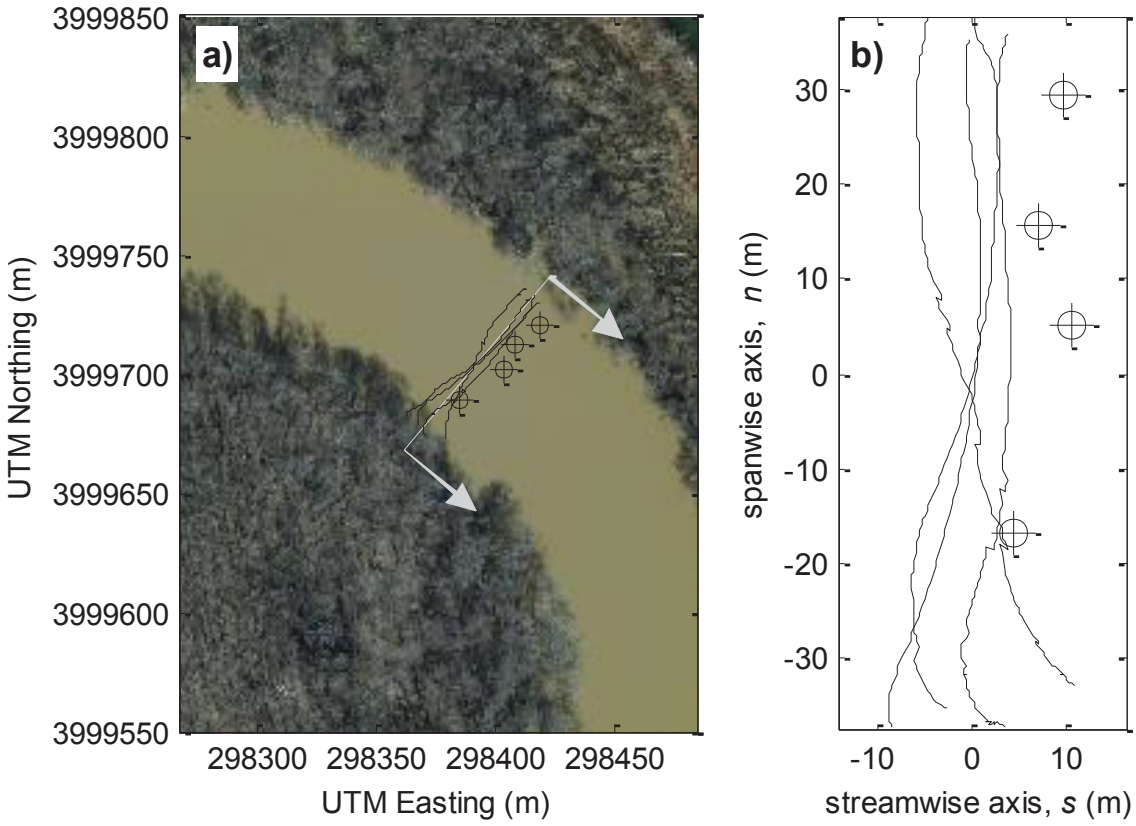

Figure 3. Locations of MV transects (black lines) and FV profiles (targets) at S1xs2 during the mean annual flow in (a) geographic coordinates and (b) stream coordinates.

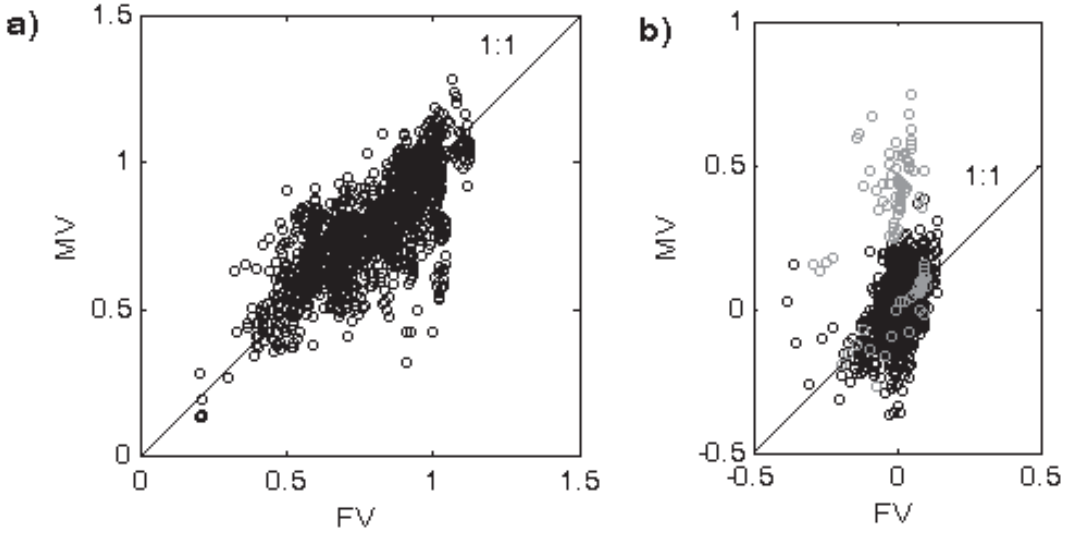

Figure 4. (a) Mean streamwise velocity, us (m s-1) and (b) mean spanwise velocity, un (m s-1) for all bins at each cross-section measured with FV and MV survey procedures.

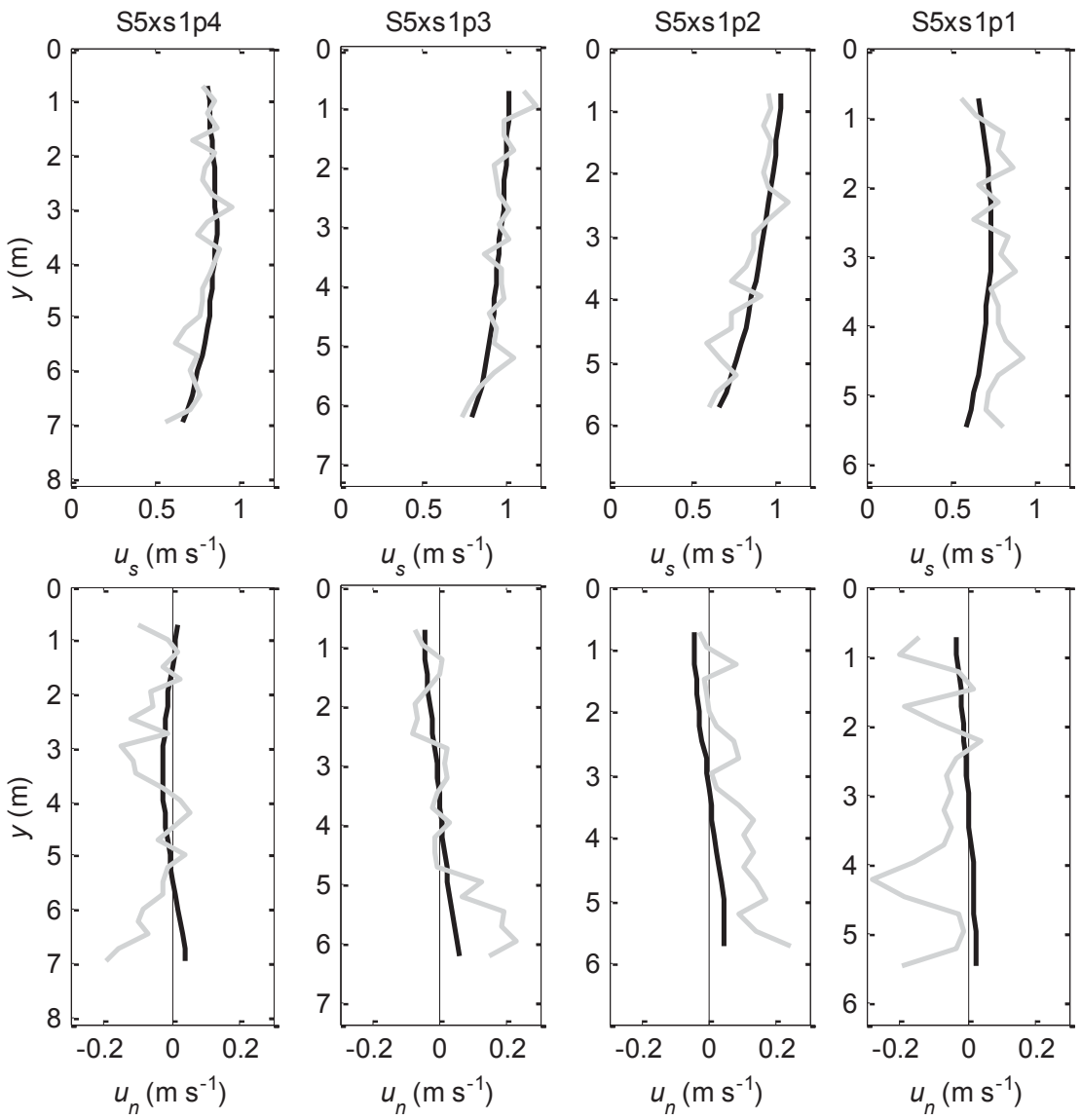

Figure 5. Streamwise and spanwise mean velocity profiles from FV (black) and MV (gray) measurements at S5xs1 during the bankfull flow.

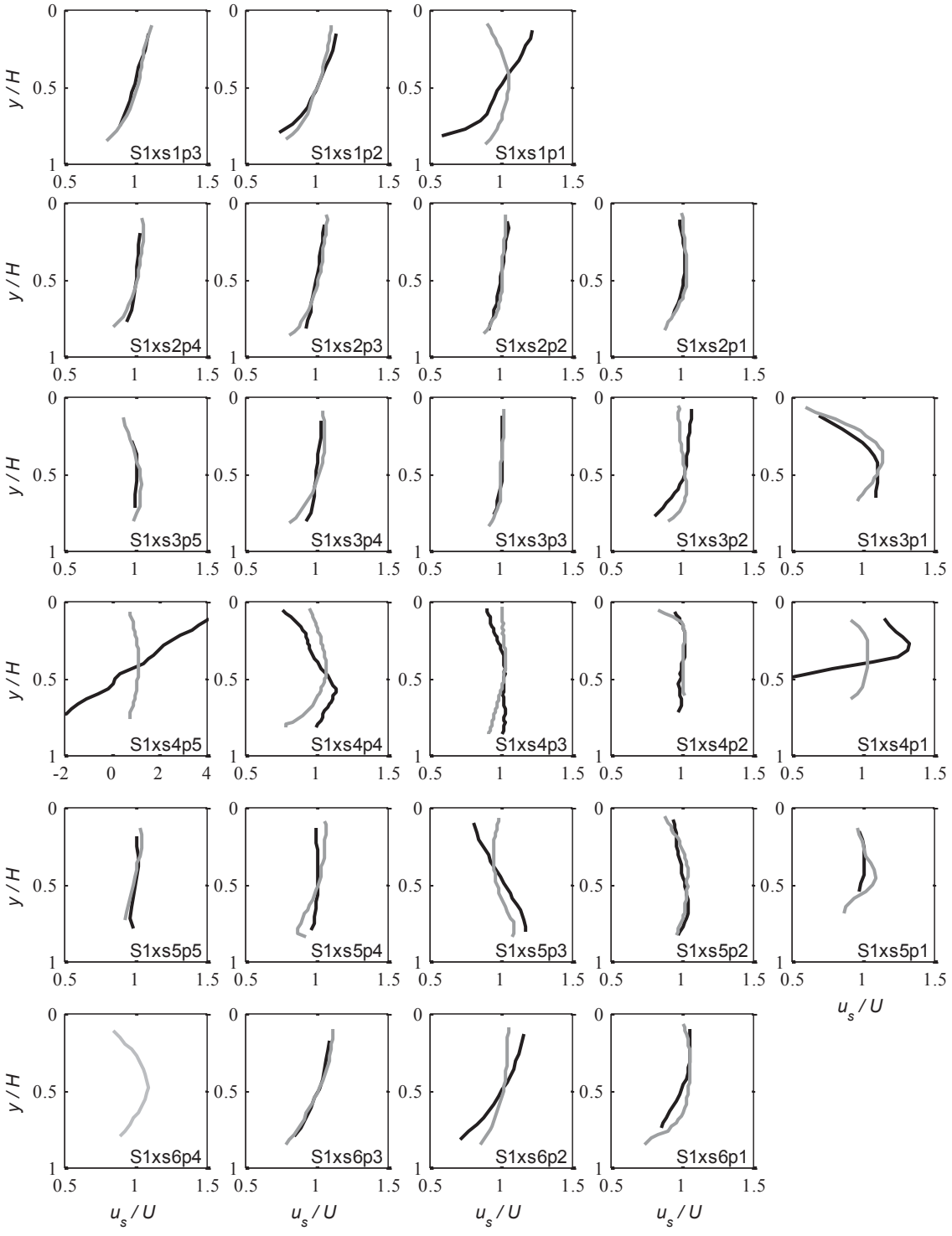

Figure 6. Mean primary velocity profiles at Site 1 for the mean annual flow (black) and bankfull flow (gray).

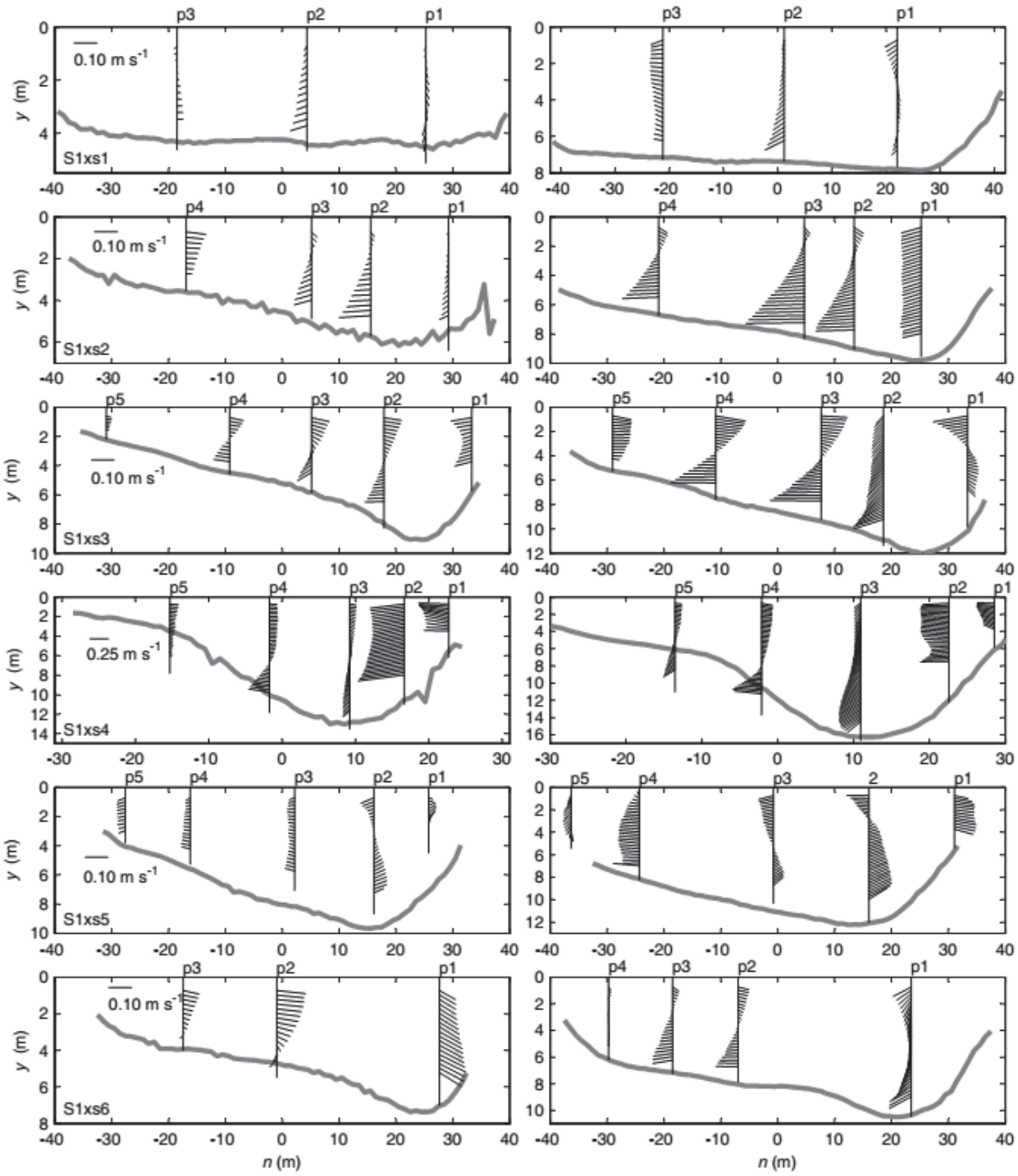

Figure 7. Mean secondary velocity profiles at Site 1 for the mean annual flow (left column) and bankfull flow (right column). The primary flow direction is out of the page.

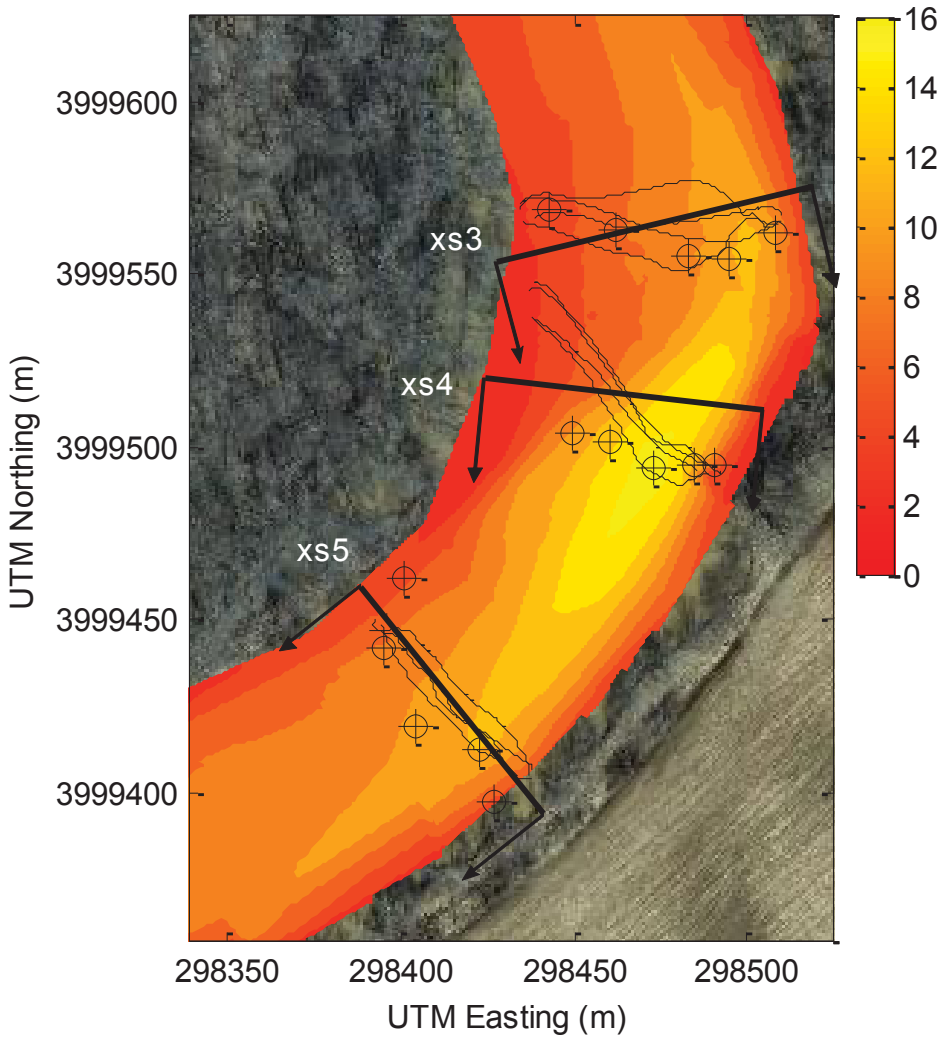

Figure 8. The FV locations (targets), boat paths for MV transects (thin lines), secondary plane orientation (thick lines) and primary flow direction (vector arrows) shown along with the measured flow depth (m) near the apex at Site 1for the bankfull flow.

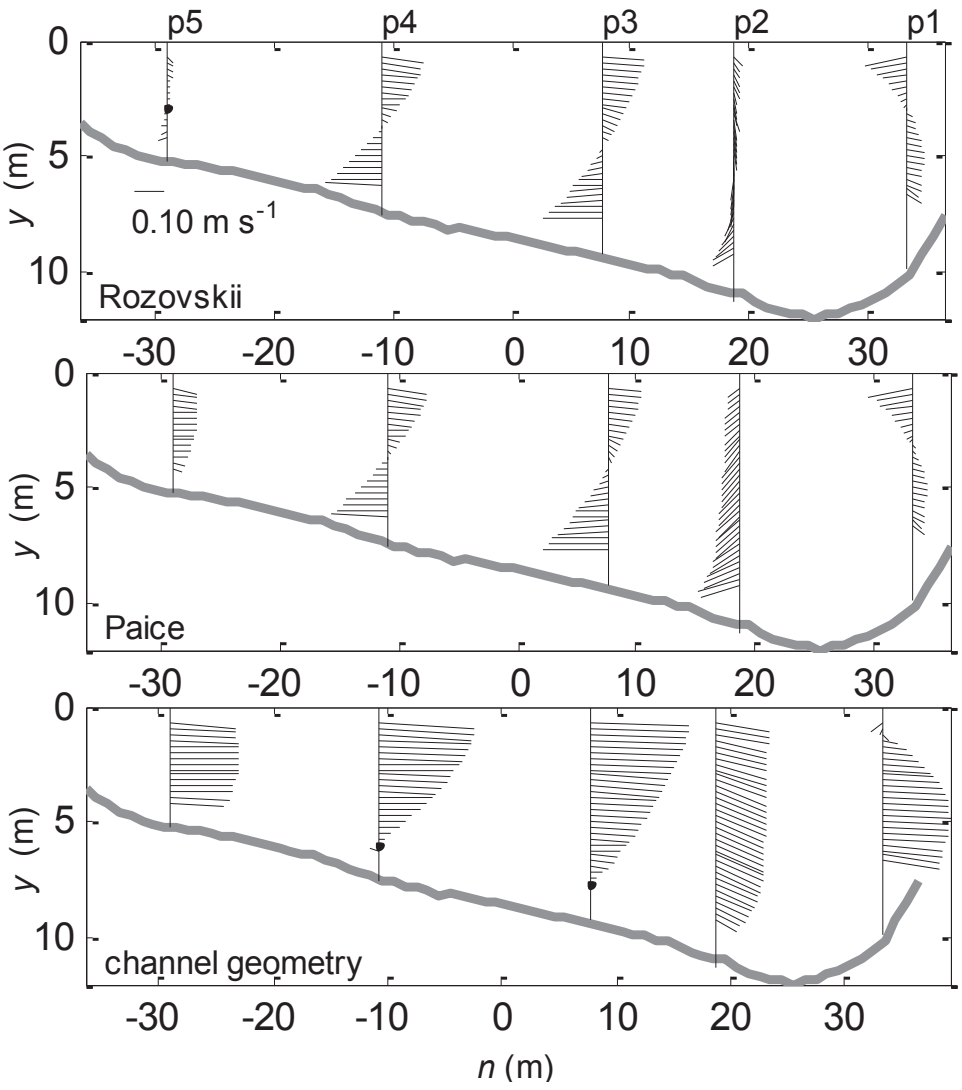

Figure 9. Secondary velocity profiles at S1xs3 for the bankfull flow using different definitions for the flow direction.

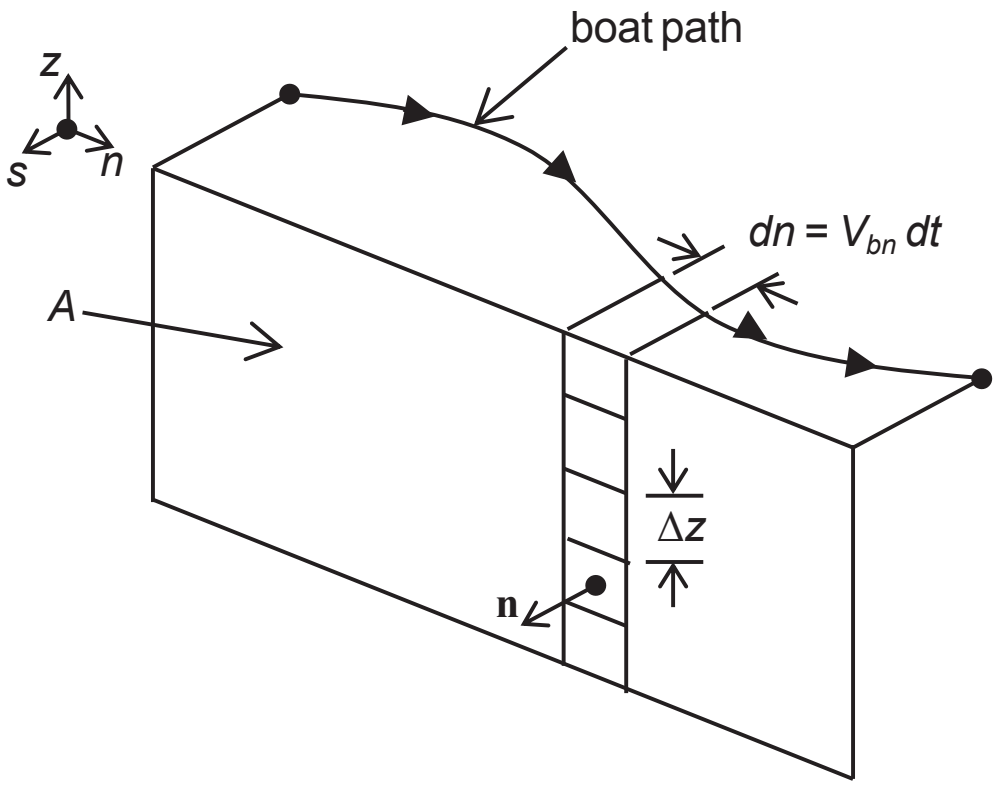

Figure A1. Definition sketch for calculating discharge in stream coordinates.

CHAPTER 4. CHARACTERIZING THE MEAN FLOW FIELD IN A RIVER FOR ASSESSING AND MONITORING HYDROKINETIC ENERGY GENERATION SITES

Abstract

The use of hydrokinetic technology for energy generation in rivers is an area of active research with potential applications in urban and remote rural settings. Negating the need for a physical barrier to the flow, in-stream hydrokinetic devices are believed to have less environmental impact than conventional hydropower. The introduction of any device that alters the flow field, however, has the potential to affect both the river and the ecosystem it supports. Characterizing the pre-installation flow conditions and monitoring changes following device installation is necessary to evaluate the ecological costs associated with this developing technology. This study presents techniques for quantifying the mean flow field throughout a study reach using an acoustic Doppler current profiler (ADCP). Depending on the stage of the project, quantities ranging from bulk flow features, such as discharge, to mean fully three-dimensional velocity profiles can be obtained. Two survey procedures are employed to determine the mean velocity profiles to best capture the spatial and temporal variation in velocity during the measurement period. In addition to environmental studies, these measurements are valuable for designing turbines and installations.

4.1 Introduction

Rivers have served as an energy source for much of human history from waterwheels to hydroelectric dams. As society seeks renewable and sustainable sources of energy to meet growing demands, hydrokinetic devices in rivers have received increasing attention. By

harnessing the kinetic energy of flowing water, hydrokinetic energy generation can be seen as an alternative to hydropower dams in low gradient regions. Questions remain regarding the actual recoverable potential of this resource. *EPRI* [2012] performed an assessment of non-tidal rivers in the continental United States with mean annual flows greater than 28 m^3 s^{-1}. The total theoretical resource was found to be 1,381 TW h yr^{-1}. There is much uncertainty, however, when determining the recoverable amount [*NRC*, 2013]. While the economic feasibility of large-scale development of this resource in developed countries is unclear, rural communities in developing countries may benefit greatly from in-stream hydrokinetic energy [*Anyi and Kirke*, 2010; 2011].

Although much can be learned from the more mature technologies of wind and tidal energy, rivers have their own unique challenges. Unlike both tidal and wind environments, river flows are typically unidirectional with a relatively predictable bulk flow direction. Depending upon the hydrologic setting, however, river velocity and flow depth can display a high degree of both spatial and temporal variability. These conditions must be considered when evaluating potential sites, as well as when designing turbines and installation, where much of the developed knowledge is not in the public domain [*Khan et al.*, 2008]. Furthermore, debris management has been recognized as a critical performance issue for hydrokinetic devices in rivers [*Anyi and Kirke*, 2010].

In addition to energy considerations, potential effects on the river morphology and supported habitat require thorough investigation. While hydrokinetic devices may directly impact aquatic species through strike, changes to the flow field may result in a number of alterations that can affect habitat [*Cada et al.*, 2007]. Changes in sediment transport rate can occur at both the local

and reach scales. Local scour around devices installed on the bed may compromise the structural integrity while also degrading local water quality. The transport of both sediment and debris within the reach may be impacted by energy extraction and alteration of the flow field. Changes in sediment and debris transport over a reach will lead to changes in the grain-size distribution of the bed, affecting bottom dwelling-species. Other potential negative environmental effects include leaching of contaminants, such as paints and lubricants, as well as acoustic effects during device operation. Monitoring of both morphological and habitat alterations following hydrokinetic device installation is required as anthropogenic-induced changes have proven difficult to predict [*Ligon et al.*, 1995]. Rivers play an important role for rural communities in developing countries and the repercussions of any changes to the river and its habitat, such as fish that may be a vital food source, require careful consideration.

While preliminary resource assessments rely on historical data and simplified models [*EPRI*, 2012], high-resolution spatial and temporal data are needed to assess local sites, design and install hydrokinetic devices, and study environmental impacts. Full characterization of a potential site includes documenting channel bathymetry, hydrodynamics, sediment dynamics, vegetation, and habitat. Extensive field data collection is required and is only practical to consider following thorough resources assessment with publically available data [*EPRI*, 2012; *Spurlock*, 2008]. Once acquired, these data can be used as a baseline to monitor post-installation changes as well as help build high resolution, e.g. 3D hydrodynamic, numerical models of the study reach to assist in site assessment and environmental impact studies.

A boat-mounted acoustic Doppler current profiler (ADCP) is particularly well-suited for hydrodynamic data collection in rivers. The two commonly used survey procedures, moving-vessel (MV) and fixed-vessel (FV), provide flexibility when considering data requirements and time constraints based on the various stages of project development. MV surveys result in measurements of three-dimensional (3D) velocity and flow depth as the boat traverses the river, where a single pass across the channel is called a transect. This relatively quick field procedure allows the determination of bulk flow characteristics, such as discharge, as well as mapping of bathymetry and depth-averaged velocity. Because the location of velocity measurements is continually changing, time-averaged or mean velocity profiles cannot be determined from MV transects. Additionally, the flow measured during a transect is not instantaneous as the turbulent flow field is changing as the boat traverses the channel. Thus, MV results are influenced by spatial and temporal changes that occur over the course of a transect. A commonly used statistical approach to analyze turbulent flow data involves decomposing the velocity time series at a location into mean and fluctuating components [*Tennekes and Lumley*, 1972]. FV measurements, where the ADCP is held at a fixed location in the river while recording, are needed to determine the mean, or time-averaged, velocity. The temporally-rich FV measurements require an increased field effort when compared to MV transects. For this reason, recent work has focused on spatial-averaging or interpolation of multiple MV transects to represent "mean" velocity profiles [*Szupiany et al.*, 2007; *Rennie and Church*, 2010]. At present, no clear guidelines exist for spatial-averaging of MV data and *Petrie et al.* [*in review*] demonstrate poor agreement between MV and FV results for secondary velocity components. Therefore, applications requiring the vertical distribution of mean velocity, such as determining the flow field entering the swept area of a turbine, benefit from FV measurements. In addition to

flow velocity and depth measurements, ADCP techniques have been demonstrated to measure bed load velocity [*Rennie and Church*, 2010] and suspended load concentration [*Dinehart and Burau*, 2005].

In this work, field survey and analysis procedures for both MV and FV boat-mounted ADCP measurements are presented using data obtained on the lower Roanoke River in eastern North Carolina, USA. While a comparison of velocity using spatial-averaging with MV transects and time-averaged with FV measurements is provided, a complementary approach is also described exploiting the relative advantages of each procedure. The data presented here are taken from an extensive field campaign to quantify the hydrodynamics of a larger study reach [*Petrie et al.*, 2013, *in review*]. The example reach was selected due to its potential as a site for a hydrokinetic device. At the present there is no plan to develop this resource on the lower Roanoke River. Thus, this work is a desk-based study exploring localized field surveys of river hydrodynamics.

4.2 Methodology

4.2.1 Field Site

The field survey was carried out in June 2009 at the study site on the lower Roanoke River in North Carolina, USA shown in Figure 1. This study site is located near the apex of a mild meander bend and is part of a reach on the lower Roanoke River that has been the focus of an intensive field campaign to characterize the hydrodynamic and geotechnical characteristics [*Nam et al.*, 2010, 2011; *Petrie et al.*, 2013, *in review*]. The discharge at the study site is primarily controlled by the Roanoke Rapids Dam—located approximately 72 km upstream. The dam was operating under flood control during the field measurements which resulted in a steady

discharge, Q, of about 565 $m^3 s^{-1}$ and a mean flow depth, H, of 7.1 m. The discharge measured at the Roanoke Rapids gaging station (U.S. Geological Survey (USGS) 2080500), located 7 km downstream from the dam, is provided in Figure 2. This figure also shows the measured gage heights at the nearest gaging stations: USGS 2081000 at Scotland Neck and USGS 2081022 at Oak City. Further details on the lower Roanoke River can be found in [*Hupp et al.*, 2009] and [*Petrie et al.*, 2013].

4.2.2 Field Equipment

The ADCP measures the velocity along beams emitting acoustic pulses into the water column. These pulses, or pings, reflect off scatterers resulting in a frequency shift which is converted to a velocity with the Doppler principle. ADCPs with three or more beams can resolve the velocity along the beams into three-dimensional (3D) Cartesian components. Velocity measurements are averaged within discrete depth cells called bins. A single measured velocity profile is an ensemble and may be contain a single ping or multiple pings that are averaged. Physical limitations of the technology prevent velocity measurements near the channel bed or water surface [*Simpson*, 2001]. For this study, a bin size of 0.25 m was used for all measurements. All FV measurements created ensembles with 20 sub-pings sent 50 milliseconds apart while the MV measurements used 1 sub-ping sent 70 milliseconds for most measurements. Data was collected using Water Mode 12 and Bottom Mode 5 [*Mueller and Wagner*, 2009]. Global positioning system (GPS) was used as the velocity reference for all measurements due to observed bed motion. Further details on ADCP operational principles can be found in [*Simpson*, 2001] and [*Mueller and Wagner*, 2009].

The ADCP, a 1200 kHz Workhorse Rio Grande by RDI Teledyne, and GPS, Trimble DSM 232, were mounted to an Oceanscience tethered boat which was secured to the starboard (right) side of a motor boat with rope. The motor boat held the operators and laptops for data acquisition. Field site locations were found during deployment with surveying software, HYPACK LITE (HYPACK, Inc.).

4.2.3 Field Measurement Procedures

ADCP measurements were performed along two cross-sections oriented approximately perpendicular to the banks as shown in Figure 1b. MV measurements were performed following the recommended procedure for measuring discharge [*Mueller and Wagner*, 2009] with four transects obtained at each cross-section. For the FV measurements, the boat was secured in the river channel using anchors. Once the boat and ADCP were in place, a minimum record length of 1200 s was obtained for all locations. The nomenclature used to describe each FV locations includes the cross section and profile number, e.g. xs1p1, where profile 1 is closest to the left bank when facing downstream. Four FV measurements were obtained at each cross-section (Fig. 3). The field survey required approximately 1 day with a three person crew. Further discussion of the field survey procedures are found in [*Petrie et al.*, 2013, *in review*].

4.2.4 Data Analysis Procedures

The software provided by the ADCP manufacturer is designed for data collection and calculation of discharge. Given the lack of standardized or commercially available software, particularly for FV measurements, customized codes were developed in MATLAB® for the analysis described

here. All data marked "bad" by the ADCP data collection software were removed or replaced. For FV measurements, bins marked as "bad" were removed from the record while spatial averaging from adjacent bins was used to replace velocity in "bad" bins for the MV measurements. All flow depths marked "bad" were removed from the record. No smoothing or filtering of the data were performed. Directional errors were observed in ensembles found at the end of transects due to the boat turning as the bank was approached. The affected ensembles were removed from the record. The results of the quality assurance procedure developed by *Petrie et al.* [2013] demonstrated that all FV measurements provided accurate measurements of mean velocity.

The ADCP software outputs velocity in geographic coordinates with east, north, and vertical components. River velocity is typically rotated to a stream-based coordinate system with streamwise, s, spanwise, n, and vertical, z, components. The horizontal geographic components are rotated to the stream-based coordinate system by the flow direction—measured clockwise from the north axis. The vertical component remains unchanged for both coordinate systems. The flow direction may be defined locally [*Bathurst et al.*, 1977] or along a cross section [*Paice*, 1990]. The local flow direction, α_l, often call the Rozovskii flow direction, is defined along a vertical profile as the direction which produces a zero net discharge in the spanwise direction. The local flow direction is calculated for ADCP measurements by

$$\tan\alpha_l = \frac{\sum_{j=1}^{m} U_{Ej}}{\sum_{j=1}^{m} U_{Nj}} \tag{1}$$

Where the profile contains j = 1, 2,…, m bins, U_{Nj} = the north velocity component of the j^{th} bin, and U_{Ej} = the east velocity component of the j^{th} bin, and α_l = the local flow direction. Equation (1) may be applied to individual ensembles from MV transects or time-averaged velocity profiles from FV measurements. The cross-sectional, α_{cs}, or Paice, flow direction is defined as the direction which produces a zero net spanwise discharge at the cross-section. A brute force algorithm is applied to determine the cross-sectional flow direction by calculating the discharge in the spanwise direction for all angles of rotation, selecting the angle that produces a discharge of zero. Spanwise discharge is calculated by

$$Q_n = \sum_{i=1}^{k}\sum_{j=1}^{m} u_{nj}(V_s)_i \Delta t_i \Delta z \qquad (2)$$

where the transect contains i = 1, 2, …, k ensembles and each ensemble contains j = 1, 2, …, m bins, u_{nj} = the spanwise velocity component of the j^{th} bin, $(V_s)_i$ = the streamwise component of the boat velocity for the ensemble, Δt_i = time elapsed between ensembles i and i–1, and Δz = the bin height. Note that the cross-sectional flow direction can only be determined from MV transects. Following the approach used for discharge determination with an ADCP, the results of multiple transects are averaged to find the cross-sectional flow direction.

A unified framework is needed to present spatially varying velocity data from both survey procedures. This is accomplished using section straightening [*Dinehart and Burau*, 2005] where velocity measurements are translated to a vertically-oriented, secondary plane representing a cross-section. The horizontal orientation of this plane is determined by the cross-sectional flow direction [*Petrie et al.*, *in review*]; thus, the plane is defined by the spanwise and vertical axes. The origin of the spanwise axis is arbitrarily set to the mean location of the MV transects to approximate the channel centerline. An advantage of this approach is that, due to the use of the

cross-sectional flow direction, spanwise and vertical velocity patterns within the secondary plane occur as shown. The orientation of the streamwise and spanwise axes at both cross-sections is provided in Figure 1b.

While MV transect cannot determine mean velocity profiles in the time-averaged sense, spatial averaging of multiple transects is often performed to reduce the uncertainty inherent in single ensembles [*Szupiany et al.*, 2007]. Following a similar approach to *Szupiany et al.* [2007], the velocity data from all MV transects are translated to the secondary plane and ensembles within a specified distance from the location of interest are averaged to create a spatially-averaged, mean profile. When comparing mean velocity profiles from MV transects to those from FV measurements, the ensembles used to create the spatially-averaged profile are within a specified search distance along the spanwise axis from the FV measurement.

The spatial and temporal resolution of the different survey procedures allows a range of velocity values to be specified from the cross section to local scale. The bulk, or cross-sectionally-averaged, velocity is determined by $U_b = Q/A$ where Q = discharge through the cross-section and A = area of the cross-section. A single transect provides estimates of both discharge and flow area. The results of multiple transects can be averaged to reduce the uncertainty in the bulk velocity. The depth-average velocity along a profile is

$$U = \frac{1}{m}\sum_{j=1}^{m} u_{sj} \qquad (3)$$

where the profile contains $j = 1, 2, \ldots, m$ bins, u_{sj} = the streamwise velocity component of the j^{th} bin. Equation (3) can be applied to individual ensembles from MV transects or mean velocity profiles from FV measurements. The direction of the depth-averaged velocity is equivalent to the

local flow direction. The vertical distribution of the mean streamwise velocity along a profile with a fully-rough boundary can be represented with the law of the wall or log law

$$\frac{u_s}{u_\tau} = \frac{1}{\kappa}\ln\left(\frac{z}{k_s}\right) + 8.5 \quad (4)$$

where u_s = streamwise velocity, u_τ = shear velocity = $(\tau_o/\rho)^{0.5}$, τ_o = boundary shear stress, ρ = fluid density, κ = von Kármán constant = 0.41, z = elevation above the bed, and k_s = characteristic roughness. Despite the fact that the log law was derived for two-dimensional flows over flat boundaries, it is often applied to velocity profiles in natural rivers [*Bathurst*, 1997]. The local flow direction minimizes the spanwise component and should be used to determine the streamwise velocity when considering the log law.

Measured velocity profiles are often used with the log law to determine the shear velocity and characteristic roughness by linear regression [*Rennie and Church*, 2010; *Petrie et al.*, 2013]. A visual survey of the streamwise velocity profiles at the study site indicated that the velocity profiles deviated from logarithmic as elevation from the bed increased. Accordingly, the extent of the logarithmic region was visually judged for each profile and only bins within the logarithmic region were used for the regression analysis. Each regression used a minimum of three bins.

4.3 Results

4.3.1 Bulk Flow Properties

The bulk flow properties, summarized in Table 1, are the average result of the four transects performed at each cross-section. The discharge and bulk velocity show good agreement between the two cross-sections. Both measured discharges, however, under predict the reported discharge

at the gaging station with the value at xs1 differing by almost 5%. This difference may be due to the fact that the study reach is not well suited for discharge measurements at the encountered flow. The flood control releases resulted in the water surface level rising above both bank edges. The presence of low-lying trees at the bank edges prevented the boat from accessing the near-bank region as well as obscured the bank edge location needed to estimate discharge in the unmeasured portion of the channel. Despite these complications, 5% is considered the acceptable range for differences amongst transects at a cross section [*Mueller and Wagner*, 2008]. Hydrologic conditions may have also contributed to the change in discharge over the 68 km from the gaging station to the study reach, including losses to groundwater and temporary storage on floodplains.

4.3.2 Flow Depth, Depth-averaged Velocity, and Flow Direction

The measured flow depth ranged from 5.0 to 8.5 m on the study reach. Flow depth interpolated from MV transects is shown in Figure 3. In addition to the four transects at each cross-section, five additional transects performed within the study reach were used for the flow depth interpolation. Typical of meander bend geometry, the flow depth increases towards the outer bank. Figure 3 also shows vectors of the mean depth-averaged velocity at each FV location. The magnitude and direction of these depth-averaged velocities are provided in Table 2. The flow directions closely follow the channel curvature and there is good agreement between the cross-sectional and local flow direction. The maximum absolute difference between the two definitions is 4.2° with a median difference of 1.0°. The accuracy of the ADCP compass is 2° [*RD Instruments*, 2007]. The distribution of depth-averaged velocity is fairly uniform in both magnitude and direction along each cross section. Additionally, the maximum value occurs at

profile 3 while the minimum occurs at profile 1 for both cross-sections. Higher velocities are usually seen on the outer half of the channel in bends.

Depth-averaged velocity may also be found from MV transects for individual ensembles or spatial averaging multiple ensembles. The mean depth-averaged velocity magnitudes from the FV measurements are shown with the depth-averaged velocity magnitude for individual ensembles from each MV transect in Figure 4. This figure demonstrates that individual ensembles can provide reasonable estimates of the mean, time-averaged, depth-averaged velocity magnitude; however, several locations do see significant differences, e.g. xs1p1 and xs2p3. To improve estimates from MV measurements, ensembles from multiple transect can be spatially-averaged. Table 3 summarizes the percent difference in depth-averaged velocity magnitude and absolute difference in flow direction between results from FV measurements and spatially-averaged MV transects considering search distances of 1, 2, 5, and 10 m. The spatial-averaged results are in reasonable agreement for both the magnitude and direction. The velocity magnitude is within 10% for all locations and search distances with median differences less than 4%. The maximum difference in flow direction is about 6° with median values of three search distances less than 2°. The number of ensembles within each search interval is also provided in Table 3. As expected, the number of ensembles increases with search distance. When selecting the appropriate search distance, features such as the distribution of depth-averaged velocity (Fig. 4) and flow depth (Fig. 3) should be considered so that ensembles obtained in regions that may have differing flow characteristics are not included in the spatial average.

4.3.3 Mean 3D Velocity Profiles

Mean 3D velocity profiles for all FV measurements are shown along with channel topography in the form of measured flow depth in Figure 5. In this figure, the horizontal axes are the same scale while the vertical axis is exaggerated to better reveal the variation of velocity with depth. The vertical velocity component, however, is the same scale as the horizontal components.

While plots like Figure 5 are useful for visualizing the velocity field in relation to the channel topography, the large streamwise component makes it difficult to interpret flow patterns in the spanwise and vertical directions. Velocity profiles can be decomposed into orthogonal components to clarify the 3D velocity field. Following the approach presented in [*Petrie et al.*, *in review*], Figures 6 and 7 provide the streamwise components and the spanwise and vertical components. The streamwise velocity profiles are typical for natural river flows with the velocity increasing from the channel bottom to near the water surface. A velocity dip—where the maximum velocity occurs below the water surface due to factors including secondary velocity patterns and wind—is seen in several profiles. The maximum streamwise velocity observed in each profile ranges from about 0.75 to just over 1.0 m s^{-1} and occurs in the upper half of the flow depth. The secondary components in the spanwise and vertical direction are typically about 5% of the streamwise component or less with a maximum of about 10% found at xs2p3. The middle profiles, 2 and 3, at both cross-sections indicate a main circulation cell is present with flow towards the outer bank near the water surface and towards the inner bank near the channel bottom. A more complex pattern appears at profile 4 which could indicate the presence of an outer bank circulation cell.

In addition to the mean components determined from FV measurements, spatially-averaged components from MV transects using a search distance of 5 m are shown in both Figure 6 and 7. For the streamwise component, ensembles from the MV transects within the search distance from the FV measurement location were averaged. For the secondary components, profiles were generated every 10 m using ensembles from the MV transects within the search distance from the profile location. This was done to illustrate the distribution of secondary velocity within each cross-section. For all components the time-averaged profiles show a smoother velocity distribution due to the larger number of ensembles averaged to create the mean profile. The spatially-averaged streamwise profiles agree well with the time-averaged profiles, reproducing the general distribution as well as reasonably predicting the magnitude. The secondary components, however, show differences in both magnitude and direction at multiple locations. Despite these differences, the general secondary velocity patterns are in agreement between the two survey procedures.

4.3.4 Log law regression fit

The results of the regression fit to the log law are given in Table 2. All profiles pass the general criteria established by [*Petrie et al.*, 2013] to evaluate linear regression fits to the log law. Each profile is described well by a general logarithmic equation as demonstrated by the high R^2-values. Between three and five bins closest to the channel bottom were used for each regression fit. The boundary shear stress, τ_o, ranges from 1.25 to 10.6 Pa with a median value of 3.78; while the k_s-values range from 0.02 to 3.0 m with a median of 0.172 m. At both cross-sections, the minimum τ_o- and k_s-values occur at profile 1 while the maximum values are found at profile 2. Due to the fact that the bed of the lower Roanoke River is comprised primarily of sand, the k_s-

values indicate that bed forms are likely present at the study reach. High resolution bathymetry measurements, such as those produced by a multibeam echo sounder, are required to describe the bed form geometry.

4.4 Discussion

An advantage of the boat-mounted ADCP for quantifying flow properties is the flexibility provided by the different survey procedures. After several sites have been identified as potential locations for hydrokinetic installations using publically available data and simplified models [*Spurlock*, 2008; *EPRI*, 2012], MV transects can be obtained throughout each reach. This initial survey provides the basic flow depth and velocity data, both bulk and depth-averaged, to evaluate the energy and economic potential of specific reaches. Depending on the length of the study reach and available time for field surveys, multiple transects should be obtained due to the increased accuracy of spatial-averaging for mean velocity. Mean depth-averaged velocities can be used to calculate the theoretical power density, $P/A_t = 0.5\ \rho U^3$, where P = power, A_t = swept area of the turbine, and ρ = density of water. The distribution of theoretical power density along each cross section is shown in Figure 8. The power density is calculated for MV transects every 5 m using a search distance of 5 m to create the spatial average and good agreement is seen with the value calculated from the depth-averaged velocity from the FV measurements. Considering the distribution of power density along with the channel bathymetry (Fig. 3) allows regions with favorable flow depths and velocity for hydrokinetic devices. The actual power generated can be estimated for various devices based on turbine blade diameter and projected device efficiency.

Once a potential site has been identified, a detailed field campaign combining both MV and FV survey procedures quantifies the site hydrodynamics. While the cross-sections on the lower Roanoke River are separated by about 50 m, finer spacing is likely required at this stage, especially in the vicinity of the proposed hydrokinetic device location. FV measurements should be performed along cross-sections at the proposed device location as well as upstream and downstream. While relatively uniform cross-stream spacing was used on the lower Roanoke River, denser measurement spacing should be considered where the flow is most likely to be impacted by the operation of a hydrokinetic device. The locations of all cross-sections and FV measurements require careful documentation to allow repeat surveys to monitor post-installation changes. The detailed site characterization will provide flow depth measurements through the reach; however, to characterize bed forms, high resolution bathymetry measurements, such as with a multibeam echo sounder [*Parsons et al.*, 2005], are required. The time necessary to complete the field campaign depends on the size of the reach and number of proposed hydrokinetic devices. Based on the experience with the lower Roanoke River, the detailed measurements at this stage will require approximately one week.

The FV measurements will provide improved estimates of the power density and bed shear stress. The power density is proportional to the velocity cubed, meaning that differences in velocity measurements are magnified. Figure 8 demonstrates that reasonable estimates of depth-averaged velocity result in more substantial differences in power density. The final economic analysis of a site will benefit from power density calculated with time-averaged FV measurements. The boundary shear stress determined by fitting the streamwise velocity profile to the law of the wall is useful for quantifying the sediment dynamics at the site. While direct

measurements of boundary shear stress in the field are not possible, a number of approaches are available to indirectly determine the applied shear stress depending on the available data [*Wilcock*, 1996; *Biron et al.*, 2004]. The various techniques, however, may produce different estimates of shear stress [*Biron et al.*, 2004]. To evaluate the shear stress along each cross-section, the average boundary shear stress along the reach is calculated with $(\tau_o)_{ave} = \gamma HS$, where γ = specific weight of water, H = average flow depth, and S = channel slope. The channel slope was estimated using the gage data at Scotland Neck (USGS 2081000) and Oak City (USGS 2081022). The average value of 4.5 Pa agrees well with averages at each cross-section: 4.5 Pa at xs1 and 4.7 Pa at xs2. In addition to providing confidence in the shear stress estimates from the log law, this analysis also demonstrates the variability of bed shear stress within a reach.

Field surveys with a boat-mounted ADCP can provide the spatial distribution of velocity, both horizontal and vertical, throughout a reach. Temporal changes in velocity limit the time available for field surveys. Extended periods of steady discharge may be difficult to find for many rivers. The flow on regulated rivers is typically easier to predict than for unregulated rivers and may also contain periods of fairly steady flow. For example, the Roanoke Rapids Dam maintains constant releases on a weekly basis to preserve spawning habitat in the spring. Additionally, flood control releases are often maintained for a week or more (see Fig. 2), though the timing is difficult to predict. For large rivers, multiple vessels equipped with ADCPs may be required to fully characterize the hydrodynamics of the site for a steady discharge.

Surveys should be performed at a range of discharges, though this is rarely practical, as site hydrodynamics may change. For example, *Petrie et al.* [2013] identify a region of flow

recirculation in a meander bend at the mean annual flow that has either moved or is not present during flood control. The difficulty obtaining measurements representing the full range of conditions and, thus, characterizing the temporal variability of velocity for a site is a limitation of field surveys. Bottom-mounted ADCP may be left in place for longs periods of time, though it is generally not practical to install more than one device. This approach can be used at the proposed location of the hydrokinetic device to obtain better estimates of energy generation potential. High resolution numerical models are a practical alternative to quantifying temporal variability. The field techniques described here provide boundary conditions as well as calibration and validation data to build models of a study site. There are many challenges to modeling river flows at the field scale including complex geometry, turbulence modeling, water surface treatment, and sediment and vegetation dynamics. Field data is an important component in evaluating model results.

4.5 Conclusions

Presently, the field of riverine hydrokinetic devices has matured to the point where prototypes are in use both in developed areas and rural developing regions. To gain a better understanding of both the energy generation characteristics of these devices and their impact on the river environment requires careful monitoring at the field scale. The hydrodynamics in the vicinity of a hydrokinetic device control, in part, the energy generation potential of the device, channel morphology, and habitat. For this reason, documentation of the site hydrodynamics is necessary prior to installation with regular monitoring following installation. This data provides representative flows for turbine design and device installation as well as benchmark data for alterations to channel morphology as well as water and habitat quality. The measurements

described here demonstrate the range of data that can be collected with a boat-mounted ADCP using both MV and FV survey procedures. The appropriate field procedure can be selected based on the project stage and desired information. While this study focuses on quantifying the site hydrodynamics, further field surveys are needed to characterize the habitat, biology, and geochemistry of the site.

Acknowledgements

The authors acknowledge the financial support of Dominion, the U.S. Army Corps of Engineers, and the Hydro Research Foundation. Ozan Celik assisted with the field measurements. Bob Graham graciously provided a boat when engine trouble threatened to cut our field campaign short.

References

Anyi, M., and B. Kirke (2010), Evaluation of small axial flow hydrokinetic turbines for remote communities, *Energy Sustainable Dev.*, *14*(2), 110-116.

Anyi, M., and B. Kirke (2011), Hydrokinetic turbine blades: Design and local construction techniques for remote communities, *Energy Sustainable Dev.*, *15*(3), 223-230.

Bathurst, J. C. (1997), Environmental River Flow Hydraulics, in *Applied Fluvial Geomorphology for River Engineering and Management*, edited by C. R. Thorne, R. D. Hey and M. D. Newson, pp. 69-93, John Wiley & Sons Ltd.

Bathurst, J. C., C. R. Thorne, and R. D. Hey (1977), Direct measurements of secondary currents in river bends, *Nature*, *269*(5628), 504-506.

Biron, P. M., C. Robson, M. F. Lapointe, and S. J. Gaskin (2004), Comparing different methods

of bed shear stress estimates in simple and complex flow fields, *Earth Surf. Processes Landforms*, *29*(11), 1403-1415.

Cada, G., J. Ahlgrimm, M. Bahleda, T. Bigford, S. D. Stavrakas, D. Hall, R. Moursund, and M. Sale (2007), Potential impacts of hydrokinetic and wave energy conversion technologies on aquatic environments, *Fisheries*, *32*(4), 174-181.

Dinehart, R. L., and J. R. Burau (2005), Averaged indicators of secondary flow in repeated acoustic Doppler current profiler crossings of bends, *Water Resour. Res.*, *41*(9), W09405, doi:10.1029/2005WR004050.

EPRI (Electric Power Research Institute) (2012), Assessment & Mapping of riverine Hydrokinetic Resources in the US, *Technical Report 1026880*, 80 pp., EPRI, Palo Alto, CA.

Hupp, C. R., E. R. Schenk, J. M. Richter, R. K. Peet, and P. A. Townsend (2009), Bank erosion along the dam-regulated lower Roanoke River, North Carolina, in *Management and Restoration of Fluvial Systems with Broad Historical Changes and Human Impacts*, edited by L. A. James, et al., pp. 97-108. doi:10.1130/2009.2451(06).

Khan, M. J., M. T. Iqbal, and J. E. Quaicoe (2008), River current energy conversion systems: Progress, prospects and challenges, *Renewable Sustainable Energy Rev.*, *12*(8), 2177-2193.

Ligon, F. K., W. E. Dietrich, and W. J. Trush (1995), Downstream ecological effects of dams, *Bioscience*, *45*(3), 183-192.

Mueller, D. S., and C. R. Wagner (2009), Measuring Discharge with Acoustic Doppler Current Profilers from a Moving Boat, *U.S. Geological Survey Techniques and Methods 3A-22*, 72 pp., U.S. Geol. Surv., Reston, VA.

Nam, S., M. Gutierrez, P. Diplas, and J. Petrie (2011), Determination of the shear strength of unsaturated soils using the multistage direct shear test, *Eng. Geol.*, *122*(3–4), 272-280, doi: 10.1016/j.enggeo.2011.06.003.

Nam, S., M. Gutierrez, P. Diplas, J. Petrie, A. Wayllace, N. Lu, and J. J. Munoz (2010), Comparison of testing techniques and models for establishing the SWCC of riverbank soils, *Eng. Geol.*, *110*(1-2), 1-10 doi: 10.1016/j.enggeo.2009.09.003.

NRC (National Research Council) (2013), An Evaluation of the U.S. Department of Energy's Marine and Hydrokinetic Resource Assessments, 141 pp., National Academies Press, Washington D.C.

Paice, C. (1990), Hydraulic Control of River Bank Erosion: An Environmental Approach, PhD. thesis, School of Environmental Sciences, University of East Anglia, Norwich, UK.

Parsons, D. R., J. L. Best, O. Orfeo, R. J. Hardy, R. Kostaschuk, and S. N. Lane (2005), Morphology and flow fields of three-dimensional dunes, Rio Parana, Argentina: Results from simultaneous multibeam echo sounding and acoustic Doppler current profiling, *J. Geophys. Res.*, *110*(F4).

Petrie, J., P. Diplas, M. Gutierrez, and S. Nam (2013), Data evaluation for acoustic Doppler current profiler measurements obtained at fixed locations in a natural river, *Water Resour. Res.*, *49*, 1-14, doi:10.1002/wrcr.20112.

Petrie, J., P. Diplas, M. Gutierrez, and S. Nam (*in review*), Combining fixed- and moving-vessel acoustic Doppler current profiler measurements for improved characterization of the mean flow in a natural river, *Water Resour. Res.*

RD Instruments (2007), *Work Horse Rio Grande Acoustic Doppler Current Profiler Technical Manual*, San Diego, Calif.

Rennie, C. D., and M. Church (2010), Mapping spatial distributions and uncertainty of water and sediment flux in a large gravel bed river reach using an acoustic Doppler current profiler, *J. Geophys. Res.*, *115*(F3), F03035, doi:10.1029/2009JF001556.

Simpson, M. R. (2001), Discharge Measurements Using a Broad-band Acoustic Doppler Current Profiler, *Open File Report 01-1*,123 pp., U. S. Geol. Surv., Sacramento, CA.

Spurlock, D. S. (2008), Modeling Flows for Assessing Tidal Energy Generation Potential, M.S. Thesis, Department of Civil and Environmental Engineering, Virginia Polytechnic Institute and State University, Blacksburg, VA.

Szupiany, R. N., M. L. Amsler, J. L. Best, and D. R. Parsons (2007), Comparison of fixed- and moving-vessel flow measurements with an aDp in a large river, *J. Hydraul. Eng.*, *133*(12), 1299-1309, doi:10.1061/(ASCE)0733-9429(2007)133:12(1299).

Tennekes, H., and J. L. Lumley (1972), *A First Course in Turbulence*, 300pp., MIT Press, Cambridge, Mass.

Wilcock, P. R. (1996), Estimating local bed shear stress from velocity observations, *Water Resour. Res.*, *32*(11), 3361-3366.

Table 1. Bulk flow properties

	Q (m^3 s^{-1})	A (m^2)	U_b (m s^{-1})	α_{cs} (°)
xs1	537	686	0.78	184.5
xs2	556	716	0.78	176.3

Table 2. Summary of FV measurements

	U (m s^{-1})	H (m)	α_l (°)	τ_o (Pa)	k_s (m)	R^2
xs1p1	0.70	6.3	180.3	1.52	0.05	0.9976
xs1p2	0.89	7.0	185.4	8.83	2.32	0.9991
xs1p3	0.94	7.4	186.6	3.75	0.18	0.9989
xs1p4	0.81	8.1	182.8	3.83	0.46	0.9995
xs2p1	0.72	6.4	176.3	1.26	0.02	0.9999
xs2p2	0.86	6.9	176.2	10.64	3.00	0.9969
xs2p3	0.98	7.7	175.5	4.10	0.17	0.9988
xs2p4	0.89	8.3	175.3	2.64	0.11	0.9967

Table 3. Comparison of U determined from multiple MV transects to FV measurements

search distance (m)	1	2	5	10
percent difference in U				
median	3.9	3.9	3.1	3.4
max	8.2	6.8	7.3	8.4
absolute difference in α_l (°)				
median	3.5	1.9	1.5	1.2
max	6.4	5.5	2.7	3.0
number of MV ensembles				
mean	18	36	89	169

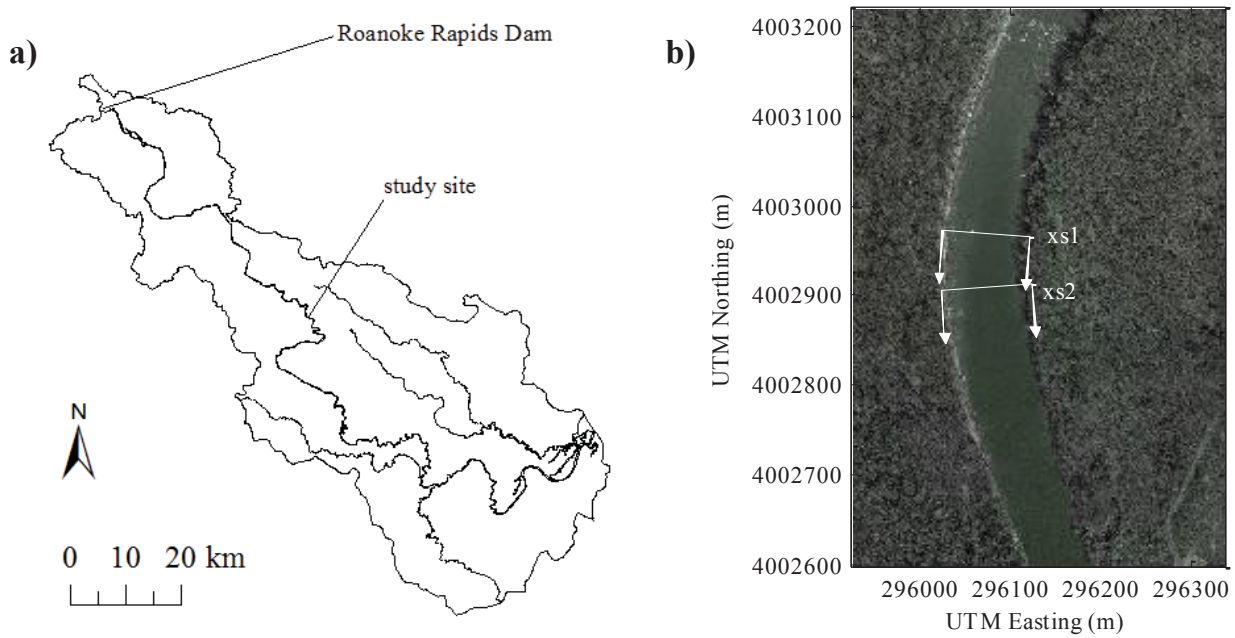

Figure 1. a) Map of the lower Roanoke River watershed in North Carolina. b) Locations of cross-section showing the cross-sectional streamwise and spanwise flow directions.

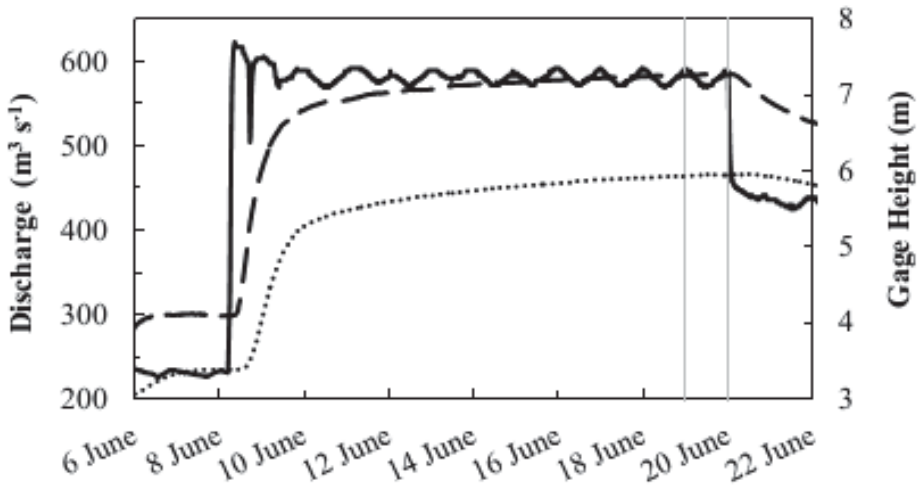

Figure 2. Discharge (Roanoke Rapids, solid line) and stage (Scotland Neck, dashed line, and Oak City, dotted line) during the field survey. The range of the field measurements is shown with gray lines.

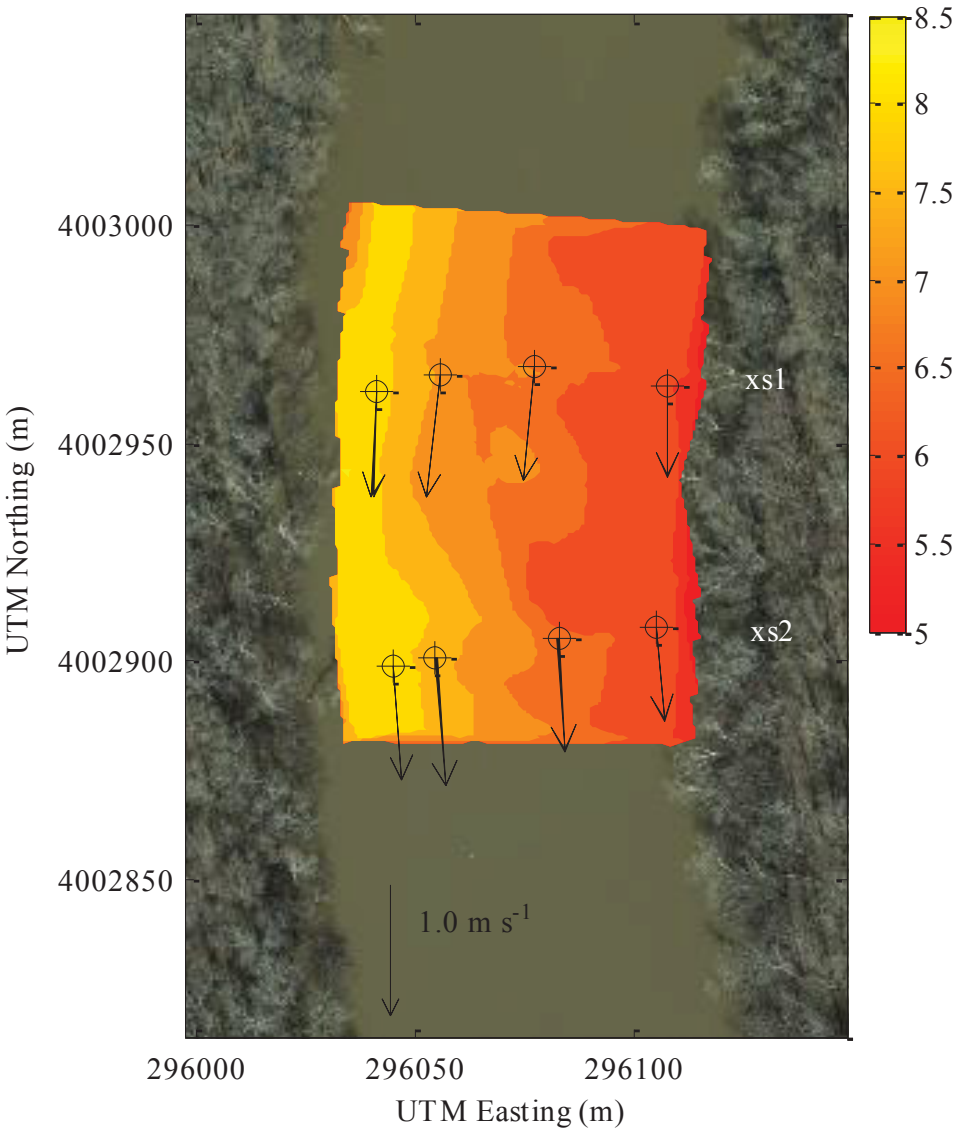

Figure 3. FV measurement locations, mean depth-averaged velocity vectors, and interpolated flow depth.

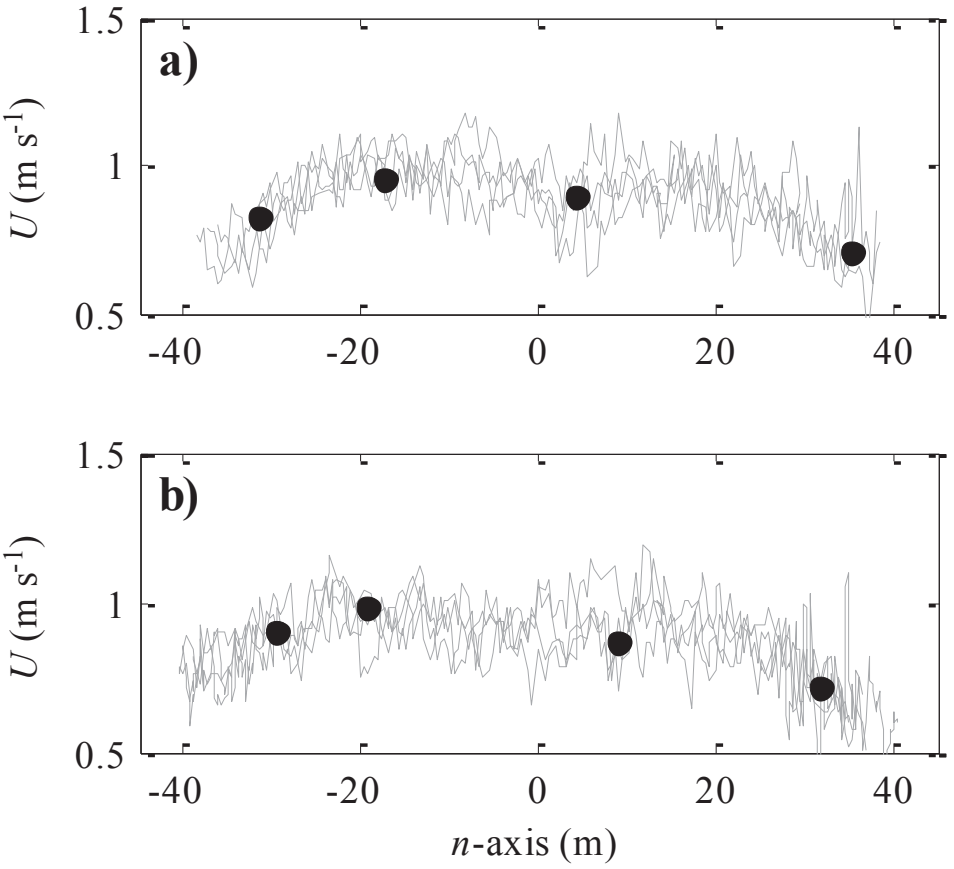

Figure 4. Magnitude of the depth-averaged velocity for the mean of all ensembles for FV measurements (circles) and individual ensembles for the MV transects (lines) at a) xs1 and b) xs2.

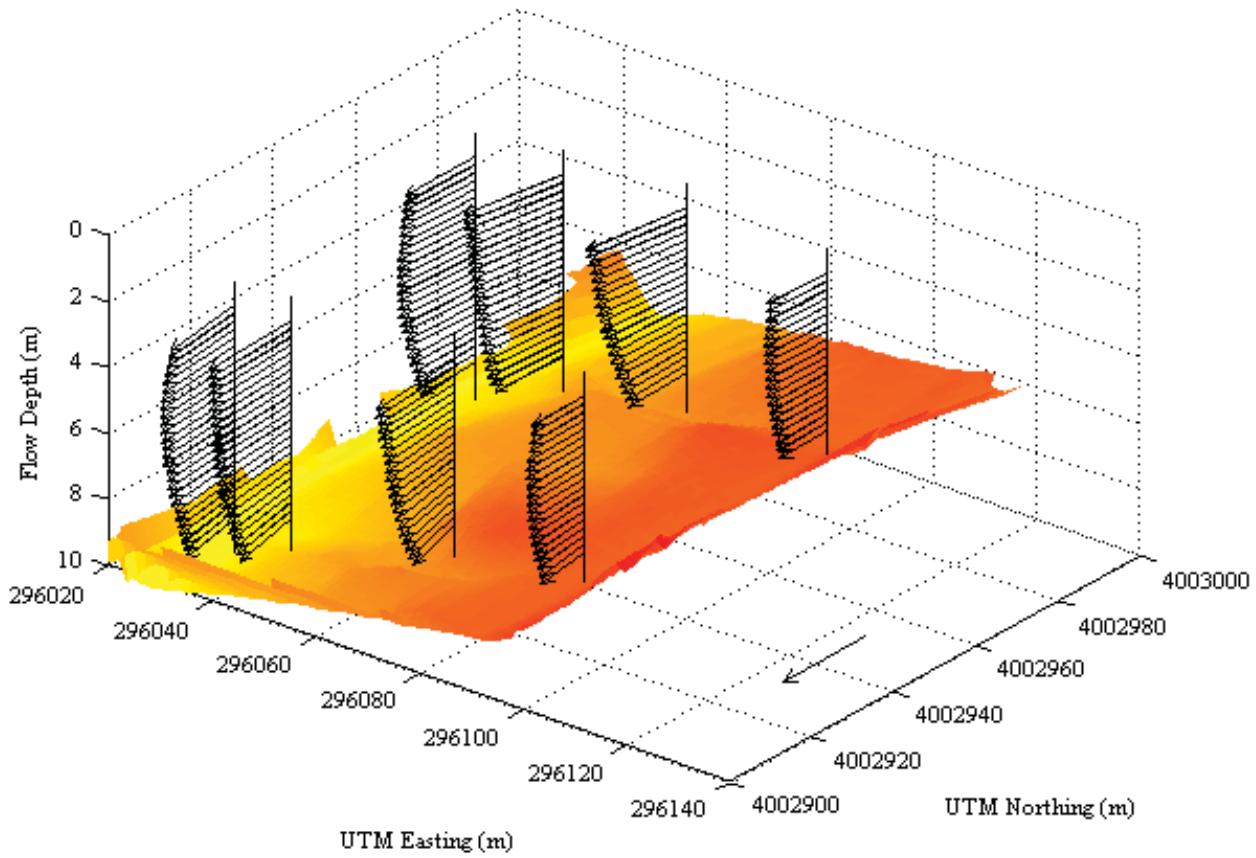

Figure 5. Mean 3D velocity vectors from FV measurements with interpolated flow depth. Reference arrow is 1.0 m s^{-1}. Flow depth scale is the same as Figure 3.

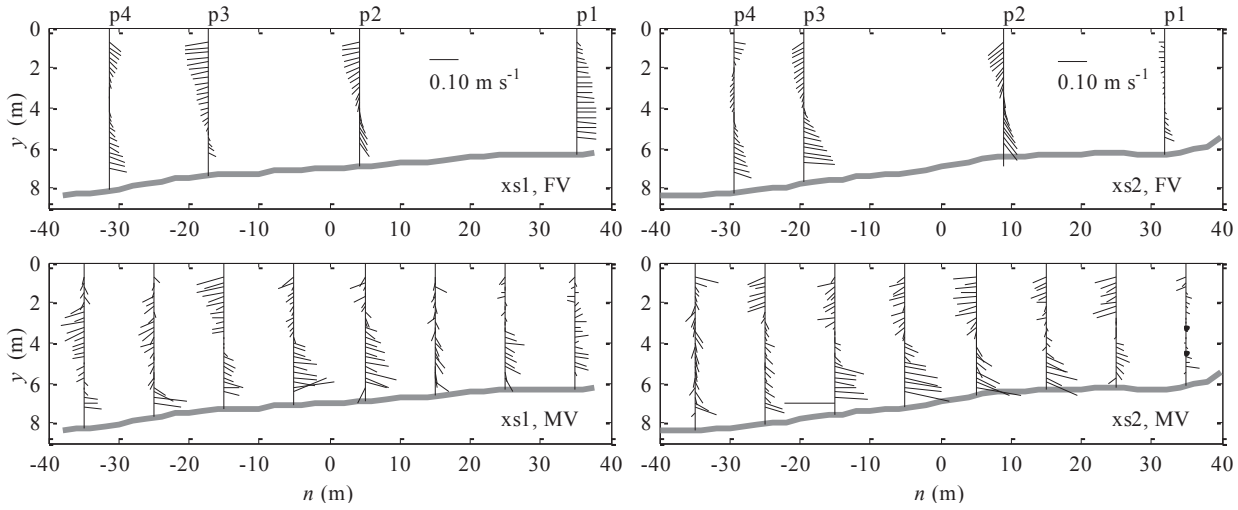

Figure 6. Mean spanwise and vertical velocity profiles at using both FV and MV measurements.

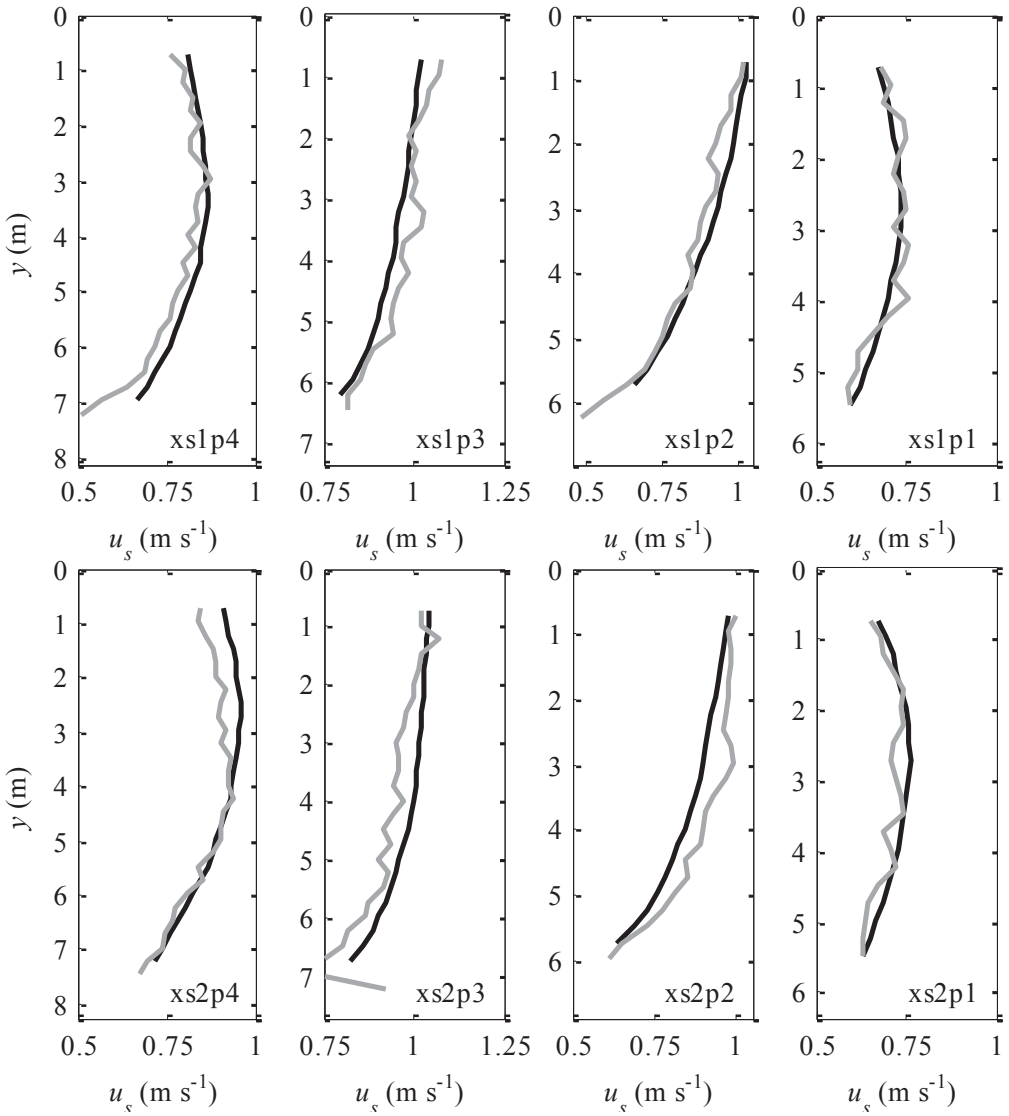

Figure 7. Mean streamwise velocity profiles using FV (black) and MV (gray) measurements.

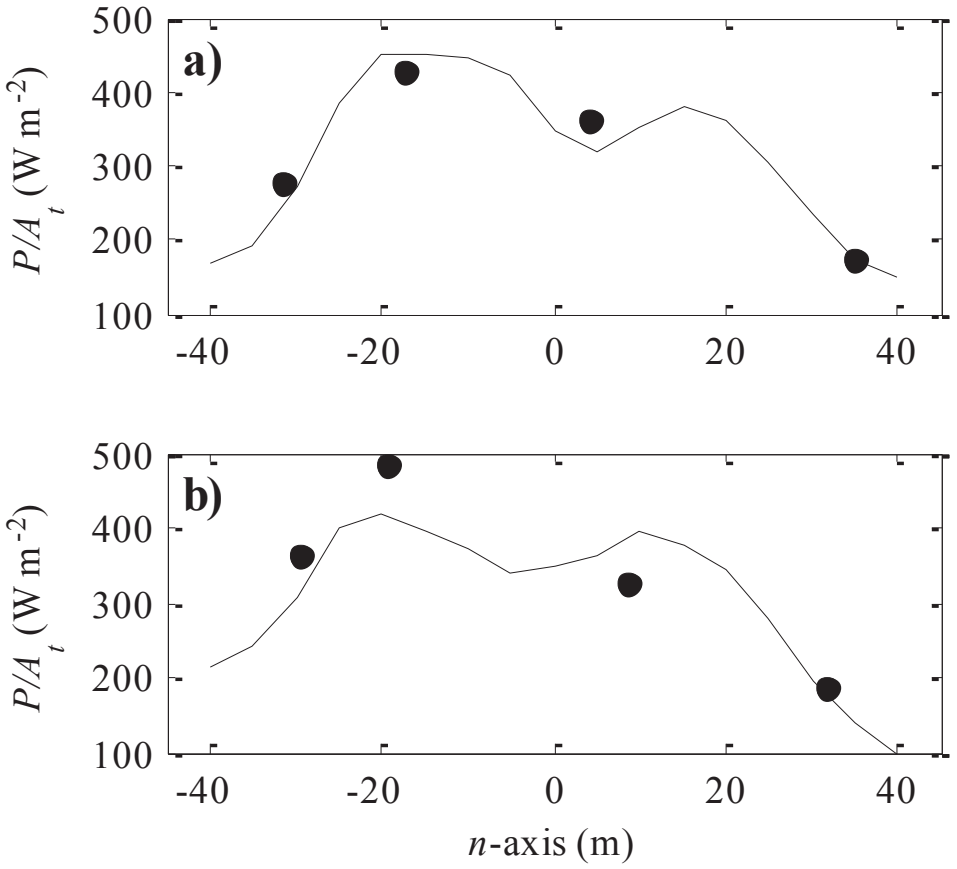

Figure 8. Distribution of power density for FV measurement (circles) and MV transects (lines) at a) xs1 and b) xs2.

CHAPTER 5. CONCLUSIONS

This research explores the use of ADCP measurements to quantify the mean flow field using data from the lower Roanoke River. Both MV and FV measurements were obtained along cross sections at two study sites for two steady discharges. This extensive dataset provides a unique opportunity to fully assess the ability of the ADCP to measure 3D velocity profiles in natural rivers.

FV surveys allow the mean 3D velocity profiles to be determined at discrete locations in the river channel. A technique employing two anchors and careful positioning of the boat was found to result in negligible motion of the ADCP for the duration of the measurement as well as during individual ensembles. A disadvantage of this procedure is that positioning the boat was found to require between 10 to 60 min, depending on location within the channel and flow conditions. Considering physical characteristics of both the flow and instrumentation, the stationarity of a velocity time series can be evaluated. The conditions during the field measurements on the lower Roanoke River were found to be stationary for both discharges. Given that such steady flow conditions are unlikely to be encountered for many field situations, an evaluation of stationarity is an important step prior to calculated mean velocity. The record length of 1200 s was found to be sufficient to both characterize the mean velocity and evaluate stationarity. The analysis of running statistics indicates that shorter records may be sufficient if stationarity of the flow field can be established a priori. The boundary shear stress applied by the flowing water to the bed can be estimated from the law of the wall. While derived for 2D flows over flat boundaries, the law of wall was found to produce reasonable results for many locations within the river. In general,

poor agreement between measured velocity profiles and the law of the wall can be attributed to (1) insufficient data to characterize the logarithmic region or (2) the law of the wall is not valid at this location, *e.g.* near the apex of a meander where highly 3D flow was observed. While FV measurements are time consuming to obtain, the results here demonstrate their utility for establishing the stationarity of the flow field, quantifying the mean velocity, and determining boundary shear stress and characteristic roughness.

Time-averaged velocity components are only available from FV surveys when using an ADCP. Spatial-averaging of MV velocity data from multiple transects has been used to approximate time-averaged velocity. Comparing streamwise and spanwise velocity components from the two survey procedures demonstrates that, while spatially-averaged MV transects can produce reasonable results at some locations, significant differences are predicted. This is especially true for the spanwise component where large velocity fluctuations are difficult to capture with MV procedures. To represent mean 3D velocity profiles, a hybrid methodology combining both MV and FV procedures is proposed. This methodology exploits the relative advantage of each procedure with MV transects providing the flow direction and bathymetry at a cross section and the mean velocity profiles determined with FV measurements. Defining the flow direction based on flow characteristics provides a consistent flow direction along a cross-section and removes the arbitrary nature of flow direction definitions based on channel geometry. Demonstrating this methodology on a meander, several well-known flow features are identified. An additional advantage is that field measurements presented along a cross section are readily available to provide boundary conditions and validation data for high resolution numerical models.

In-stream hydrokinetic energy convertors are an emerging technology that can benefit from the ADCP field measurement and analysis procedures developed here. Characterizing the flow field helps to identify appropriate locations for hydrokinetic devices as well as estimate the energy generation potential. Given the uncertainty regarding the environmental impacts, benchmark data is needed to quantify changes to the flow field and channel morphology. Velocity data collected following the installation of hydrokinetic devices can be analyzed for changes in bulk properties such as flow direction as well as changes to the mean 3D flow field.

Further work is anticipated to investigate the ability of FV measurements to determine turbulence characteristics such as profiles of turbulent kinetic energy and Reynolds stresses. The ability of the ADCP to capture small scale fluctuations is limited by the relatively large sample volume and low sampling frequency. Some studies, however, have found reasonable agreement between measured quantities with an ADCP and theoretical relations. The extensive dataset from the lower Roanoke River may provide insight in turbulence measurements in large natural rivers. Additional work is also anticipated to integrate the field data with high resolution numerical models. Computational fluid dynamics has become a valuable tool for riverine studies. Most studies are limited to simulation of laboratory scale flows. As computational resources increase, models of actual field sites will become practical and require high resolution field data. The field measurement and analysis techniques developed here can be incorporated with numerical simulations for a more complete representation of flow in natural rivers.